Effects of drought and the role of auxin on barley stamen maturation

Dissertation

zur

Erlangung des Doktorgrades (Dr. rer. nat.)

der

Mathematisch-Naturwissenschaftlichen Fakultät

der

Rheinischen Friedrich-Wilhelms-Universität Bonn

vorgelegt von

Richard Johannes Lange

aus

Berlin

Bonn, 2023

Angefertigt mit Genehmigung der Mathematisch-Naturwissenschaftlichen Fakultät
der Rheinischen Friedrich-Wilhelms-Universität Bonn

1. Gutachter: Prof. Dr. Lukas Schreiber
2. Gutachter: Prof. Dr. Frank Hochholdinger

Erscheinungsjahr: 2023
Tag der Promotion: 20.06.2023

Table of contents

List of figures

List of tables

List of abbreviations

%	Percent
°C	Degree Celsius
µ	Micro
ABA	Abscisic acid
ACN	Acetonitrile
ANOVA	Analysis of variance
ARF	Auxin response factor
ATP	Adenosine triphosphate
AuxRE	Auxin responsive element
bp	Base pair
cpm	Counts per million
CSA	CARBON STARVED ANTHER
DAPI	4’,6-diamidino-2-phenylindole
DAPs	Differentially abundant proteins
DDA	Data dependent analysis
DEGs	Differentially expressed genes
DNA	Deoxyribonucleic acid
DPPs	Differentially phosphorylated proteins
FC	Fold change
FDA	Fluorescine diacetate
FDR	False discovery rate
GA	Gibberellin
GC	Gas chromatography
GO	Gene ontology
GPF	Golden Promise Fast
h	Hours
IAA	Indole-3-acetic acid
IL	Introgression line
IPA	Indole-3-pyruvic acid
IVR	Invertase
JA	Jasmonate
LA	Lactic acid
LFQ	Label free quantification

LC-MS/MS	Liquid chromatography-tandem mass spectrometry
MAR	Missing at random
MNAR	Missing not at random
min	Minutes
ml	Milliliter
MOC	Metal-oxide chromatography
MSG38	MALE STERILE GENETIC 38
n	Sample size
PCR	Polymerase chain reaction
PI	Propidium iodide
Ppd-H1	PHOTOPERIOD 1
qRT-PCR	Quantitative real-time PCR
RNA	Ribonucleic acid
RT	Room temperature
RWC	Relative water content
SD	Standard deviation
SnRK1	SUCROSE NON-FERMENTING 1-RELATED PROTEIN KINASE 1
SWC	Soil water content
TCA	Tricarboxylic acid
TDR	Time domain reflectometry
TFA	Trifluoroacetic acid
TOR	TARGET OF RAPAMYCIN
W	Waddington
w/v	Weight per volume
YUC	YUCCA

Summary

Drought is a major abiotic stress that reduces crop yields all over the world. Climate change, the most prevalent crisis of our time, is predicted to increase the frequency and intensity of drought events in the future. Concomitantly, the increasing world population will require a rise in global crop production. To prevent a severe food insecurity situation, it is a pressing need to create varieties with robust yields under water deficit conditions, in economically important crops such as barley. Drought stress, occurring during the phase shortly before anthesis, is especially harmful to male reproductive development, which takes place in the stamens. Thus, understanding the molecular aspects that are essential for stamen development and that are also disrupted by drought stress should provide a firm basis for targeted crop improvement.

First, this work investigated the effects of transient drought stress on barley stamen development during the post-meiotic maturation phase. Drought treatment started around the phase of microspore release caused the highest reduction in barley spikelet fertility and was mainly caused by impaired male fertility, although female organ development was also negatively affected. Stamens that showed an altered morphology upon drought harbored viable but starch-less pollen that is infertile. Accordingly, comparative transcriptome analysis of stamens revealed that drought downregulates genes involved in central carbon metabolism, ranging from sucrose degradation to ATP synthesis, and in starch metabolism. Furthermore, drought-stressed stamens contained reduced levels of sucrose, hexoses and succinate, a tricarboxylic acid (TCA) cycle intermediate required for energy production. Drought also downregulated the expression of genes related to auxin synthesis, response and signaling in stamens. Thus, this work supports that auxin upregulates central carbon metabolism to ensure pollen starch accumulation, hence male fertility. Therefore, controlling auxin response and signaling in stamens may offer a valuable approach to improve pollen maturation and yield under drought. Moreover, the screening of a subset of the wild barley introgression line population S42IL and the genotypes Golden Promise Fast (GPF) and GB2 identified potential drought-tolerant accessions that could serve as genetic resources in future crop improvement programs.

Next, comparative omics analyses between stamens of the auxin-deficient mutant *male sterile genetic 38* (*msg38*) and the fertile cultivar Bowman were conducted to study the role of auxin in barley stamen maturation, with a special focus on auxin response and central carbon metabolism factors. Transcriptome analysis indicated that auxin predominantly regulates well-known primary targets of auxin signaling at early stages of stamen maturation. However, auxin has even stronger effects in gene expression during the phase of pollen starch accumulation, particularly by boosting genes involved in energy production pathways. Decreased expression of auxin-dependent energy production genes in *msg38* stamens often correlated well with

lower levels of the corresponding proteins. Moreover, auxin was found to control the phosphorylation of sugar utilization enzymes and other factors of heterotrophic energy generation. These findings underline the importance of auxin as major regulator of the stamen energy production pathway. Additionally, we identified MSG38-dependent candidates participating in auxin response and signaling that we hypothesize may exert direct regulation of carbohydrate metabolism genes. This work provides a basis for future analysis of the auxin signaling cascade as well as targeted molecular engineering of central carbon metabolism in stamens that could help to improve male fertility under adverse environmental conditions such as drought.

1 General introduction

Achieving food security remains one of the most fundamental challenges for the global community. Throughout recent years, geopolitical conflicts, climate-change-related disasters, and the unprecedented impact of a global pandemic have exacerbated food insecurity all over the world (FAO, 2022a). A clear illustration of this deteriorating situation is that between 702 and 828 million people faced hunger in 2021 – 150 million people more than in 2019 (FAO, 2022a). The growing world population is projected to reach 9.7 billion by the middle of the 21st century (United Nations, 2019), which will require a doubling of agricultural crop production (Tester and Langridge, 2010; Tilman et al., 2011). However, yields have been stagnating or are increasing too slowly to meet future demands (Brisson et al., 2010; Ray et al., 2012; Ray et al., 2013). Simultaneously, climate change facilitates extreme weather events such as floods, storms, heat spells or drought waves that are major threats to food security as they directly or indirectly jeopardize yields around the globe (Mall et al., 2017; Holleman et al., 2020; Hasegawa et al., 2021). For example, a heat and drought period in 2003 reduced European agricultural production by 30% (Ciais et al., 2005). In the United States, crop yield and insurance data analysis has shown that excessive rainfalls have caused an average 17% maize yield reduction from 1981 to 2016 (Li et al., 2019). Models predict that future climate-change-related stresses will occur with increased frequency and magnitude (Dai, 2011; Cook et al., 2015; Haile et al., 2020), and will additionally cause a 1.7% decrease of global arable land (Zhang and Cai, 2011). Thus, it is crucial to generate high-yielding and stress-tolerant crops to cope with these future scenarios and prevent severe food insecurity and malnutrition, especially in poor countries that will likely face the most devastating climate change threats (Mendelsohn et al., 2006).

Nutrition of the world population predominantly relies on cereal grains that provide the majority of consumed calories (Awika, 2011; Poole et al., 2021). Only in 2021, cereal crop production amounted to 2.8 billion tons (FAO, 2022b). Barley (*Hordeum vulgare* spp. *vulgare*) is mainly a source for fodder and malting but also serves as staple crop in parts of the Middle East and Africa (Grando and Gomez-Macpherson, 2005; Baik and Ullrich, 2008). Barley is the fourth most grown cereal with an annual production estimate of 157 million tons in 2020 (FAOStat, 2022). Due to its simple diploid genetics and adaptation to a range of adverse conditions such as cold, salinity or drought, barley is an excellent model to study the physiological and molecular effects of abiotic stress in cereal crops (Gürel et al., 2016; Giraldo et al., 2019). Moreover, barley genetic resources carry great potential for crop improvement because of their rich adaptive genetic variability and the possibility of enhancing genetic diversity by crossing cultivated barley with the wild progenitor *Hordeum spontaneum* (Nevo and Chen, 2010; Lakew et al., 2011).

1.1 Cereal reproductive development under drought stress

Plant reproductive development follows the vegetative phase and encompasses the formation of floral and reproductive structures, establishment of the male and female gametophytes, fertilization upon anthesis and subsequent grain set (Senapati et al., 2019). Spikelets are the basic developmental units of cereal inflorescences that bear one or more florets. These in turn contain stamens and/or pistils, the gametophyte-carrying structures. During the early phase of reproductive development, the number of spikelets within an inflorescence determines the potential grain number, which is the most important factor of cereal crop yield (Bingham, 1966; Dolferus et al., 2011). Adverse environmental conditions can disturb reproductive processes, leading to reduced yield (Dolferus et al., 2011; de Storme and Geelen, 2014). In cereals, drought is a major abiotic stress that jeopardizes reproductive development (Saini and Aspinall, 1981; Dorion et al., 1996; Sheoran and Saini, 1996; Ji et al., 2010). The damage on yield depends on the severity of the stress and the plant's growth stage (Dolferus et al., 2011). When it occurs after anthesis, drought mainly limits grain or seed weight (Plaut et al., 2004; Honsdorf et al., 2017). At reproductive stages before anthesis, water deficit in cereals causes reduced spikelet fertility or grain number, the predominant factor of yield losses in cereal crops under drought (Saini and Aspinall, 1981; Ji et al., 2010; Liu et al., 2015). Due to its implications for economy and food security, it is of high importance to investigate the effects of drought stress on reproductive development (Ma et al., 2020) and to identify genetic components that enable stable yields under stress.

Drought stress in plants results from tissue water deficit that evokes a multitude of biochemical, physiological and molecular alterations, and impairs elementary processes such as photosynthesis, respiration, assimilate partitioning and cell growth (Farooq et al., 2009; Taiz and Zeiger, 2010; Sallam et al., 2019). Plants have evolved different strategies to resist and survive water-limiting conditions (Farooq et al., 2009; He et al., 2018). For example, plants can accelerate growth to complete their life cycle (escape strategy) (Shavrukov et al., 2017), or they can optimize water uptake or close stomata to reduce water loss (avoidance strategy) (Turner et al., 2001; Tuteja, 2007; Farooq et al., 2009). These strategies require that plants initiate morphological, physiological and molecular mechanisms, such as root system modification, antioxidant defense, osmoprotection, as well as hormonal and transcriptional regulation (Farooq et al., 2009; Singh et al., 2019).

Various studies have investigated the effects of water deficit during vegetative development and unveiled a range of molecular players that control vegetative growth under drought (Bechtold and Field, 2018; He et al., 2018; Singh et al., 2019; Pradhan et al., 2020). Although research has also started to focus on drought during reproductive development, the number of studies that describe specific, drought-induced morphological and molecular changes at

different stages of reproductive development is still limited (Ma et al., 2020). Moreover, only few reports have identified molecular mechanisms that mitigate defects in floral organs, hence loss of grain yield, under drought conditions in Arabidopsis (Sukiran et al., 2019), rice (Guo et al., 2013; Guo et al., 2016), maize (Nuccio et al., 2015) and wheat (Ji et al., 2010). In barley, studies have investigated the effects of drought stress on early reproductive development (Gol et al., 2021) and grain filling (Honsdorf et al., 2017). However, little is known about the impact of drought stress at stages close to anthesis. Identification of the most vulnerable aspects of reproductive development during this phase and subsequent molecular dissection of stress-induced defects will provide basis for the identification of drought tolerance sources in barley germplasm.

1.2 Importance of carbohydrate metabolism in male reproductive development

Male gametophyte development is crucial for fertility, hence cereal grain yield. Pollen grains are heterotrophic entities that depend on sporophytic sugars to fuel essential processes required for successful development and function (Ruan et al., 2010; Liu et al., 2021). Sucrose is the main carbohydrate delivered from photosynthetically active sites to anther sink tissues (Ruan et al., 2010). During microsporogenesis, sucrose is transported symplasmically through the terminal phloem to the anther endothecium and middle layer, and apoplasmically to the anther tapetum cell layer, which feeds the microspores (Gómez et al., 2015; Liu et al., 2021). During gametogenesis or pollen maturation, sugars enter the symplasmically isolated microspore through sucrose and hexose transporters (Castro and Clément, 2007; Oliver et al., 2007; Hirose et al., 2010). Within the developing pollen grain, invertases hydrolyze sucrose into hexoses that are not only channeled into glycolysis and tricarboxylic acid (TCA) cycle pathways to fuel energy production but also used for the synthesis of starch (Oliver et al., 2005; Lee et al., 2020; Liu et al., 2021). In contrast to Arabidopsis pollen, which harbors mainly lipid bodies for energy storage (Zheng et al., 2018), cereal pollen accumulates starch in modified plastids (amyloplasts) at late maturation stages (Amanda et al., 2022). Such starch reserves provide energy for the terminal functions of pollen grains: germination, pollen tube growth and fertilization (Dickinson, 1968; Clement et al., 1994; Franchi et al., 1996; Lee et al., 2016).

Disruption of anther carbohydrate metabolic pathways, including synthesis, degradation, transport and metabolic regulation of sugars can impair pollen development and cause male sterility (Liu et al., 2021). A common feature of sterile pollen in cereals is the lack of starch accumulation. For example, mutations in rice genes involved in glycolysis (*OsHXK5*) and starch synthesis (*OspPGM* and *OsAGPL4*) result in reduced pollen starch accumulation and male sterility (Lee et al., 2016; Lee et al., 2020). Moreover, sugar transport and partitioning, orchestrated by the MYB transcription factors CARBON STARVED ANTHER (CSA) and CSA2, are crucial for pollen development (Zhang et al., 2010; Wang et al., 2021).

Pollen silencing of the sugar sensor SUCROSE NON-FERMENTING 1-RELATED PROTEIN KINASE (SnRK1) leads to abnormal pollen shape and lack of starch accumulation, supporting that regulation of carbohydrate metabolism is critical for successful male reproductive development (Zhang et al., 2001). A connection between sugar metabolism and hormone signaling in pollen has also become clear in recent years. Downregulation of the sucrose transporter *CsSUT1* causes male sterility associated to lower expression of auxin synthesis and signaling genes (Sun et al., 2019). Barley pollen produces auxin, which is required to enhance heterotrophic energy generation and starch synthesis during maturation (Amanda et al., 2022). Despite the progress brought about by research in Arabidopsis and rice (Liu et al., 2021), the complex molecular network that governs carbohydrate metabolism in male reproductive tissues is still not fully understood. Moreover, understanding this network in cereal crops will potentially open new avenues to control male fertility and facilitate hybrid crop breeding (Amanda et al., 2022), which is another promising technology to safeguard future yields.

1.3 Research aims

This dissertation comprises two chapters. The first chapter covers the major project of this work, which aimed to describe the morphological and molecular effects of short-term drought stress on barley stamen and pollen maturation. In the second chapter, the project investigated the changes in the stamen transcriptome and proteome of the barley pollen-sterile and auxin-deficient mutant *msg38* to better understand the role of auxin in pollen carbon metabolism and starch accumulation.

2 Chapter I – Effects of drought on barley stamen maturation

2.1 Introduction

Throughout their life cycle, plants are exposed to a range of unfavorable environmental conditions (Mochida et al., 2015). Among them, drought stress is a major threat that jeopardizes rain-fed agricultural crop production by limiting the vegetative and reproductive capability of plants (Barnabas et al., 2008). In the past, drought has affected approximately 75% of the global harvested areas of crops, causing economic losses of 166 billion U.S. dollars in the period between 1983 and 2009 (Kim et al., 2019). Driven by anthropogenic-caused climate change, the adverse impact of drought and heatwaves on crop production has tripled throughout the last decades (Brás et al., 2021). In cereals, which provide the majority of global consumed calories (Poole et al., 2021), droughts are consistently increasing production losses, overall imposing 7% more damage to yields than in the past (Lesk et al., 2016; Brás et al., 2021). A recent meta-analysis has estimated that drought stress reduces yields of wheat and rice by average 27.5% and 25.4%, respectively (Zhang et al., 2018). As humanity-driven climate change alters the global environment, the frequency and intensity of drought periods will likely increase in the future (Hoerling et al., 2012; Dai, 2013; Lehner et al., 2017; Haile et al., 2020; Hari et al., 2020), thus posing an elevated threat to crop yields.

In self-fertilizing cereals such as rice or wheat, abiotic stresses (e.g. cold or drought) are causing the highest loss of grain number when they occur during the reproductive phase, shortly before anthesis (Oliver et al., 2005; Ji et al., 2010; Jin et al., 2013). The development of male reproductive organs is especially vulnerable to drought stress as transient water deficiency episodes around meiosis and mitosis can irreversibly abort stamen and pollen development, resulting in stress-induced male sterility (Dorion et al., 1996; Liu and Bennett, 2011; Jin et al., 2013). In contrast, the development of female reproductive organs remains mostly unaffected by drought stress in wheat and rice (Bingham, 1966; Saini and Aspinall, 1981; Ji et al., 2010). Therefore, male sterility is widely considered the major driver of drought-induced loss of grain number in cereals (Dolferus et al., 2011; Yu et al., 2019).

An important part of male reproductive development in flowering plants is the formation and maturation of male gametophytes in form of pollen grains (Scott et al., 2004). First, differentiation of male sporogenous cells and subsequent meiosis (microsporogenesis) give rise to haploid microspores that are released into the anther locule (Scott et al., 2004; Wilson and Zhang, 2009). Subsequently, microspores acquire a multi-layered pollen wall and become vacuolized (Christensen et al., 1972; Owen and Makaroff, 1995). In cereal crops, developing gametophytes undergo two rounds of asymmetric mitosis to become tricellular, thus containing two generative cells and one vegetative cell (Eady et al., 1995). Moreover, late stages of pollen development in cereals are characterized by the accumulation of large starch stocks (Amanda

et al., 2022). Finally, anther sacs open to release mature pollen that goes on to germinate and elongate a pollen tube that carries the generative cells to the female gametophyte for fertilization (Scott et al., 2004).

Throughout the last decades, research has investigated the adverse effects of transient drought stress on male reproductive development. This has identified meiosis and the stages shortly after microspore release as most vulnerable to drought stress (Dolferus et al., 2011; Yu et al., 2019). Water deficit during wheat meiosis decreases grain number without necessarily affecting the water relations within spikelet tissues (Morgan, 1980; Saini and Aspinall, 1981; Dorion et al., 1996). Moreover, drought stress during male meiosis in wheat, rice and tomato can lead to morphological defects (e.g. abnormal vacuolation and degeneration) and impaired function of the tapetum (Lalonde et al., 1997; Ji et al., 2010; Guo et al., 2013; Jin et al., 2013; Lamin-Samu et al., 2021), an anther layer that is critical for microspore development (Pacini, 2010) and highly active during microsporogenesis (Clément et al., 1996). Anthers subjected to drought at meiosis or during the early phase of maturation can be smaller, pale and shriveled (Sheoran and Saini, 1996; Jin et al., 2013). Moreover, histological cross-sections of drought-stressed rice anthers reveal hypertrophy of endothecial cells and deformation of whole locules (Jin et al., 2013; Guo et al., 2016), suggesting that intense drought can impact all anther tissues. Drought-induced male sterility has been frequently linked to abnormal microspore development (Yu et al., 2019), associated to microspore disorientation, abnormal vacuolation and, in extreme cases, complete degeneration (Jin et al., 2013; Guo et al., 2016). Pollen of drought-stressed anthers often show wall defects and reduced or complete absence of starch (Saini et al., 1984; Sheoran and Saini, 1996; Lalonde et al., 1997; Jin et al., 2013).

In cereals, all these drought-induced defects have been associated with impaired carbohydrate metabolism (Saini et al., 1984; Dorion et al., 1996; Sheoran and Saini, 1996; Lalonde et al., 1997; Jin et al., 2013). In anthers of wheat and rice, short-term drought stress irreversibly represses on the one hand the activity of acid invertases (IVRs), important enzymes of sugar utilization (Sheoran and Saini, 1996; Lalonde et al., 1997; Koonjul et al., 2005; Nguyen et al., 2010), and, on the other hand, soluble starch-synthase and ADP-glucose pyrophosphorylase, two key enzymes required for starch biosynthesis (Dorion et al., 1996). Moreover, in rice anthers, drought downregulates the genes encoding not only invertases (e.g. IVR1, IVR5, CIN4 or INV2) but also glycoside hydrolases, 6-phosphofructokinase and UDP (uridine diphosphate)-galactose/UDP-glucose transporters (Koonjul et al., 2005; Nguyen et al., 2010; Jin et al., 2013). Notably, maintenance of anther sink strength through elevated expression of genes participating in carbohydrate metabolism can contribute to drought tolerance (Ji et al., 2010; Dong et al., 2017). For example, drought and heat tolerance of rice cultivar N22 could be partially explained by increased transcript levels of genes encoding the cell wall invertase

OsINV4 and the monosaccharide transporter OsMST8 in anthers (Li et al., 2015). Furthermore, expression of the invertase encoding gene *TaIVR1* in drought tolerant accessions SYN604 and Jinmai47 remained unaffected and increased significantly under drought-stress, respectively, whereas it was mostly repressed in drought-susceptible wheat lines (Ji et al., 2010; Dong et al., 2017).

Drought stress also affects hormone homeostasis in anthers (Yu et al., 2019). Abscisic acid (ABA), a central player in the regulation of abiotic stress responses (Sah et al., 2016; Weiste et al., 2017), accumulates in drought-stressed male reproductive tissues and correlates with repression of carbohydrate metabolism genes, thus contributing to pollen sterility (Morgan, 1980; Ji et al., 2010; Liu and Bennett, 2011). Other studies suggest that auxin, a powerful regulator of plant growth and male reproductive development (Cecchetti et al., 2008; Ozga et al., 2016), participates in the regulation of plant responses to drought stress (Shi et al., 2014; Sharma et al., 2018). In rice panicles, drought stress imposed during the anthesis stage decreased the endogenous content of indole-3-acetic acid (IAA), the main bioactive auxin in plants (Sharma et al., 2018). This decline was accompanied by the downregulation of genes encoding nine auxin synthesis enzymes (YUCCAs), their upstream transcription factors, auxin co-receptors and auxin response factors (ARFs) (Sharma et al., 2018). Accordingly, exogenous application of IAA mitigated the negative effects of heat and drought stress on pollen viability and overall spikelet fertility (Sharma et al., 2018). Auxin application during pre-anthesis drought stress in Arabidopsis, also improves drought stress tolerance, possibly due to altered regulation of reactive oxygen species (ROS), sugar metabolism and upregulation of stress-related genes (Shi et al., 2014).

To ensure sufficient grain yield in the future, it is an urgent task to improve the tolerance of cereal crops against drought (Farooq et al., 2009). However, this requires in-depth knowledge of the mechanisms that orchestrate plant responses to the stress (Farooq et al., 2009) and the identification of the most vulnerable aspects of development (Dolferus et al., 2011). The studies just described have already made advances in wheat, rice and tomato, some of them through transcriptomic, proteomic and metabolite analyses to identify major pathways that are affected in drought-stressed reproductive tissues (Liu and Bennett, 2011; Jin et al., 2013; Li et al., 2015; Mehri et al., 2020; Lamin-Samu et al., 2021). On the other hand, although adverse effects of pre-anthesis drought stress on grain formation in barley are known (Rajala et al., 2011), detailed descriptions of drought-induced changes in maturating barley stamens are lacking. Here, in addition to classical physiological and morphological studies, high-throughput omics datasets may provide a first broad glance on stage-dependent changes in male reproductive tissues in response to drought. Moreover, exploiting the high genetic variability of exotic barley

germplasms could lead to the identification of genetic resources carrying enhanced drought tolerance, thus, contributing to future crop improvement breeding programs.

In this work, the main goal was to investigate the effects of short-term drought stress on barley stamen maturation using the two row spring-barley cultivar Scarlett as model crop. The specific aims were to (i) describe the phenotypic effects of drought stress during stamen maturation on anther and pollen development, including pollen starch accumulation; (ii) investigate the transcriptome of drought-stressed stamens to provide insight into the molecular changes and regulatory pathways affected by drought stress in male reproductive tissues; (iii) conduct comparative metabolite profiling of drought-stressed stamens at late maturation stages to elucidate the effects on sugars and intermediates required for energy production in pollen starch filling; (iv) evaluate spikelet fertility under drought of different barley accessions to identify potential sources of drought tolerance.

2.2 Material and methods

2.2.1 Plant material

In this study, we used the spring-barley elite cultivar Scarlett to investigate the effects of short-term drought stress on barley stamen development. Scarlett seeds were kindly provided by Ali Naz (Rhenish Friedrich Wilhelm University of Bonn). Moreover, 17 ILs of the S42IL collection, created by Schmalenbach et al. (2008), were screened for drought-tolerance. Seeds for those lines were kindly provided from Klaus Pillen (Martin Luther University Halle-Wittenberg). We also tested the genotypes Golden Promise Fast (GPF) and GB2 for drought-tolerance. GPF, a fast-flowering genotype harboring the wild allele of the flowering time gene *Ppd-H1* (Gol et al., 2021), was kindly provided by Maria von Korff (Heinrich Heine University of Düsseldorf). The fast-flowering Iraqi landrace GB2 (WB-111) originates from a panel of barley genotypes selected by the GENDIBAR consortium and was obtained from the WHEALBI collection.

2.2.2 Growth conditions and drought treatments

All plants were grown in a controlled greenhouse chamber (16 h light at 22°C, 8 h dark at 18°C, light intensity: 100 μEinsteins $m^{-2}s^{-1}$). Barley seeds were sown in 96-well trays filled with a 1:1 mix of soil ED 73 Einheitserde® (Einheitserdewerke Werkverband e.V., Sinntal-Altengronau, Germany) to BVB Substrates (1:1 vermiculite to coconut fiber). After one week, seedlings were transplanted to round 1-liter pots, filled with 500 g of the above described substrate. Time domain reflectometry (TDR) field operating meter FOM2/mts (E-Test, Lublin, Poland) was used to monitor the volumetric soil water content (SWC) of pots. Measurements were carried out daily shortly before watering. Plants were watered on demand to maintain an average control SWC levels before and after the drought stress treatment. Fertilization was done once per week with WUXAL® Super 8+8+6 (0.25% concentration) (Hauert MANNA Düngerwerke GmbH, Nürnberg, Germany).

Our standard setup for drought-stress experiments included two plants per genotype per pot and a control SWC of ~25%. We adjusted these conditions for screening the fast-flowering genotypes S42IL-107, GPF and GB2 by lowering the SWC to ~10% and subsequently increasing the number of plants per pot to four. Drought treatments were conducted when plants reached stages of stamen maturation, predicted by our modified Waddington scale (Figure 1) (Waddington et al., 1983). Primary, secondary and tertiary barley tillers were tagged and pots were randomly assigned to control and treatment blocks. In the drought group, water was withheld for 72 h, whereas control group SWC was maintained at control levels. Thereafter, drought-treated plants were re-watered and maintained at control SWC levels until harvest.

2.2.3 Relative water content measurements

Relative water content (RWC) of the penultimate leaf was used as indicator of the plant water status. We obtained the RWC following the protocol by Liu et al. (2006) with some modifications. Sections of the middle part of the penultimate leaf blade were cut every morning throughout the treatment, weighted and immediately transferred into a fresh 2 ml tube, filled with distilled H_2O. Tubes were kept for 24 h at 4 °C. Leaf pieces were then blotted dry with a tissue paper to remove excess water and turgid weight was determined. Leaf blades were then transferred into a fresh 2 ml tube and dried in an oven at 60 °C for 48 h. Subsequently, dry weight was determined. RWC was calculated using the equation by Schonfeld et al. (1988): RWC = [fresh weight – dry weight] / [turgid – weight – dry weight].

2.2.4 Imaging of reproductive organs and plant tissues

Florets were carefully dissected using fine forceps and a common stereomicroscope and subsequently placed on a black velvet. A Discovery.V12 stereomicroscope and a Stemi 503 color camera (Carl Zeiss, Oberkochen, Germany) were used to visualize and image the reproductive organs. Determination of scale and image export was performed with the ZEN v2.3 blue edition software (Carl Zeiss, Oberkochen, Germany).

For imaging of microspores within anthers at stages W7.5 – W8.25, anthers were mounted in perfluoroperhydrophenanthren (Sigma-Aldrich/Merck) and examined using a Axio Scope.A1 microscope combined with an Axiocam 512 color camera (Carl Zeiss, Oberkochen, Germany).

Photographs of whole plants and inflorescences were taken with a Canon EOS 500D camera mounted with a Canon EF 16–35 mm F/4 L IS USM lens (Canon, Tokyo, Japan). Images were processed using the ImageJ v1.53 software (https://imagej.nih.gov/ij/).

2.2.5 Reciprocal crosses

Control and drought-stressed Scarlett plants were used in cross-pollination experiments to assess the effect of drought stress on pollen and pistil fertility, respectively. To prevent self-pollination, spikelets containing W9.35 florets were carefully opened with clean forceps, emasculated and covered with plastic wrap one to two days before the crosses. Reproductive organs of florets coming from the middle of an inflorescence were used for the crosses. Crosses were conducted when pistils of emasculated plants showed full spreading of stigmatic branches, using fresh pollen of recently-opened control anthers or drought-stressed anthers, respectively. Subsequently, inflorescences were covered with a paper bag. At maturity, grain set in individual inflorescences was calculated as fraction of grains divided by the number of pollinated pistils.

2.2.6 Pollen starch staining and visualization

Anthers were opened using fine forceps and pollen grains were immersed in I_2/KI solution (0.3 g / 1.5 g per 100 ml H_2O) on a glass slide (Carl Roth, Karlsruhe, Germany). Starch staining of in pollen was visualized with an Axio Scope.A1 and imaged with an Axiocam 512 color camera (Carl Zeiss, Oberkochen, Germany).

Whole-anther starch staining was conducted using fresh anthers fixed in Carnoy's solution (6:3:1 :: ethanol: chloroform: glacial acetic acid) for 1 – 2 h. Anthers were transferred into a new 1.5 ml tube filled with staining solution (0.5 g / 2.5 g I_2/KI in 100 ml 8:2:1 :: chloral hydrate: glycerol: water) and kept on a rotating wheel for approximately 4 – 6 h. Subsequently, staining solution was discarded and anthers were cleared in chloral hydrate solution for 24 h on a rotary wheel. Clearing solution was then replaced with fresh chloral hydrate and anthers were cleared for another 24 h. Stamen samples were mounted in chloral hydrate on a cover slide and visualized and imaged with a Discovery.V12 stereomicroscope and a Stemi 503 color camera (Carl Zeiss, Oberkochen, Germany), respectively.

2.2.7 Pollen nuclei visualization

We used 4',6-diamidino-2-phenylindole (DAPI) staining to visualize pollen nuclei in control and drought-stressed anthers at stage W9.5. For one sample, 6 – 9 anthers, originating from a single inflorescence, were dissected with fine forceps and placed in a 1.5 ml tube containing DAPI solution (1 µg/ml DAPI, 0.0013% (w/v) Toluidine Blue, 1% Triton-X in 1x PBS, pH 7.4). Samples were vortexed, briefly spinned down and subsequently flicked gently. Tubes were covered with aluminum foil and samples were incubated for 1 h at room temperature (RT). After a short centrifugation, the bulk of pollen accumulated at the bottom of the tubes were carefully pipetted on a microscope slide and perhydroperfluorophenanthren (Sigma-Aldrich/Merck, St. Louis, USA) was added on top of the pollen. Examination of pollen nuclei was performed with an SP8 laser confocal scanning microscope (Leica Microsystems, Wetzlar, Germany) using a 405 nm laser beam and a HyD detector capturing the emitted fluorescence between 410 – 505 nm.

2.2.8 Pollen viability assay

A combined staining with fluorescine diacetate (FDA) and propidium iodide (PI) was used to assess viability of control and drought-stressed pollen. For each sample, a minimum of nine anthers originating from a single inflorescence were dissected and placed in a 1.5 ml tube filled with staining solution (FDA: 10 µl/ml FDA and 20% sucrose (w/v) in 1x PBS; PI: 20 µl/ml PI and 20% sucrose (w/v) in 1x PBS). Samples were vortexed and incubated at RT in the dark for 5 min. After brief centrifugation, the pellet with stained pollen was pipetted into a fresh 1.5 ml tube and washed with 1x PBS with 20% sucrose. The washing step was repeated one time before and pollen were mounted on a microscope slide. Pollen were visualized with an Axio

Scope.A1 (Carl Zeiss, Oberkochen, Germany) mounted with filters that cover the emission spectra of FDA (517) nm and PI (617 nm), respectively, and imaged with an Axiocam 512 color camera (Carl Zeiss, Oberkochen, Germany). Only those pollen were considered as viable which exhibited a strong green FDA fluorescent signal and weak red autofluorescence signal for PI, respectively.

2.2.9 RNA extraction

For RNA extraction, stage W8.5, W8.75 stamen material was collected at days two and three of the drought-stress treatment, respectively. Stage W9 stamen material was collected one day after the end of the stress. Stage W9.25 and W9.35 stamen material was collected two to three days after the end of the stress treatment. For each replicate, we collected stamens from 13 – 15 florets of one individual inflorescence for stages W8.5 and W8.75 and 7 – 9 florets from one individual inflorescence for W9, W9.25 and W9.35, respectively. Stamen material was collected in 1.5 ml tubes and immediately frozen in liquid nitrogen. Samples were grinded at 30/s frequency for 1 min using a TissueLyser II (Qiagen, Venlo, Netherlands). Tube-holders were pre-cooled for 10 min at -80 °C and soaked in liquid nitrogen before grinding. RNA extraction was conducted following the method described by Onate-Sanchez and Vicente-Carbajosa (2008) with some modifications. RNA was resuspended in 24 µl DEPC-water and 6 µl of DNase mix (3 µl 10x DNase buffer, 3 µl DNase I (RQ1 RNase-free DNase by Promega, Madison, USA)) and incubated for 60 min at 37 °C. Subsequently, 70 µl DEPC-water, 10 µl sodium-acetate (pH 5.2, 3 M) and 400 µl 100% ethanol were added. Samples were mixed by inversion, centrifuged for 20 min at 4 °C. The supernatant was discarded and the pellet was washed with 70% ethanol. RNA was resuspended in 10 – 50 µl DEPC-water and quantified using the Qubit assay (Thermo Fisher Scientific, Waltham, USA) following the manufacturer's instructions.

2.2.10 Oligonucleotides

All used oligonucleotides have been used in the study by Amanda et al. (2022).

Table 1. Oligonucleotides used in this study.

ID	Oligonucleotide sequence	Target	Target name
P683	TGGAGAGGCAGGGGTTGGAT	HORVU.MOREX.r2.1HG0062140	*HXK5*
P684	TGCTGCGTTTGTACCAGTGCC	HORVU.MOREX.r2.1HG0062140	*HXK5*
P685	TCTCGATGTTGGAACCATAGCG	HORVU.MOREX.r2.3HG0205730	*Msg38*
P686	TGAAAGCACCGCACAGCAGG	HORVU.MOREX.r2.3HG0205730	*Msg38*
P679	TTGGGAGGCAGTCTGGAACA	HORVU.MOREX.r2.3HG0256400	*Cyt-C*
P680	TGAGGCTTCTTCAGTCCAGGGA	HORVU.MOREX.r2.3HG0256400	*Cyt-C*
P681	TCACAAGCACAAGGGCCACAC	HORVU.MOREX.r2.1HG0075760	*AGP-L1*
P682	AGGTGCGGTGAATGTGGCGA	HORVU.MOREX.r2.1HG0075760	*AGP-L1*
P62	AGCTTGGCCTGCACTCTCTG	HORVU.MOREX.r2.3HG0246760	*ADP*
P63	CCCTTCACCAGATGTCGCGC	HORVU.MOREX.r2.3HG0246760	*ADP*

2.2.11 cDNA synthesis and qRT-PCR

RNA was diluted to a 200 ng/ul concentration and cDNA was synthesized with 500 ng total RNA using 80 units of the M-MLV Reverse Transcriptase RNase H(-) (Promega, Madison, USA) in a 10 µl reaction volume. Subsequently, cDNA was diluted with 190 µl of H_2O. qRT-PCR was performed in 384-well plates with 6.25 ng cDNA using 0.25 units of the GoTaq® G2 Hot Start Polymerase (Promega, Madison, USA) and 0.5X SYBR Green I (Thermo Fisher Scientific, Waltham, USA) in a 10 µl reaction volume. LightCycler® 480 II (Roche, Basel, Switzerland) was used to run the qRT-PCR. We selected the putative ADP-ribosylation factor gene *HvADP* (HORVU.MOREX.r2.3HG0246760) as normalization factor of gene expression levels. Raw data was analyzed with the LingRegPCR 2020.0 software (Ruijter et al., 2009) and expression values were calculated in Microsoft Excel 2019.

2.2.12 Transcriptome analysis

We performed two separate transcriptome analyses of Scarlett control and drought-stressed stamens, one including stamens at stages W8.5 and W8.75, and the second including stamens at stages W9.25 and W9.35. For each stage, four biological replicates per treatment were collected. RNA was obtained as described in 2.2.9. Both transcriptome analyses were conducted as described below.

Sample processing, including ribosomal RNA depletion, library preparation and RNA sequencing (20 million 150-bp single reads per sample), was conducted at the Max Planck Genome Centre in Cologne with a HiSeq 2500 System (Illumina, San Diego, USA). RNAseq transcripts were quality-checked with FastQC v0.11.5 and reads were trimmed with Trimmomatic v0.35 (Bolger et al., 2014) using following parameters: ILLUMINACLIP: Trimmomatic-0.35/adapters/TruSeq3-SE.fa:2:30:10 LEADING: 3 TRAILING: 3 HEADCROP: 10 SLIDINGWINDOW: 4:15 MINLEN: 50. We quantified RNAseq transcripts with the mapping-based mode of Salmon v1.4 (Patro et al., 2017). Previously, we created a decoy-aware index of the predicted confidence transcriptome in the Morex V2 genome (Monat et al., 2019), using the entire genome as decoy sequence. Output *.sf files were fused and downstream analysis was conducted with R software. Transcripts were filtered for >1 counts per million (cpm) in at least three replicates. We used the TMM method of *edgeR* package (Robinson et al., 2010) for data normalization and assessed clustering of replicates according to all expressed genes with principal component analysis and Euclidean distances plotted with *pheatmap*. Differentially expressed genes (DEGs) between control and drought at each stage were obtained with an approach using the *limma* package (Ritchie et al., 2015). In short, counts were transformed to log2 cpm values with the *voom* function and a linear model was created by applying the *limFit* function on the transformed data. Differences between the groups (log fold-changes) were displayed as *contrasts* of the fitted linear models with P adjustment for false discovery rate (FDR). Subsequently, DEGs were filtered for a |fold change (FC)| ≥ 1.5 and FDR-adjusted P ≤ 0.05. We performed hierarchical clustering on DEGs utilizing Pearson correlation coefficients as distance metric. Heatmaps were created with the *annHeatmap* 2 function of the *Heatplus* package. Gene Ontology (GO) enrichment in each DEG hierarchical cluster was performed with the *weigh01* algorithm of the *TopGO* package (Alexa et al., 2006) and the *de novo* GO term annotation of the Morex V2 high confidence transcriptome received from J. Zhong (Zhong et al., 2021). Moreover, statistical significance of enrichment in gene categories related to auxin, sugar transport and energy metabolism under drought across all investigated stages was evaluated by Fisher's exact test in R. We independently confirmed the enrichment in those categories using the manually and semi-automatically curated resources by Amanda et al. (2022).

2.2.13 Metabolite profiling and starch measurements

Sample material was collected in five independent experiments. We dissected stamens from 19 – 34 florets coming from three inflorescences for each W9 – W9.5 control replicate. For each W9.35 drought replicate, 29 – 46 florets from four to five inflorescent were pooled. Every replicate contained stamen material originating from one single experiment, except for two W9.35 drought replicates, in which stamens of two experiments were pooled. Stamens of each replicate were collected in a 1.5 ml tube. Fresh weight was measured and samples were immediately frozen in liquid nitrogen. In total, 5 – 9 control replicates per stage and five W9.35 drought replicates were analyzed, respectively.

Metabolite profiling and starch measurements were conducted in the group of Prof. Dr. Alisdair Fernie at the Max Planck Institute of Molecular Plant Physiology in Potsdam and performed as described by Amanda et al. (2022). In brief, gas chromatography (GC)–mass spectrometry (ChromaTOF software v1.00, Pegasus driver 1.61; LECO, St. Joseph, USA) was conducted for metabolite profiling as previously described (Michard et al., 2017). Xcalibur software (Thermo Fisher Scientific, Waltham, USA) was used to evaluate the chromatograms and mass spectra. Metabolite identification was manually verified using the mass spectral and retention index collection of the Golm Metabolome Database (Kopka et al., 2005). Peak heights of the mass fragments were normalized based on the fresh weight of the sample and the added amount of an internal standard (ribitol). Relative levels of each metabolite were calculated as the ratio between each log transformed replicate and the mean of all nine log transformed control replicates at stage W9.35.

Stamen starch measurements of the same barley stamen samples were performed as previously described (Rosado-Souza et al., 2019). In short, the pellet was resuspended in 1 ml of deionized water. Subsequently, the sample was divided in two aliquots, which were boiled at 95 °C in a water bath for 20 min. Samples were then cooled and spinned at 20,000 g for 1 min and the water was discarded. Subsequently, 50 ml of starch digestion mix (200 mM sodium acetate, 6.3 U/ml amyloglucosidase, 50 U/ml a-amylase, freshly prepared) was added to the first aliquot for digestion at 37 °C for 4 h. Afterwards, 100 ml of glucose assay mix (100 mM 2-(4-[2-hydroxyethyl]-1-piperazinyl)-ethanesulfonic acid-KOH (HEPES-KOH), pH 7.5, 2 mM $MgCl_2$, 20ml 10 mM ATP, 20ml 10 mM NAD+, 0.3ml 1500 U/ml hexokinase) was added to both digested and undigested samples to bring them to a final volume of 200 ml in a 96-well flat-bottom microtiter plate. An absorbance plot of glucose standards at 340 nm was obtained to determine the linear range and calculate the slope of the standard curve. Baseline absorbance of samples at 340 nm was recorded. Next, 0.45 U of Glucose 6-phosphate dehydrogenase (G6PDH) was added and absorbance at 340 nm was again recorded again as ODG6PDH. The starch content was calculated as (ODG6PDH of digested samples- ODG6PDH of

undigested samples) – (ODbaseline of digested samples - ODbaseline of undigested samples).

2.2.14 Statistical analysis

Statistical tests and values of n are described in the figure legends. Differences of means between control stages were tested in Excel 2019 with one-tailed Student's t-tests after evaluating homogeneity of variances with *F*-tests. Significant differences between means in multiple comparisons were tested by Kruskal-Wallis ANOVA and a subsequent Conover-Iman test with Bonferroni correction. All tests were performed with a significance threshold of $P<0.05$. Compact letter display in figure 2F and figure 8 was obtained with the *multcompView* package in R. Plots were created using the R package *ggplot2*.

2.3 Results

2.3.1 Staging the phase of stamen maturation in barley cultivar Scarlett

The barley inflorescence (“spike”) is hidden inside the leafy pseudostem during most of its development. Under our greenhouse conditions, it extrudes out of the sheath of the last (flag) leaf only after fertilization. Thus, destructive dissection is required to determine the exact stages of stamen development in a given inflorescence, which prevents further experimentation. Therefore, we established first a non-destructive method to predict stamen development in hidden Scarlett inflorescences, based on three tiller features: the flag leaf sheath extension out of the penultimate leaf, the distance of the hidden spike tip to the auricle of the penultimate leaf, and the perceived length of the hidden spike (Figure 1A). These features correlated with advancing anther and pistil development as determined with our previously modified Waddington (W) morphological scale (Figure 1B, C) (Amanda et al., 2022). Scarlett anthers at stage W7.5 harbor either tetrads or recently released microspores (Figure 1D), which represent the end of meiosis. At stages W8 and W8.25, the thickening wall and expansion of free microspores indicate the initiation of stamen and pollen maturation (Figure 1D).

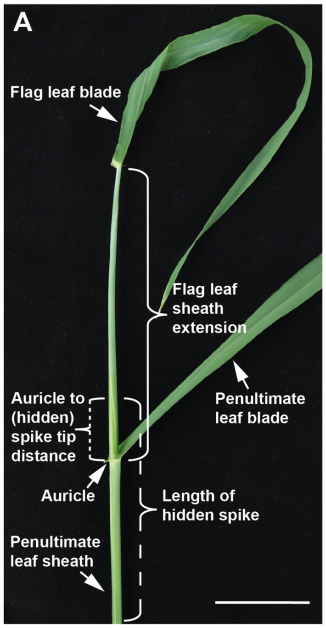

B

Waddington stage (W)	Flag leaf sheath extension (cm)	Auricle-to-spike-tip-distance (cm)	Length of hidden spike (cm)	Pistil morphology after Waddington *et al.* (1983) and Amanda *et al.* (2022)	Anther morphology
7.5	not visible	≤ -12.5	2.5 – 3.5	Stigmatic branches appear	Transparent
8 – 8.25	not visible	-12.5 to -10	3.5 – 4.5	Styles and stigmatic branches elongate	Pale green
8.5	0 – 3	-10 to -7.5	4.5 – 5.5	Hairs on ovary wall differentiate	Green
8.75	2 – 7	-8 to -4	5.5 – 7	Stigmatic branches and hairs on ovary wall elongate	Matte green
9	6 – 9	-4.5 to -1	7 – 8		Honeycomb -like structure visible
9.25	8 – 12	-2 to 2	7.5 – 9	Styles and stigmatic hairs erect	Yellow-green
9.35	10 – 14	-1 to 5	>8	Stigmatic branches start to spread outwards	
9.5	13 – 17	5 to 7	>9	Styles and stigmatic branches spread	Yellow

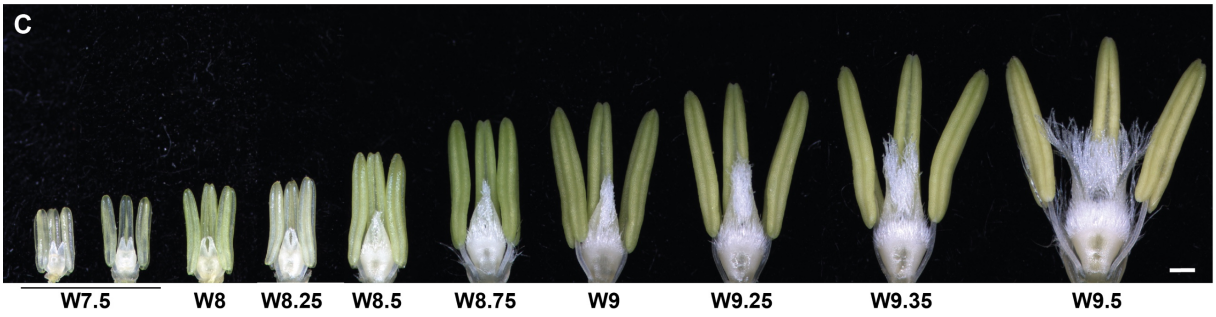

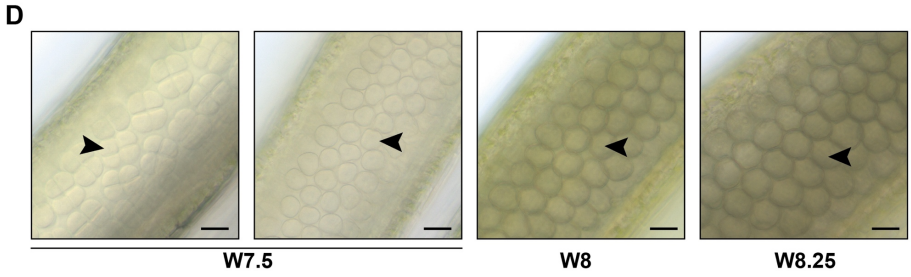

Figure 1. Morphological scale of stamen maturation in cultivar Scarlett under normal greenhouse conditions. A) Tiller morphology and features used to predict floral organ development. Bar, 5 cm. **B**) Modified Waddington (W) scale of pistil and anther development and its correlation with external tiller features. The hidden spike tip is positioned below or above the auricle of the penultimate leaf at early or late stages, respectively, resulting in negative or positive auricle-to-spike-tip distances. **C**) Stamen and pistil morphology between stages W7.5 and W9.5. Bar, 500 µm. **D**) Male gametophytes visualized through fresh anthers mounted in perfluorperhydrophenanthren. Arrowheads indicate tetrads (W7.5, left), recently released microspores (W7.5, right) and expanding free microspores with thicker cell walls (W8 and W8.25). Bars, 200 µm.

2.3.2 Short-term drought stress during the phase of stamen maturation affects vegetative and reproductive development

Next, we established a system to perform short-term drought treatments during the stamen maturation phase in pairs of Scarlett plants grown in 1-liter pots under greenhouse conditions (see details in Methods). We began experiments approximately 6 weeks after sowing, when the flag leaf sheath of the first tiller started extending and we could tag and predict the stage of stamen development in the first three tillers. Maintaining the soil water content at ~25% in control pots sustained the relative water content of the penultimate leaf above 90% (Figure 2A). Instead, withholding water dropped the soil water content to around 0% after 2 days and to completely undetectable levels after 3 days, which ultimately reduced the average leaf water content to 57% (Figure 2A). Moreover, drought-stressed plants exhibited leaf wilting and reduced height by the end of the 3-day treatment (Figure 2B). Thereafter, we re-watered these plants, maintained them at control levels and examined spike morphology approximately two weeks later. Control inflorescences appeared mostly well hydrated and with grain-filled spikelets (Figure 2C, D). Although some inflorescences from drought-stressed plants also appeared hydrated, they showed various degrees of empty (sterile) spikelets (Figure 2C). Moreover, other inflorescences either carried a fraction of pale and dehydrated spikelets, predominantly at the top of the spike, or were completely dehydrated, thin and stunted (Figure 2C). Inflorescences that were stressed at earlier stages of stamen maturation tended to show more hydrated morphologies, while partial and fully dehydrated inflorescences tended to occur more often when the drought stress was started at later stages of stamen maturation (Figure 2D). However, the frequencies of the different (de)hydration types show some variability between different experiments, so that we cannot conclude that the initial stage of a drought-stressed inflorescence unequivocally determines the final hydration status. While drought seems to elicit an overall fatal stress in fully dehydrated spikelets, we hypothesize that it specifically impairs the development of floral organs in hydrated-but-sterile spikelets. Therefore, we quantified the impact of drought on the fertility of hydrated spikelets. When the treatment started at stages W7.5 and W8 – W8.25, some inflorescences were completely sterile (58% and 42% of all spikes analyzed, respectively), while the fertility of the rest dropped an average of 73% and 55%, respectively (Figure 2E). Spikelet fertility declined an average of 20% when the treatment started at W8.5 – W8.75, while it remained unaffected when started at stage W9 or later (Figure 2E). These findings suggest that inflorescences at the early phase of stamen maturation undergo drought-sensitive processes that are essential for later fertility, whereas inflorescences at later stages are more robust to drought stress, as long as they do not reach a critical dehydration point. We selected stages W8 – W8.25 as starting point of all subsequent drought experiments of this work, to specifically target the stamen maturation phase and avoid spikelets that had not exited meiosis.

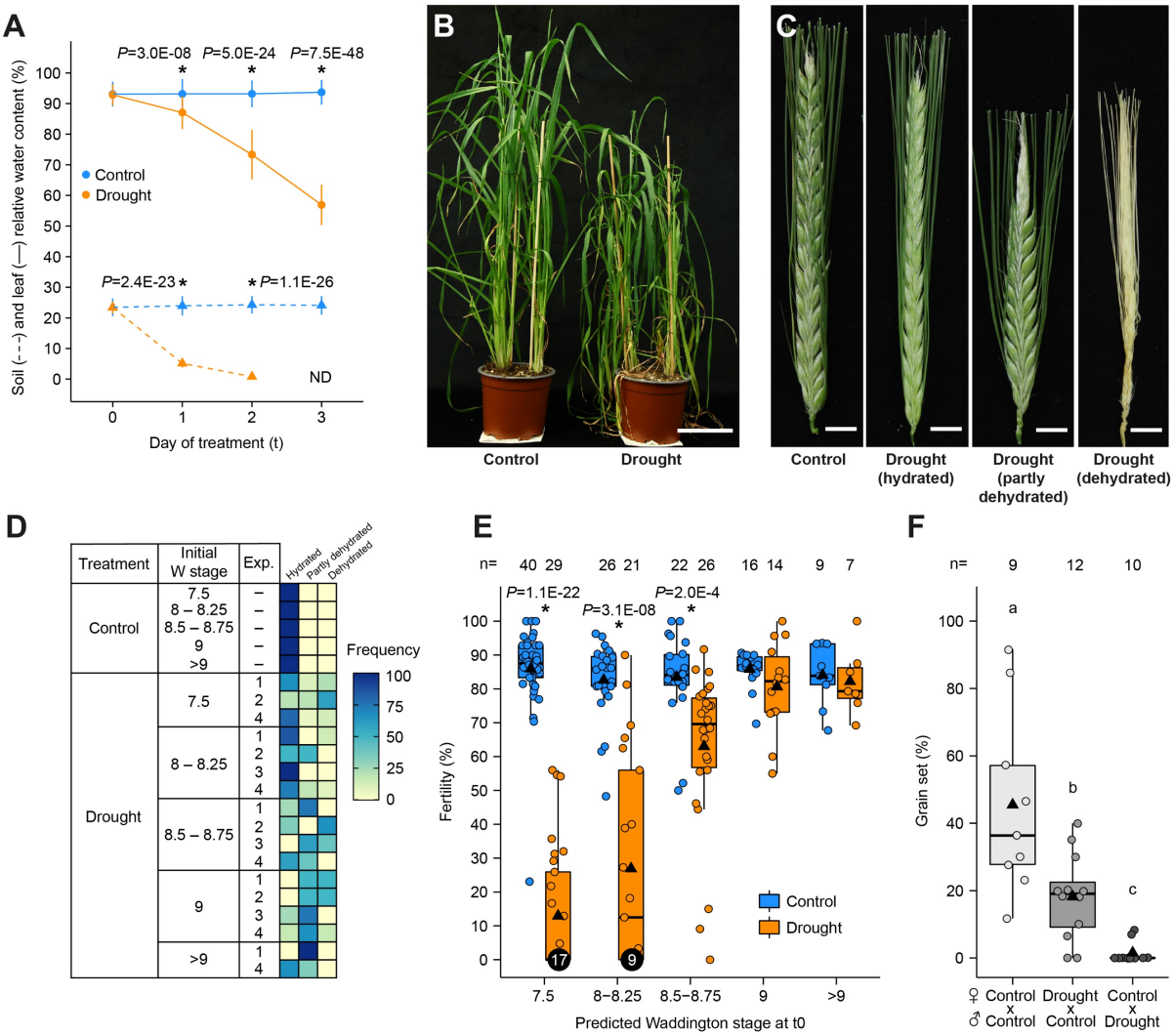

Figure 2. Effects of drought stress applied during Scarlett's stamen maturation phase. A) Soil water content (dash lines) and relative water content of the first tiller's penultimate leaf (solid lines) under control and drought stress conditions during a 3-day period. Data pooled from three independent experiments (n= 48 [leaf relative water content] and 24 [soil water content]) and plotted as mean ±SD. Asterisks indicate significant differences between control and drought at each time point (one-tailed t-test). Soil water content at day 2 was detectable in only 15 out of 24 drought samples. ND, not detectable. **B**) Representative plant morphology three days after the start of a drought trial. Bar, 5 cm. **C**) Representative spike morphologies around two weeks after the end of a drought trial. Bars, 1 cm. **D**) Frequency of spike hydration phenotypes around two weeks after the end of four independent experiments (Exp.). Frequencies were calculated within all inflorescences predicted to be at the same W stage at the start of the drought stress, and are presented separately for each experiment. Stages W7 – W7.5 and > W9 were not found in every experiment. **E**) Final fertility of hydrated spikelets after the drought treatments start (t0) at different maturation W stages. Fertility calculated as the ratio of filled spikelets over the total number of spikelets. Box plot whiskers represent ±1.5x the interquartile range; triangles, means; horizontal lines, medians; circles, individual measurements. Data pooled from four independent experiments. Numbers above the boxes correspond to sample sizes (n) for each group. Asterisks indicate significant differences between control and drought at each stage, determined with one-tailed t-tests. **F**) Grain set in cross-pollination tests, calculated as the number of grain-filled spikelets over the total number of crossed spikelets. Letters indicate significant differences between the crosses determined with a Conover-Iman test after a Kruskal-Wallis ANOVA indicated differences between crosses ($P < 0.05$). Box plot features as in (E).

To clarify if drought impairs the development of male and/or female reproductive organs, we conducted reciprocal crosses between control and drought-treated plants. The efficiency of hand-pollinated control crosses was highly variable and only achieved an average grain setting rate of 45% (Figure 2F). Yet, when we pollinated pistils of drought-treated plants with fresh control pollen, grain set was significantly reduced to 18% (Figure 2F). Moreover, most spikes of control plants that were pollinated with drought-stressed pollen showed no grains (Figure 2F). These results indicate that defects in the development or function of both male and female floral organs can contribute to the loss of fertility induced by drought from the early phase of barley stamen maturation. Nevertheless, male fertility defects alone explain most of the reduced grain production under drought.

We also followed the progress of stamen and pistil morphology in a 6-day time course during and after the drought treatment. Floral organs of control florets advanced approximately by one to two Waddington stages per day (Figure 3A). During the first three days of treatment, the morphology of stamens and pistils in all drought-stressed florets was undistinguishable from the control, and progressed at the same pace to reach stages W8.75 and W9 (Figure 3A). Thereafter, only 28% of the drought-treated florets examined between days 4 and 6 continued this trend, showing a normal morphology and reaching the end of maturation by day 6 (“drought, unaffected stamens”, Figure 3A). Instead, the remaining 72% of the florets in the stress group exhibited an altered stamen morphology (“drought, affected stamens”, Figure 3A). Still, regardless of the stamen morphology, we did not observe a slowdown in floret development according to the Waddington scale, which is mainly based in pistil features. In contrast, short-term drought stress causes visible changes in plant morphology (Figure 1A). Hence, we matched the Waddington stages of the inflorescences collected during the 6-day time course to the flag leaf sheath extension and the auricle-to-spike-tip distance of their tillers. These two length features were significantly reduced in drought-treated tillers from stages W8.75 and W8.5 onwards, respectively (Figure 3B). Since these stages occur mainly during the first days of the time course, these results show that drought starts impairing vegetative growth of tiller tissues during the stress treatment, whereas drought-induced changes in floret and stamen morphology occur later, after the end of the stress period.

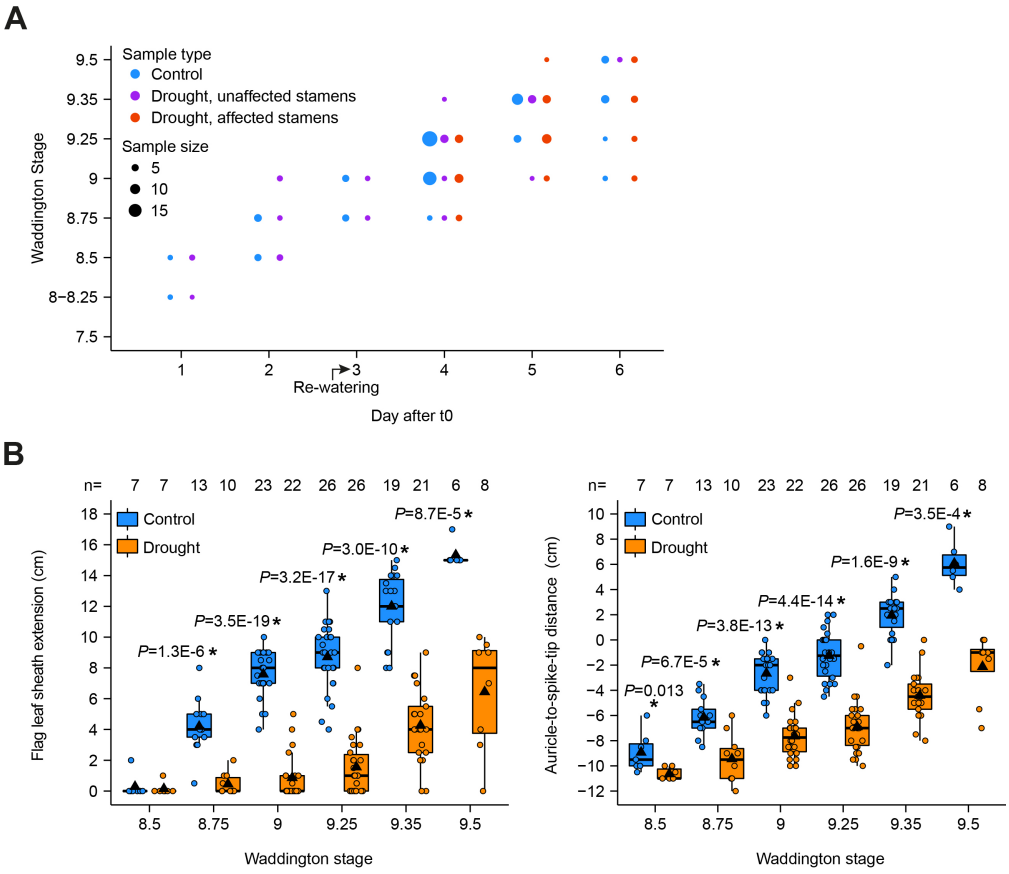

Figure 3. Progression of Scarlett reproductive and vegetative development under drought. **A**) Time course of stamen maturation stages according to our modified Waddington scale. **B**) Flag leaf sheath extension and auricle-to-spike-tip distance of tillers with inflorescences at different Waddington stages. Box plot features as in Figure 2E. Asterisks indicate significant differences between control and drought at each stage (one-tailed t-test). All data in this figure originates from 10 independent experiments.

2.3.3 Short-term drought during stamen maturation blocks pollen starch accumulation

We then focused on identifying the specific defects that drought induces in stamen maturation and that ultimately account for the loss in male fertility. First, we investigated pollen starch accumulation, an essential feature of cereal crops that is required for pollen fertility (Saini et al., 1984; Dorion et al., 1996; Jin et al., 2013) and that occurs at late stamen maturation stages in barley (Amanda et al., 2022). Under control conditions, starch becomes visible as individual granules in Scarlett pollen at stage W9.35 and fills the entire pollen grain at stage W9.5. Concomitantly, anthers increase in size and change color from green to yellow (Figure 4). Drought-treated stamens that maintain a mostly normal morphology also accumulate pollen starch between stages W9.35 and W9.5 (Figure 4, unaffected). In contrast, drought-affected anthers not only appear pale yellow and smaller from stage W9.25 but also display no starch at any maturation stage (Figure 4, affected). From here on, we used this obvious change in stamen morphology as indicator of failed pollen starch accumulation caused by drought stress. However, we have not formally tested if pollen grains from drought-unaffected stamens are fertile. Even if they appear to accumulate starch normally, they could be impaired in other functions necessary for fertility, such as pollen tube germination or growth.

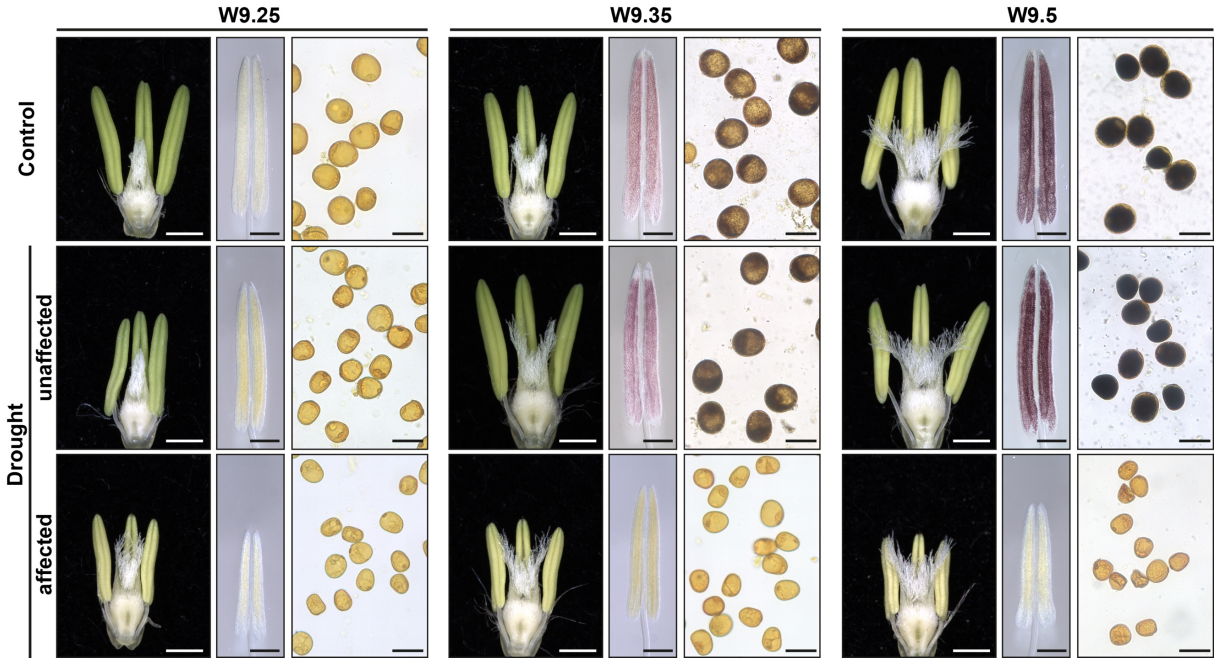

Figure 4. Stamen morphology and pollen starch filling during late maturation stages. Each panel displays reproductive organs (left, bars: 1 cm) and potassium iodide staining in whole anthers (middle, bars: 500 µm) or in pollen grains (right, bars: 50 µm). Iodide reveals starch deposition with a purple or dark blue color.

Second, we evaluated the products of pollen mitosis with DAPI staining of pollen nuclei. This revealed that both control and drought-affected pollen contain a vegetative nucleus and two sperm cells at stage W9.5 (Figure 5A), indicating that pollen mitosis occurred under drought. Third, we quantified pollen viability with a double staining of fluorescein diacetate (FDA) and propidium iodide (PI), which distinguish alive and dead cells, respectively (Figure 5B). We found that, in average, 86% of control and 78% of drought-affected pollen are viable, with only a slight difference between the treatments (P = 0.053, Figure 5C). Together, the results support that the majority of pollen grains survive the stress and are able to complete two rounds of mitosis. However, drought impairs pollen starch accumulation in 72% of all spikelets and we conclude that this is a major cause of reduced male fertility and grain set under this stress.

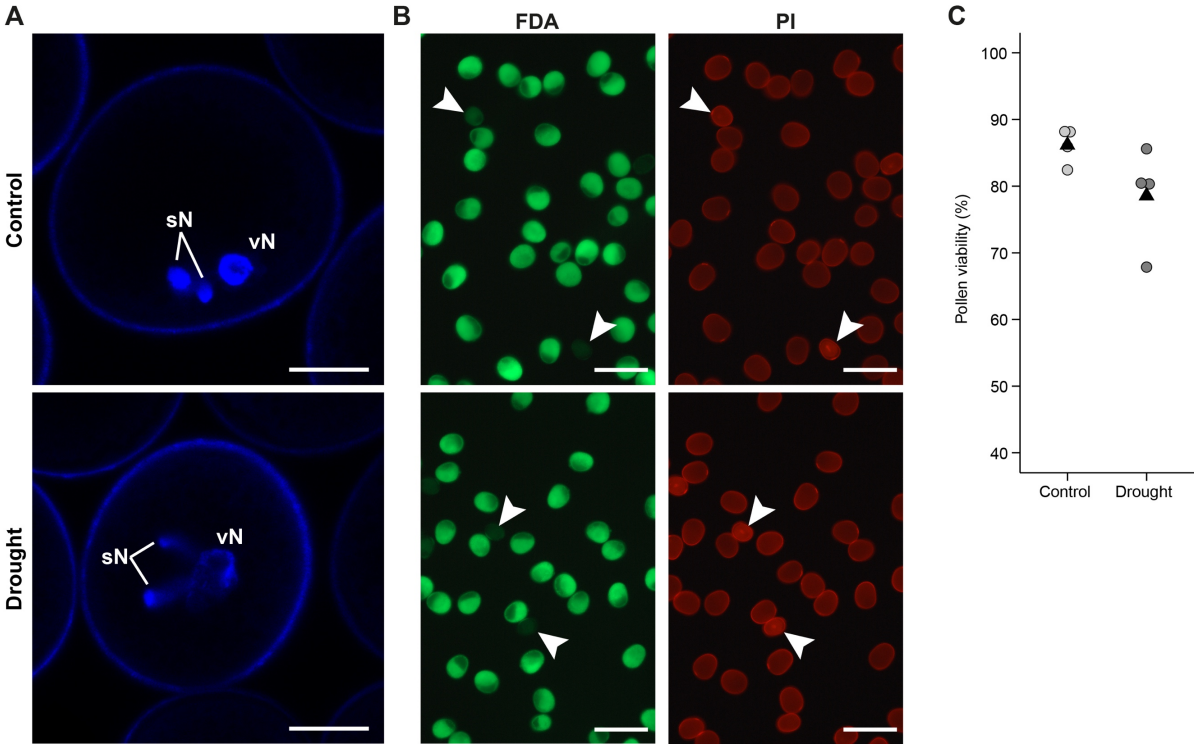

Figure 5. Characterization of pollen at stage W9.5. A) DAPI staining of pollen nuclei. vN, vegetative nucleus. sN, sperm cell nuclei. Bars, 10 µm. **B**) Pollen viability in control or drought-affected stamens (confirmed failure of starch accumulation) assayed simultaneously with fluorescein diacetate (FDA) and propidium iodide (PI) dyes. FDA fluoresces (green) in viable cells. Arrowheads indicate pollen with only background fluorescent signal, and thus considered non-viable or dead. Instead, PI accumulates inside dead cells and increases the intensity of fluorescence (red, arrowheads). Note that all pollen grains have a relatively high red signal, a combination of both autofluorescence and emission from PI accumulated on the surface of viable cells (images obtained with a normal epifluorescence microscope). Bars, 200 µm. **C**) Quantification of pollen viability determined by FDA-PI staining. Each data point is the ratio of viable pollen counted from three different florets in one inflorescence. Significance of difference between control and drought was determined with a one-tailed t-test. n = 4 inflorescences (598 and 464 total pollen grains scored for control and drought, respectively).

2.3.4 Short-term drought affects auxin signaling and energy metabolism in maturing stamens

To study the consequences of drought in gene expression, we analyzed the transcriptome of Scarlett stamens at stages W8.5 and W8.75, collected on days two and three of the treatment, respectively. Principal component analysis of all gene expression data revealed that the differences between the transcriptomes of W8.75 stamens under drought and all other samples explained 51% of the total variance (Figure 6A). The second component separated control stamens at W8.75 from the other samples and explained 27% of the variance, probably reflecting the developmental differences between the two stages analyzed. Sample distance analysis confirmed this overall separation of the transcriptomes (Figure 6B). We identified 5,598 differentially expressed genes [DEGs, |fold change (FC)| ≥ 1.5; FDR-adjusted P ≤ 0.05] between control and drought samples and their number increases from 1,008 at stage W8.5 to 5,183 at W8.75. Altogether, the data indicates that, by the third and final day of drought, when the relative water content in vegetative tissues reaches a minimum, the transcriptome of maturing stamens undergoes a major reprogramming.

Furthermore, the principal components, sample distances and hierarchical clustering of DEGs (Figure 6A – C) show that one replicate at each stage of drought-treated stamens are outliers, with a transcriptional profile lying between the control and the rest of the drought samples. This suggests that such replicates did not receive the full extent of the drought treatment or were less affected by it.

DEGs form seven clusters (Figure 6C, D), four (1, 2, 5 and 7) of which contain mostly drought-downregulated genes (65% of all DEGs), while the remaining clusters harbor drought-upregulated genes (Figure 6C, D). To investigate the putative role of DEGs, we conducted a gene ontology analysis on each cluster. Upregulated clusters are enriched for genes related to water and osmotic stress responses, proline synthesis, trehalose metabolism, and signaling through the stress hormones jasmonate (JA), ethylene and ABA (Table 2). These upregulated pathways may represent stamens' attempts at resisting the drought stress.

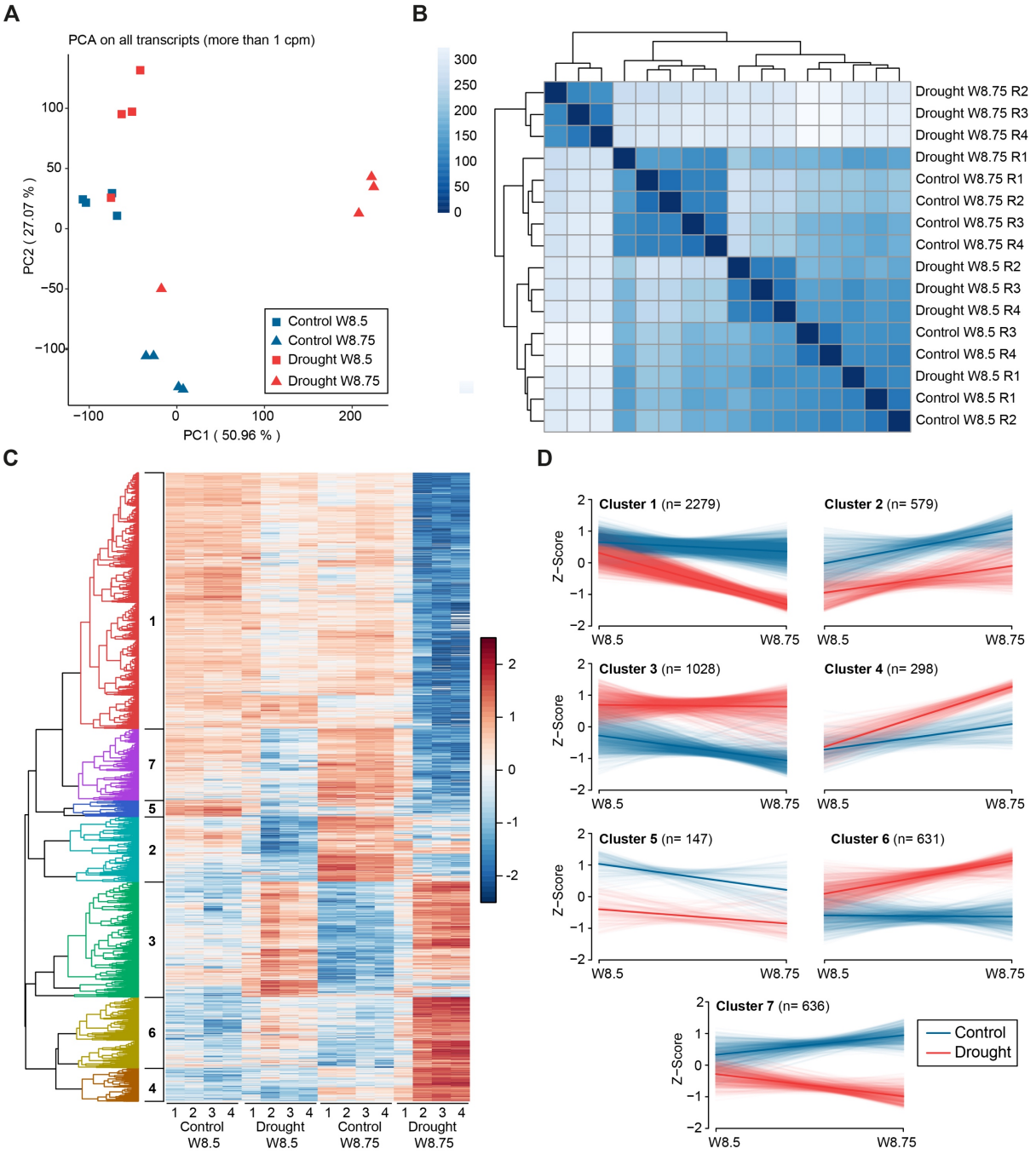

Figure 6. Transcriptomic analysis of Scarlett stamens under drought. A) Principal component analysis of normalized expression levels (counts per million, cpm) of all expressed genes. **B**) Heatmap of Euclidean distances between samples calculated from normalized cpm values of all expressed genes. **C**) Hierarchical clustering of DEGs. Each column is a biological replicate (n = 4 per treatment and stage). Scale represents mean-centered cpm values. **D**) Expression profiles of all DEGs within each cluster. Z-scores are mean-centered and scaled transcript levels in cpm. Light-colored thin lines connect Z-scores at each stage of individual transcripts. Dark-colored thick lines connect the mean Z-Scores across all transcripts at each stage.

Table 2. Representative TopGO categories of upregulated genes under drought.

GO ID	Term	weight01Fisher	Cluster
GO:1901001	Negative regulation of response to salt stress	0.00248	3
GO:1902584	Positive regulation of response to water deprivation	0.00256	3
GO:0070413	Trehalose metabolism in response to stress	0.00643	3
GO:0005992	Trehalose biosynthetic process	0.02704	3
GO:0055129	L-proline biosynthetic process	0.00013	6
GO:2000022	Regulation of jasmonic acid mediated signaling pathway	0.01501	3
GO:0009871	Jasmonic acid and ethylene-dependent systemic resistance	0.0027	3
GO:0009723	Response to ethylene	0.01039	6
GO:0009738	Abscisic acid-activated signaling pathway	0.00412	6
GO:0009737	Response to abscisic acid	0.00443	6
GO:0031098	Stress-activated protein kinase signaling cascade	0.02065 0.0091 0.00293	3 4 6

Clusters 1 and 7 contain the genes most strongly downregulated by drought at stage W8.75. These two clusters differ only because cluster 7 genes seem expressed at lower levels already at stage W8.5, while downregulation of cluster 1 genes is obvious only at W8.75. Both clusters include, among others, genes associated to auxin signaling and carbohydrate metabolism (Table 3). These categories are in agreement with a recent report that barley pollen produces auxin to boost the expression of energy-generation pathways, which in turn sustain the production of pollen starch (Amanda et al., 2022). In that work, the authors curated all barley genes associated to auxin signaling, sugar transport and heterotrophic ATP production, and found specific subsets that are likely induced by auxin and expressed at high levels during the starch filling stages W9.25 and W9.35.

Table 3. Representative TopGO categories of downregulated genes under drought.

GO ID	Term	weight01Fisher	Cluster
GO:0005975	Carbohydrate metabolic process	6.20E-07 0.00208	1 7
GO:0006006	Glucose metabolic process	0.00362 1.40E-11	1 7
GO:0030388	Fructose 1,6-bisphosphate metabolic process	0.00675	1
GO:0009734	Auxin-activated signaling pathway	0.01218 0.00782	1 7

Therefore, we followed the expression kinetics of all genes from these categories under drought in the W8.5 and W8.75 stamen transcriptomes, and in additional transcriptomes at W9.25 and W9.35, which we collected on days 2 and 3 after the end of the stress, and focusing exclusively on stamens with drought-induced altered morphology. At these later stages, drought affects the expression of 12,188 genes, which represent 62% of the entire transcriptome (19,584 detected transcripts) and a two-fold increase in the number of DEGs from stage W8.75. Overall, we detected a significant enrichment of genes related to auxin signaling, sugar transport, heterotrophic ATP production and starch metabolism (Table 4). Clustering the fold-change data for all these genes unveiled three expression patterns (Figure 7A). First, drought causes a strong downregulation of gene subsets in all categories at stages W9.25 and/or W9.35. Several genes in these subsets already show reduced expression at W8.75, particularly in the auxin response, sucrose degradation and glycolysis categories. Second, a few subsets contain genes downregulated only at W8.75 (auxin response, ARF and glycolysis). Finally, drought also upregulates the expression of gene subsets in almost every category.

Table 4. Enrichment of drought-induced differentially expressed genes (DEGs) related to auxin response, sugar transport, ATP production and starch metabolism. Numbers of genes are pooled across all stages W8.5 – W9.35. Significance of enrichment of each category was determined using Fisher's exact test ($P < 0.05$).

Category	Annotated genes	Expressed genes	DEGs	*P* value of Fisher's exact test
Auxin response	150	84	68	0.006995
Sugar transport	96	60	49	0.01549
Energy production and starch metabolism	263	239	198	2.469E-07

Barley pollen synthesizes bioactive auxin through the flavin monooxygenase HvYUC4. Moreover, the expression of the *HvYUC4* gene is controlled both developmentally and through an auxin-mediated positive feedback loop (Amanda et al., 2022). Given the lower expression of auxin signaling genes under drought, we used qRT-PCR to test if drought also reduces the expression of *HvYUC4*. We found 10- to 100-fold downregulation of *HvUC4* transcripts under drought at the three stamen maturation stages tested (Figure 7B). A similar effect was also confirmed for two energy production genes (*HvHXK5*, glycolysis; *HvCyt-C*, electron transport chain) and the starch synthesis gene *HvAGP-L1* (Figure 7B), previously shown to depend on auxin accumulation (Amanda et al., 2022). In sum, our analyses support that drought may impair pollen starch accumulation by blocking normal expression of genes required for auxin synthesis and signaling, sugar transport and utilization, heterotrophic energy production, and starch synthesis.

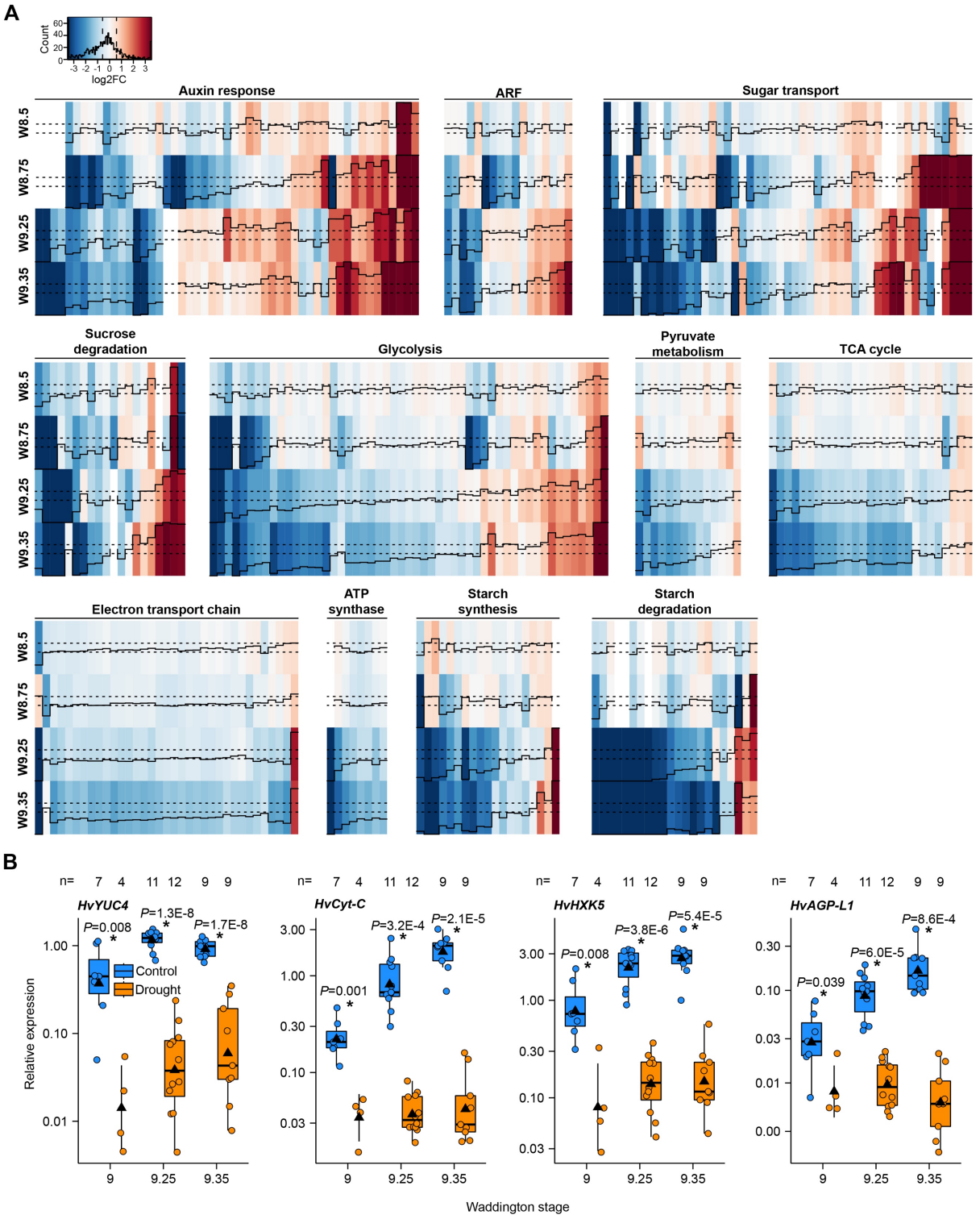

Figure 7. Drought stress during stamen maturation affects the expression of genes related to auxin signaling, sugar transport and energy metabolism. **A**) Heatmaps of log2 fold change values (FC, black solid line) of genes from different pathways that are differentially expressed under drought at least at one Waddington stage. Dashed black lines indicate log2 FC values of +/- 1.5, representing the threshold of significance for up- and downregulation. Blank cells without a trace line indicate no expression of a gene at a particular stage **B**) qRT-PCR of representative DEGs. Box plot features and statistics as in Figure 2E, except for drought stage W9, which shows the mean, SD and the individual data points of only four samples. Total number of biological replicates per sample is a pool from two independent experiments.

To test this interpretation, we evaluated the dynamics of sugars, pyruvate and TCA cycle organic acids in maturing stamens and assessed whether drought affects the levels of those metabolites at the starch-filling stage W9.35. Under control conditions, the contents of sucrose, glucose, fructose and trehalose decline after stage W9.25 (Figure 8A). This correlates with an increase in succinate, the entry point from the TCA cycle into the mitochondrial electron transport chain, at W9.35 and W9.5. On the other hand, pyruvate, citrate and malate tend to decline from stages W9-W9.25, similar to the sugars, while oxoglutarate remains stable (Figure 8A). However, citrate levels increase sharply at final stage W9. This kinetics supports that starch accumulation in pollen grains correlates with increased sugar utilization and channeling of TCA cycle intermediates into succinate to support energy production.

In drought-affected stamens, all sugars are significantly lower at stage W9.35 compared to control stamens (Figure 8A). Accordingly, the increase of succinate levels after stage W9.25 cannot be sustained, although pyruvate and oxoglutarate remain unchanged (Figure 8A). Overall, this suggests that drought leads to the disruption of photosynthate acquisition by the stamen sink-tissue, which in turn reduces the flow of succinate into the electron transport chain for ATP generation. However, drought-affected W9.35 stamens over accumulate citrate to relative levels similar to W9.5 control stamens (Figure 8A).

We confirmed that under control conditions starch levels of Scarlett stamens at stages W9 and W9.25 are low (Figure 8B). However, they increase exponentially at W9.35 and W9.5 (Figure 8B). As expected, this increase fails to occur in drought-stressed stamens.

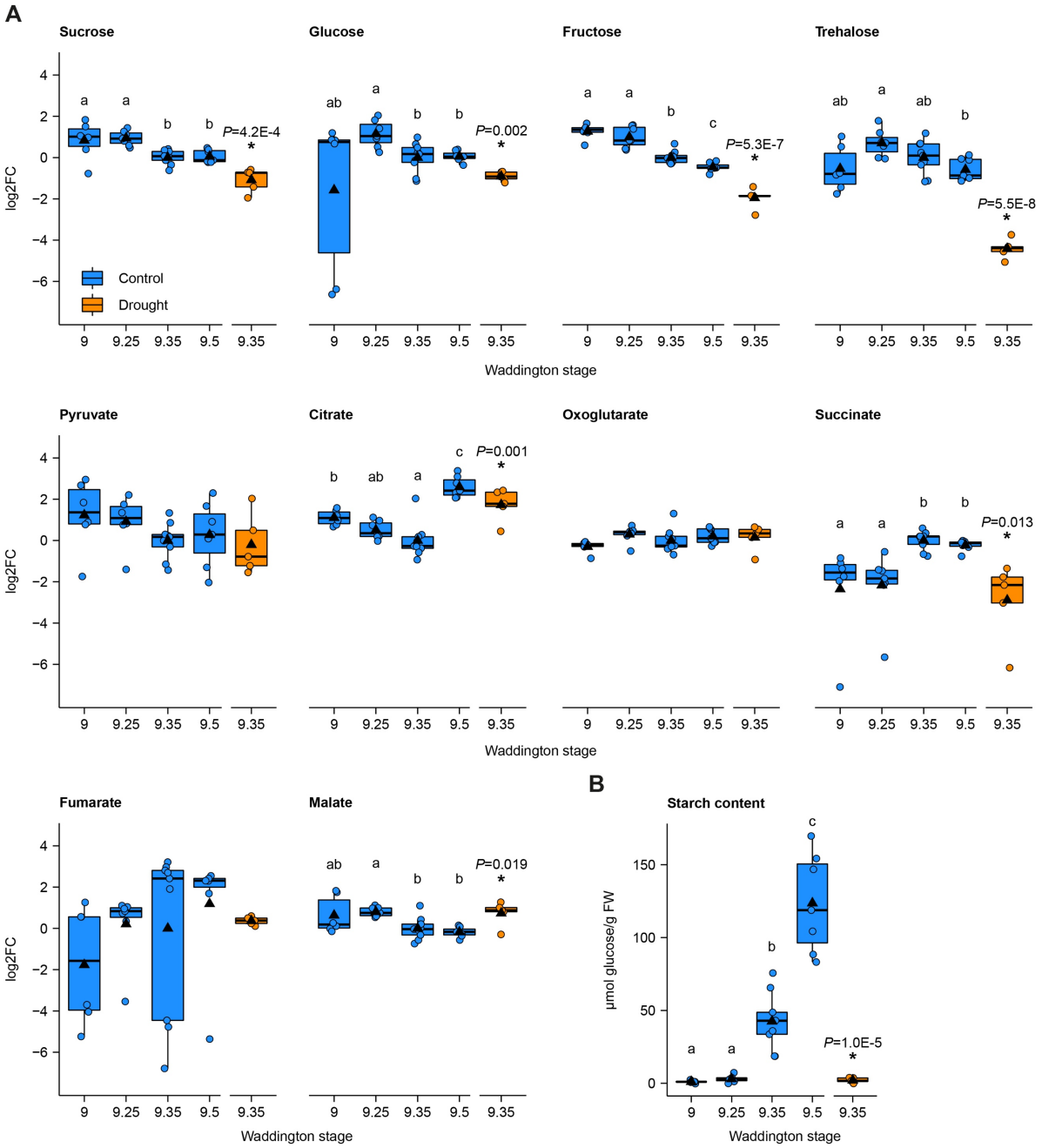

Figure 8. Metabolite profiling of stamens during maturation. A) Log2 relative levels of disaccharides, hexoses, pyruvate and TCA cycle organic acids calculated from the ratio of normalized values of each replicate to the mean of control W9.35 values. **B**) Starch content. Box plot features as in Figure 2E. Letters indicate significant differences between control stages determined with a Conover-Iman test following a Kruskal-Wallis ANOVA ($P < 0.05$). Asterisks indicate significant differences between control and drought at stage W9.35, determined with a one-tailed t-test. n= 6 (control W9); 7 (control W9.25, W9.5); 9 (control W9.35); and 5 (drought W9.35), except for pyruvate control W9.25 (n=6), where one outlier with the value 4.62 was excluded from the analysis.

2.3.5 Pre-screening a collection of wild barley introgression lines in Scarlett for short-term drought responses

In the next part of this study, we aimed to explore a subset of the barley introgression line population S42IL to identify genotypes that show tolerance to drought stress at stages of stamen maturation. The S42IL collection was created by a cross between cultivar Scarlett and the wild barley accession ISR42-8 (*Hordeum vulgare* ssp. *spontaneum*), followed by subsequent rounds of marker-assisted selection and backcrossing with Scarlett as recurrent parent (von Korff et al., 2004; Schmalenbach et al., 2008). Each introgression line comprises one or multiple marker-defined chromosomal regions of ISR42-8, collectively covering about 86.6% of the wild donor genome (Schmalenbach et al., 2008). We grew 53 of the lines (S42IL-101 – S42IL-153) under our greenhouse conditions to determine flowering time and growth uniformity. We found that S42IL-107, 108, 109 and 110 flowered earlier than the other lines, as previously reported (Schmalenbach et al., 2009; Honsdorf et al., 2017). Moreover, S42IL-107 and 108 are smaller and tiller less. The rest of the population showed a similar phenology as Scarlett, which allowed the prediction of stamen developmental stages based on our previously established developmental scale (Figure 1B). We conducted three drought-stress experiments with a low number of samples in a subset of 16 introgression lines. These include, among others, S42IL-121 and 143, since both have exhibited enhanced tolerance to drought stress (Honsdorf et al., 2017; Muzammil et al., 2018), and S42IL-118, 119, 120 and 123, which share overlapping genomic regions with S42IL-121 (Honsdorf et al., 2017).

Spikelet fertility was significantly reduced in Scarlett and seven introgression lines under drought conditions (Figure 9A). Moreover, although the data was quite variable for the rest of the lines, some appeared to show normal fertility under stress. We conducted further experiments with better replication and a more accurate estimate of developmental stage at the beginning of the experiment (W8 – W8.25), for the two most promising lines, S42IL-120 and 121, along with overlapping lines S42IL-119 and 123. However, we were not able to recapitulate the results of the first screening and S42IL-120 displayed opposite results in separate trials (Figure 9B). Thus, additional intensive screening of the complete S42IL collection is required to identify reliable drought-tolerant genotypes.

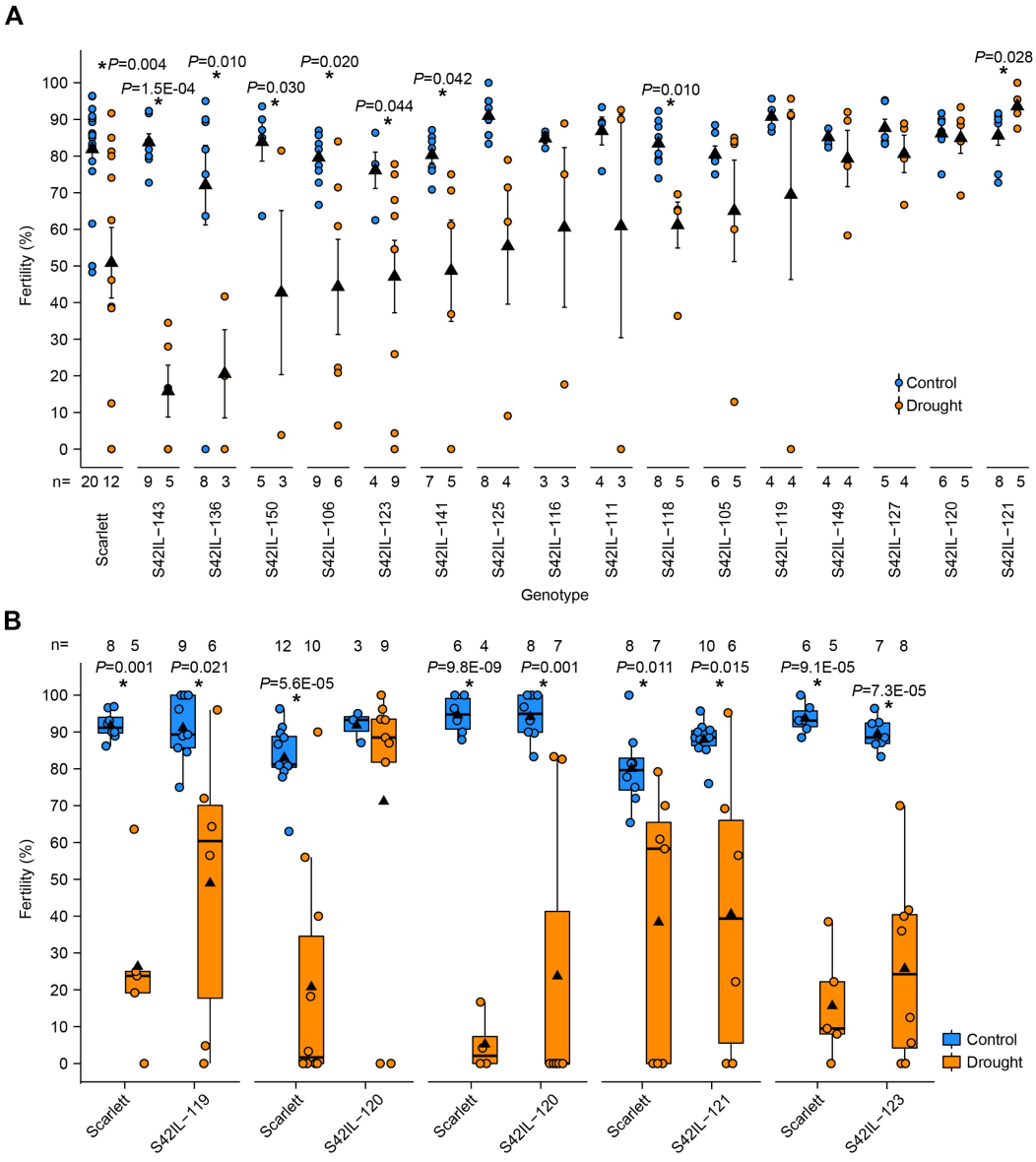

Figure 9. Screening of 16 introgression lines of the S42IL collection. A) Fertility of hydrated spikelets when the treatments start at Waddington stages W8 – W8.75. Filled circles, individual data points; vertical black lines, ±SD; triangles, means. Scarlett data is pooled from three independent experiments, while each S42 introgression line was tested in one experiment. Numbers below the plot correspond to sample size (n, number of independent plants) for each group. Asterisks indicate significant differences between control and drought in each line, determined with one-tailed t-tests. **B**) Fertility of hydrated spikelets of selected S42ILs when the treatments start at stages W8 – W8.25. Lines were tested in individual experiments with Scarlett as control genotype. Box plot features as in Figure 2E. Numbers above the plot correspond to sample size (n) for each group.

Furthermore, we conducted pilot screening experiments to explore drought tolerance during stamen maturation in three fast-flowering barley genotypes that harbor the wild allele of *Photoperiod-H1* (*Ppd-H1*). S42IL-107 and Golden Promise Fast have been linked to drought tolerance in vegetative tissues and young inflorescences (Honsdorf et al., 2017; Gol et al., 2021), while GB2 is a Mediterranean accession that shows tolerance to heat stress during stamen maturation (unpublished). Since the three genotypes develop very fast with a smaller

plant size and lower tiller number than Scarlett, we had to adjust our scale of vegetative features to predict stamen development (Figure 10A). Moreover, the lines require less watering than Scarlett so that a soil water content of ~9% is sufficient to maintain the relative leaf water content above 90% (Figure 10B). Yet, although drought-stress from early stages of stamen maturation resulted in unmeasurable soil water content after 3 days with S42IL-107 and GPF plants, the average leaf water content decreased only an average of 4% and 6%, respectively (Figure 10B). Under these conditions, spikelet fertility remained at control levels in S42IL-107, whereas it decreased 5% in GPF (Figure 10C). It should be noted, however, that these results indicate that a short period of water scarcity during the early stamen maturation phase in S42IL-107 or GPF does not cause the same levels of stress and spikelet sterility as in Scarlett.

We performed another experiment with 4 instead of 2 GPF plants per pot, to attempt increasing the water demand in each pot. In this case, a 3-day water deficit caused not only a fast depletion of soil water content but also a reduction in relative leaf water content to 75% (Figure 10B). Nevertheless, this is not yet close to the water deficit observed in Scarlett (57%, Figure 2A), which suggests that GPF is more resilient to water scarcity. Furthermore, even at 75% leaf water content, the fertility of GPF spikelets was not different from the control (Figure 10C). This result contrasts with the slight decrease in fertility observed under drought in the previous experiment. This could be explained because in the second experiment the fertility values of both control and drought samples were more widely spread, and half of the control samples showed a mild fertility reduction.

Next, we applied our adjusted drought treatment approach on accession GB2, which resulted in the same depletion of soil and leaf water content just described in GPF (Figure 10B). However, in this case, there was a clear reduction in spikelet fertility (on average 61% of control values, Figure 10C). In sum, under more water demanding conditions, drought stress causes a similar reduction of leaf water content in GPF and GB2 but has contrasting effects on spikelet fertility in both genotypes. This may support the hypothesis that GPF is more resilient to short-term drought and suggests the two genotypes as a potential pair of contrasting lines for further analyses. However, additional tests are needed to verify these results.

A

Genotype	Flag leaf sheath extension (cm)	Auricle-to-spike-tip-distance (cm)	Length of hidden spike (cm)
S42IL-107	not visible	-8 to -6	2 – 3
Golden Promise Fast	0 – 4.5	-8 to -3	2 – 4
GB2	not visible	-9 to -7	1.5 – 2

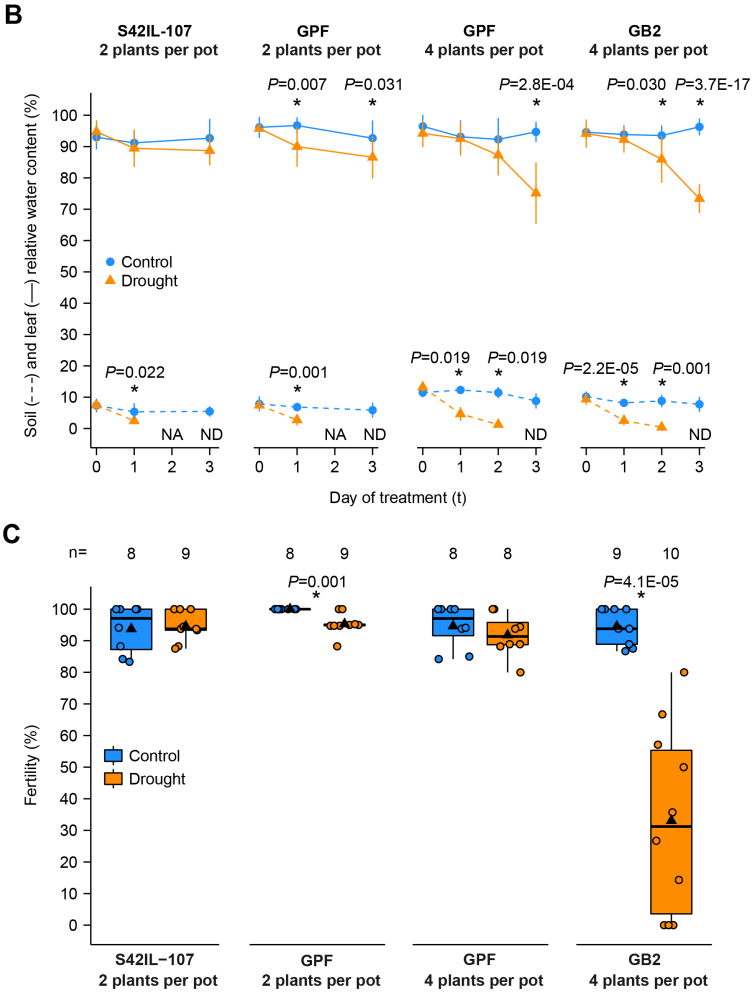

Figure 10. Screening of fast-flowering barley genotypes for short-term drought responses. A) External tiller features correlating with modified Waddington (W) stages W8 – W8.75 in three fast-flowering barley genotypes. Features as defined in Figure 1A – B. **B**) Soil water content (dashed lines) and leaf relative water content (solid lines) under control and drought stress conditions and two experimental setups (2 or 4 plants per pot). Each plot represents a single experiment (n= 4 – 9 [leaf relative water content] and 3 – 6 [soil water content]) and displays means ± SD. Asterisks indicate significant differences between control and drought at each time point (one-tailed t-test). NA, no data available; ND, not detectable. **C**) Fertility of hydrated spikelets. Treatments started at early stamen maturation stages (W8 – W8.75). Each box plot represents a single experiment. Box plot features as in Figure 2E. Asterisks indicate significant differences between control and drought at each stage, determined with one-tailed t-tests. Numbers above the plot correspond to sample size (n) for each group.

2.4 Discussion

2.4.1 Effects of drought stress on barley stamen maturation

In this work, we established a method to apply a short-term water deficiency stress during barley stamen maturation. In cultivar Scarlett, this simulated drought wave strongly reduces the leaf relative water content and visibly stunts vegetative growth (Figure 2A, B; Figure 3B), yet plants survive the stress and continue their life-cycle. Still, in some cases, the stress leads to full dehydration of individual spikelets or complete inflorescence (Figure 2C), suggesting that drought may be fatal for spikelet tissues when it exceeds a critical level. Similar abnormal morphology of whole spikelets has been documented in rice after a one-week drought treatment during stamen development (Jin et al., 2013). Our results show that initiating drought stress during the early stamen maturation phase causes a dramatic loss of spikelet fertility, while no or only slight effects are seen when the stress starts at advanced maturation stages. Wheat inflorescences show a similar stage-specific response to short-term water deficiency (Ji et al., 2010).

Based on our reciprocal crosses, defects in both male and female reproductive structures cause the reduction in spikelet fertility under drought, although male sterility is seemingly the major contributor to the loss of spikelet fertility (Figure 1F). This agrees with the accepted view that development of male organs in cereals is the reproductive process most vulnerable to drought stress (Dolferus et al., 2011; Yu et al., 2019). Moreover, several studies have documented that drought does not affect ovule fertility (Bingham, 1966; Saini and Aspinall, 1981; Ji et al., 2010). Nevertheless, recent pollination experiments with drought-stressed pistils have shown significant reduction in grain set of four wheat genotypes (Onyemaobi et al., 2017). Future work should examine drought-treated pistils throughout maturation to identify potential morphological abnormalities. Furthermore, assays investigating stigma receptivity could test if drought disturbs the interaction between pollen and pistils.

Our work also shows that drought stress from the early stages of barley stamen maturation does not impair pollen viability or prevents the completion of the two rounds of pollen mitosis. However, it results in lack of pollen starch (Figure 4, Figure 8B), which is also in line with studies in other cereals (Ji et al., 2010; Jin et al., 2013). Moreover, anthers that harbor starch-less pollen are pale and seem smaller than normal (Figure 4), indicating that drought not only affects male gametophyte development but also anther sporophytic tissues. In the past, similar abnormal anther morphology upon pre-heading drought stress was described in rice (Liu and Bennett, 2011).

Staining of pollen originating from stamens with a drought-affected morphology showed that the male gametophytes were able complete two round of mitotic divisions and were mostly viable (Figure 5). Thus, we assume that developing the majority of microspores is able to

survive our drought-stress treatment but is unable to drive processes required for starch synthesis at terminal maturation stages. We conclude that the inability to accumulate starch under drought is the most important cause of male sterility in barley cultivar Scarlett. Remarkably, we did find that a proportion of drought-treated stamens maintain a normal morphology and harbor pollen that accumulate starch (Figure 4). We hypothesize that this is the pollen that contributes to the partial and variable grain set that we observed under drought. This should be tested with further pollination experiments with drought-treated stamens bearing either starch-full or starch-less pollen. It is possible that the variable fertility between inflorescences of independent plants reflects differences in water deficiency between pots and plants. However, the partial fertility within inflorescences indicates that some spikelets may withstand the stress better than others. Small differences in developmental timing between spikelets of the same inflorescence could explain their sink capacity, that is, spikelets that are more developmentally advanced could be stronger sinks than their slightly younger counterparts and benefit first from the limited carbohydrate resources under water deficiency. To attempt identifying molecular mechanisms or processes of stamen maturation that favor pollen starch accumulation in some spikelets, it would be interesting to compare transcriptomes of drought-affected versus drought-unaffected stamens. Among the early-stage transcriptomes that we analyzed in this work, we found at each early stage one drought-treated replicate with transcriptional profiles intermediate between the control and the rest of the drought samples. We hypothesize that such replicates contained stamens less affected by the water stress and that would go on to have normal morphology and starch accumulation at later stages (recall that at early stages W8.5 and W8.75 morphology alone cannot distinguish affected from non-affected stamens).

2.4.2 Impact of drought on stamen carbon metabolism and energy generation

Carbon in the form of sugars is essential to fuel energy generation and starch synthesis in heterotrophic pollen (Ruan et al., 2010; Liu et al., 2021). Accordingly, we found that, as Scarlett stamen maturation proceeds, sugars decrease while pyruvate levels remain constant, indicating a continuous flux of glycolytic intermediates into pyruvate production. On the other hand, sugars are reduced in drought-affected stamens at the starch-filling stage W9.35. Similar results have been reported for wheat anthers under drought at late maturation stages, and for rice anthers under combined drought and heat stress [but not heat alone] (Dorion et al., 1996; Li et al., 2015). Together, our data indicates that short-term drought stress leads to impaired photoassimilate supply to barley stamens, which manifests in a mild anther carbon starvation. This is likely a consequence of hampered photosynthesis in leaves of drought-stressed plants, which results in decreased photoassimilate production and altered transport of sugars to the sink tissues (Farooq et al., 2009; Basu et al., 2016; Du et al., 2020).

Our transcriptome analysis revealed that the expression of genes encoding sugar transporters in stamens is extensively altered under drought stress (Figure 7A). In rice, the R2R3 MYB transcription factor encoding gene *CSA* regulates sugar partitioning into anthers and is crucial for male fertility (Zhang et al., 2010). Our data shows that the barley ortholog of *CSA* is downregulated during drought at stage W8.75 but upregulated at post-stress, starch-filling stages W9.25 and W9.35. A similar increased expression of *CSA* was observed in response to low sucrose content in anthers under combined heat and drought stress (Li et al., 2015). On the other hand, the barley ortholog of the rice monosaccharide transporter *OsMST8*, a direct target of *CSA* (Zhang et al., 2010), shows an opposite trend (upregulated during drought but downregulated at stage W9.25), which does not agree with the observed expression of *HvCSA*. Similarly, a homolog of the sucrose transporter gene *SUT1*, which is critical for pollen development in cucumber and rice (Hirose et al., 2010; Sun et al., 2019), is also repressed at later stages. Overall, the data suggests that drought-induced downregulation of critical gene sugar transporter genes emerges after the stress. We hypothesize that this may be one the main causes of lower sucrose import and hexose availability in drought-stressed stamens.

Invertases perform the hydrolytic cleavage of sucrose into hexoses that subsequently undergo hexokinase-mediated phosphorylation, the initial step of hexose utilization pathways including glycolysis or starch synthesis (Roitsch and González, 2004; Claeyssen and Rivoal, 2007; Ruan et al., 2010). Genes participating in sucrose degradation were mostly downregulated in drought-treated stamens (Figure 7A). Among them, one cell wall invertase encoding gene, which is highly expressed at all investigated stages under control conditions, was consistently repressed in drought-treated stamens after stage W8.5. Similarly, its rice ortholog *OsCIN2*, was irreversibly downregulated by meiotic drought stress in previous studies in rice (Ji et al., 2005; Jin et al., 2013). Our analysis also revealed that drought negatively regulates glycolysis, pyruvate metabolism as well as starch synthesis at late maturation stages post drought stress. Accordingly, the expression of the hexokinase gene *HvHXK5* and the *ADP-glucose pyrophosphorylase large subunit* gene *HvAGP-L1*, a key player in starch synthesis, was not altered or even upregulated during the treatment, respectively, but significantly downregulated in drought-affected stamens at stages W9.25 and W9.35. Overall, these results suggest that drought disrupts sugar utilization and mobilization processes that are relevant for male gametophyte development, which is in agreement with findings in previous studies (Dorion et al., 1996; Jin et al., 2013; Lamin-Samu et al., 2021). Strikingly, our metabolite profiling showed that pyruvate levels remain unaffected in drought-treated stamens, which might be a result of decreased conversion of pyruvate into downstream metabolites or increased generation of pyruvate through alternative sources like alanine (O'Leary, 2021).

Reaching the terminal stages of maturation, barley pollen increases mitochondrial respiration to produce high amounts of ATP (Amanda et al., 2022), one of the major limiting factors of starch synthesis (Geigenberger et al., 2004). The mitochondrial TCA cycle is a central component of energy production as it channels pyruvate, the product of glycolysis, into an interconversion sequence of organic acids that provides reducing equivalents for the ATP generating electron transport chain (Fernie et al., 2004; Zhang and Fernie, 2018). Previously, it has been speculated that failure to use sugars under drought may result in lack of energy for developing microspores (Nguyen et al., 2010). In our work, drought negatively affects the expression of the majority of genes related to the TCA cycle, electron transport chain and ATP synthesis (Figure 7). Moreover, we found reduced levels of the TCA organic acid succinate in drought-affected stamens (Figure 8A). Succinate is the entry point to the electron transport chain (Fernie et al., 2004; Schertl and Braun, 2014) and reaches highest levels in normal barley stamens at starch-filling stages W9.25 and W9.35. Thus, it likely plays an important role in energy production at terminal stages of stamen and pollen maturation. Accordingly, drought-induced reduction in succinate levels in stamens could disrupt the mitochondrial electron transport chain, leading to insufficient ATP generation and hampered pollen starch synthesis. On the other hand, drought-affected stamens over accumulate the TCA intermediates citrate and malate (Figure 8A). Both organic acids are essential players in plant metabolism are key compounds of numerous metabolic pathways such as gluconeogenesis or synthesis of amino acids, fatty acids, hormones or flavonoids (Fatland et al., 2005; Zhang and Fernie, 2018; Lee et al., 2021; Tahjib-Ul-Arif et al., 2021). Malate and citrate have been demonstrated to increase in leaf and fruit tissues under water-deficit in numerous plant species and are associated with alleviation of drought stress-induced damage (Timpa et al., 1986; Guicherd et al., 1997; Sağlam et al., 2010; Levi et al., 2011; Obata et al., 2015; Nahar and Ullah, 2018). While studies in ash imply a role of malate in osmotic adjustment under drought (Guicherd et al., 1997), citrate is considered to participate in antioxidative defense and osmoprotection in response to a variety of abiotic stresses including drought (Tahjib-Ul-Arif et al., 2021). For instance, exogenous application of citrate increased leaf antioxidative enzyme activity, content of the compatible osmolyte proline and improved yield traits of drought-stressed cotton plants (Gebaly et al., 2013). Osmotic adjustment through accumulation of compatible solutes like sugars, amino acids and organic acids, as well as the antioxidant defense are two common strategies of plant drought tolerance (Farooq et al., 2009; Singh et al., 2019). Interestingly, mature stamens contain increased citrate levels at stage W9.5, when pollen seemingly reaches a mostly dehydrated state that precedes anther opening (Amanda et al., 2022). Therefore, it is possible that malate and citrate are general protective molecules to face low water states in barley pollen and/or anthers, perhaps at the expense of their function in the TCA cycle.

In summary, our transcriptome and metabolite data support a model where maturing barley stamens are active sugar consumers to respond to the high demand of energy and building blocks for starch synthesis. Accordingly, insufficient sugar supply after short-term drought stress results in altered flux of succinate into the electron transport chain, reduced energy generation and, ultimately, failure of pollen starch accumulation. The transcriptomic data indicates that drought stress alters processes related to energy and starch synthesis from stage W8.75. Moreover, starch accumulation is obvious from stage W9.25. Still, it will be important to carry on additional metabolite analyses in drought-stressed stamens at all development stages considered here (W8.5 to W9.25), in addition to W9.35, to test whether drought stress immediately alters the stamen metabolome during the treatment (stages W8.5, W8.75) or only at later stages of development.

2.4.3 Effects of drought on expression of genes related to ABA

Plant hormones are essential regulators of reproductive development under adverse conditions (Yu et al., 2019). ABA is one of the most conspicuous hormones in plant abiotic stress responses and it accumulates in reproductive tissues under drought stress, which has been associated with reduced male fertility (Morgan, 1980; Ji et al., 2011; Liu and Bennett, 2011; Dong et al., 2017). Not unexpectedly, we found an enrichment of upregulated genes related to ABA in drought-stressed stamens, including two *9-cis-epoxy-carotenoid dioxygenases* (*NCED*s) that are involved ABA synthesis (Huang et al., 2018). One of them, *HvNCED1*, was upregulated 30-fold in drought-treated stamens at stage W8.75 and remained highly upregulated at later stages. Importantly, two genes encoding *cytochrome P450 family ABA 8'-hydroxylases*, which are essential for ABA catabolism by converting ABA to phaseic acid (Kushiro et al., 2004), were downregulated at different stages of the drought treatment and during pollen starch-filling. Together, our results are essentially similar to previous findings in drought-susceptible wheat cultivars (Ji et al., 2011) and indicate that drought stress increases ABA content in barley stamens. In past studies, it was demonstrated that ABA regulates male reproductive development by repressing crucial players in carbohydrate metabolism such as invertases (Oliver et al., 2007; Ji et al., 2011). Thus, ABA in drought-affected stamens may contribute to the downregulation of sugar utilization genes that are essential for the normal development and function of heterotrophic barley pollen.

2.4.4 Effects of drought on auxin synthesis, response and signaling

Auxin and its signaling pathway are indispensable for floral organ formation (Nemhauser et al., 2000; Cheng et al., 2006) and regulates several aspects of male reproductive development such as pollen development, anther dehiscence and filament elongation (Nagpal et al., 2005; Cheng et al., 2006; Cecchetti et al., 2008). Past research has already investigated the role of auxin in reproductive development under abiotic stress including heat (Sakata et al., 2010) or

drought (Lamin-Samu et al., 2021). In rice, decreased *YUC*-mediated IAA synthesis, lower IAA content and impaired auxin signaling in panicles has been considered a major cause of spikelet sterility in response to drought at the anthesis stage (Sharma et al., 2018). In barley, the accumulation of IAA in stamen during the terminal phase of maturation, necessary for pollen starch synthesis, is determined by the flavin monooxygenase encoding gene *HvYUC4*, also called *MSG38*. Non-functionality of *MSG38* results in significantly reduced IAA levels in barley stamens, lack of pollen starch and male sterility (Amanda et al., 2022). Our RNA-Seq and qRT-PCR data show that *MSG38* expression is significantly downregulated after rewatering, at stages W9.25 and W9.35, which is precisely the peak phase of *MSG38* expression in normal barley stamens (Amanda et al., 2022)., Thus, we propose that drought-induced downregulation of *MSG38* may impede auxin synthesis and accumulation in Scarlett stamens. Furthermore, half of auxin response genes that were consistently downregulated in *msg38* stamens (see chapter II) also show lower expression in drought-stressed stamens. Members of the ARF transcription factor family bind to auxin responsive elements (AuxREs) present in the promoters of auxin-induced genes to regulate their expression (Liscum and Reed, 2002; Li et al., 2016). In our study, three drought-repressed ARFs are regulated by *MSG38* (discussed in chapter II) at similar maturation stages, indicating that the transcriptional effects of drought not only affect auxin synthesis genes but also auxin signaling genes. Importantly, 115 out of 198 drought-responsive genes related to energy metabolism were also found to be dependent on auxin (Amanda et al., 2022; chapter II). This supports that drought partially mimics the physiological and molecular effects of impaired auxin synthesis in the *msg38* mutant. Thus, impaired MSG38-mediated auxin synthesis and signaling are also major factors underlying hampered energy metabolism and pollen starch synthesis under drought. However, in clear contrast to drought stress, *msg38* mutant stamens over accumulate sugars, which supported the interpretation that auxin signaling is not required for stamen sugar acquisition but rather to promote sugar utilization (Amanda et al., 2022). Moreover, these authors proposed that sugar accumulation and signaling may trigger auxin synthesis in barley pollen. Our work with drought provides circumstantial support to that model: lower sugar acquisition on drought-treated stamens may directly prevent *MSG38* expression and, therefore, auxin production and signaling. In this scenario, failed starch accumulation in drought-stressed pollen is compounded by a reduction in both photosynthate acquisition and the hormone that boosts carbon utilization.

Furthermore, we found that barley orthologs of Arabidopsis' *AtARF6* and *AtARF8* were both downregulated in drought-stressed stamens at stage W8.75. In Arabidopsis, ARF6 and ARF8 regulate the maturation of the gynoecium and stamen. Double-loss of function mutant *arf6arf8* exhibits arrested floral organ development (Nagpal et al., 2005). Thus, drought may also impair other MSG38-independent pathways of auxin signaling that are needed for successful stamen

and pistil maturation. It is also possible that drought impacts hormone pathways that interact with auxin-signaling genes, hence alter their expression. For instance, direct crosstalk between ABA and auxin signaling in plant tissues such as roots is well documented (Harris, 2015; Emenecker and Strader, 2020).

2.4.5 Barley germplasms with varying drought tolerance

Exploiting exotic germplasms is key to identify genetic resources that confer tolerance against abiotic stresses such as drought (Zamir, 2001; Honsdorf et al., 2017). In wheat and rice, studies have already successfully identified tolerant germplasm by applying transient waves of drought during stages shortly before anthesis (Liu et al., 2006; Ji et al., 2010). Here, we aimed to assess drought tolerance during stamen maturation of 16 barley genotypes originating from the wild barley introgression line population S42IL, which has shown to harbor valuable genetic resource that confer drought tolerance in vegetative tissues or early reproductive development (Muzammil et al., 2018; Gol et al., 2021). However, we were unable to consistently reproduce independent drought-stress experiments with some of these lines. Remarkably, line S42IL-121 is drought-tolerant during juvenile and grain-filling stages and the tolerance was associated to an unknown quantitative trait locus on chromosome 4H (Honsdorf et al., 2014; Honsdorf et al., 2017). Thus, it might be attractive to perform further testing to determine whether these lines reliably show spikelet fertility when subjected to drought during stamen maturation. To ensure precise application of drought waves at different stages of stamen development as in Scarlett, it will be important to establish individual scales for floral development in these lines.

We also identified two early flowering lines that appear to show contrasting responses to short-term drought, namely Golden Promise Fast (tolerant) and GB2 (susceptible). These can be used to identify mechanisms that maintain spikelet fertility under drought stress. Further investigations will require reciprocal crosses to test whether the susceptibility of GB2 to drought stress lies within the female and/or male organs. Both GPF and GB2 contain the wild allele of the flowering time gene *Ppd-H1*, which was associated to drought tolerance during early inflorescence development (Gol et al., 2021). This suggests that the tolerance of GPF to drought stress during stamen maturation involves a different mechanism.

2.5 Conclusion

This work shows that pollen sterility due to failed starch accumulation is a major determinant of barley spikelet sterility after a 3-day drought treatment started at the beginning of stamen maturation. Moreover, our evidence suggests that the starch accumulation defect is associated with decreased sugar content in stamens, which suggests that drought impairs carbon supply from photosynthetic tissues to the anther sinks. Lower carbon supply is in turn associated to lower expression of sugar transport genes. Furthermore, water deficiency has additional, compounding effects on the expression of genes required for auxin synthesis and signaling, as well as genes on all metabolic pathways related to sugar utilization and heterotrophic energy production. Auxin normally boosts energy pathways in barley pollen; thus, the impairment of both processes under drought supports their connectivity and importance in pollen function and development. We also found that genes participating in ABA homeostasis are altered in response to drought stress, suggesting an accumulation of ABA in drought-affected stamens. We suggest that drought-induced disruption of auxin and ABA signaling networks is also a critical factor in preventing pollen fertility after drought.

3 Chapter II – The role of auxin in barley stamen maturation

3.1 Introduction

Male reproductive development in flowering plants takes place in the stamens and is controlled by a sequence of precisely coordinated events that ensure successful formation of the male gametophyte (Scott et al., 2004; Wilson et al., 2011; Hafidh and Honys, 2021). In cereals, the post-meiotic phase of male reproductive development, called microgametogenesis or pollen maturation, includes crucial milestones of pollen development such as construction of the pollen wall, asymmetric mitosis and starch accumulation (Christensen et al., 1972; Eady et al., 1995; Lee et al., 2020). The latter serves as energy storage for germination and growth of the pollen tube (Clement et al., 1994; Lee et al., 2020), and, therefore, is a reliable indicator of pollen fertility in cereals. Energy availability and respiration rate are determinants for starch production in heterotrophic tissues (Dickinson, 1968; Geigenberger et al., 2004). Thus, as non-photosynthetic structures, pollen grains change their metabolism at late stages of maturation to a state of high energy production to enable starch synthesis (Amanda et al., 2022). To perform this transition, the pollen relies on the sporophyte, which provides photosynthetic assimilates, mainly in the form of sucrose (Ruan et al., 2010; Liu et al., 2021). To date, various molecular players involved in anther and pollen carbon metabolism have been identified (Liu et al., 2021). However, the regulatory mechanisms that underlie the timely expression of the corresponding genes and protein factors during pollen maturation are poorly understood.

Plant hormones are key signaling molecules that integrate environmental cues to regulate growth and development (Ozga et al., 2016). There is extensive evidence that they are of great importance for male reproductive development (Ozga et al., 2016). For example, in Arabidopsis, JA activates MYB21 and MYB24, two R2R3 MYB transcription factors that are crucial for pollen maturation, anther dehiscence and filament elongation (Mandaokar et al., 2006; Song et al., 2011; Reeves et al., 2012). Gibberellin (GA) signaling regulates programmed cell death of tapetal cells as well as pollen wall deposition through the MYB transcription factor GAMYB (Aya et al., 2009). Moreover, GA promotes filament growth in Arabidopsis, presumably by increasing the expression of JA synthesis genes (Cheng et al., 2009).

The hormone auxin is also required for multiple aspects of male reproduction (Sundberg and Østergaard, 2009). IAA, the most abundant bioactive auxin in plants, is predominantly synthesized via the tryptophan-dependent pathway (Kasahara, 2016). First, tryptophan is converted to indole-3-pyruvic acid (IPA), which is subsequently transformed into IAA via flavin monooxygenases of the YUCCA (YUC) family (Mashiguchi et al., 2011). Auxin synthesis through Arabidopsis' *YUC2 and YUC6* genes is necessary for pollen mitosis (Yao et al., 2018). Additionally, auxin regulates the timing of anther dehiscence and filament elongation (Cecchetti et al., 2008), and the pollen-specific auxin transporter *PIN-FORMED 8* regulates

auxin homeostasis and male gametophyte development (Ding et al., 2012). Moreover, ARFs, central players of auxin signaling, are crucial for successful male development. Arabidopsis' *ARF17* is essential for pollen viability and pollen wall patterning (Yang et al., 2013), whereas *ARF6* and *ARF8* are necessary for stamen maturation and filament growth (Nagpal et al., 2005). Maturing rice anthers contain high levels of IAA and express auxin synthesis and -signaling genes (Hirano et al., 2008). Even if there is extensive evidence of the importance of auxin in pollen and stamen development (Salinas-Grenet et al., 2018), it is not fully understood yet which molecular processes in male reproductive tissues are regulated by auxin. Therefore, studying the molecular landscape on a transcript and protein level could assist greatly in uncovering putative candidate targets of auxin signaling.

Recently, Amanda et al. (2022) reported reduced IAA levels in stamens of the barley mutant *male sterile genetic 38* (*msg38*), carrying a loss-of-function allele of the pollen-specific auxin synthesis gene *HvYUC4*. This results in lack of pollen starch accumulation and male sterility, and is associated to decreased expression of carbon metabolism genes and reduced levels of important organic assimilates required for energy production during stages of pollen starch accumulation (Amanda et al., 2022). Together, the data indicates that auxin controls the timing and buildup of pollen starch by regulating central carbon metabolism, thus ensuring completion of male gametophyte development (Amanda et al., 2022).

In this chapter, we extend the studies of the *msg38* barley mutant to provide additional insight into the implications of auxin accumulation in stamens for barley stamen and pollen development. Our aims were to (i) perform comparative transcriptome analysis of *msg38* stamens at developmental stages W8.5, W8.75 and W9 to identify early auxin-mediated processes and investigate the expression kinetics of auxin-responsive and carbon metabolism genes at stages prior to pollen starch synthesis; (ii) analyze the proteome and phosphoproteome of normal and *msg38* stamens at stages W9, W9.25 and W9.35 to examine posttranscriptional and posttranslational changes in proteins involved in auxin response, auxin signaling and carbohydrate metabolism.

3.2 Material and methods

3.2.1 Plant material

The barley cultivar Bowman and segregating populations of *msg38* were obtained from the GRIN-USDA seed bank. The spontaneous mutation was found in the cultivar Ingrid (Franckowiak and Hockett, 1988; Franckowiak and Lundqvist, 2012) and was backcrossed at least six times into the cultivar Bowman (Druka et al., 2011). In this study, we used the introgression line, designated as *msg38*.

3.2.2 Growth conditions

Barley seeds were sown in 96-well trays filled with a 1:1 mix of soil ED 73 Einheitserde® (Einheitserdewerke Werkverband e.V., Sinntal-Altengronau, Germany) to BVB Substrates (1:1 vermiculite to coconut fiber). One week later, seedlings were transplanted to round 1-liter pots, filled with the above described substrate. Plants grew in a controlled greenhouse chamber under long-day conditions (16 h light at 22°C, 8 h dark at 18°C, light intensity: 100 μEinsteins $m^{-2}s^{-1}$).

3.2.3 RNA extraction and transcriptome analysis

We analyzed the transcriptome of Bowman and *msg38* stamens at stages W8.5, W8.75 and W9. For each stage, stamens from 8 – 11 florets from one inflorescence were collected as one replicate. In total, four replicates per genotype and stage were analyzed. Sample collection, RNA extraction and transcriptome analysis were conducted as described in 2.2.9 and 2.2.12, respectively.

To investigate the expression kinetics of MSG38-dependent auxin-responsive, sugar transport and energy metabolism genes throughout an extended period of stamen maturation (Waddington stages 8.5 – 9.35), we used Salmon output *.sf files of stages W8.5 – W9 and stages W9.25, W9.35 generated by Amanda et al. (2022) in one analysis. Downstream analysis was performed in R software as described in 2.2.12. Curated lists of genes related to auxin, sugar transport, energy generation and starch metabolism were acquired from Amanda et al. (2022).

3.2.4 Preparation of total proteome, library and phospho-enriched samples

Stamen proteome and phosphoproteome analysis based on liquid chromatography-tandem mass spectrometry (LC-MS/MS), including preparation of the total proteome, libraries and phospho-enriched samples, as well as data acquisition and data analysis, was conducted in the group of Dr. Hirofumi Nakagami at the Max Planck Institute for Plant Breeding Research in Cologne.

Stamens of Bowman and *msg38* were collected at stages W9, W9.25 and W9.35. For each replicate, stamens of 9 – 14 florets of a single inflorescence were collected in a 1.5 ml tube and immediately frozen in liquid nitrogen. In total, five biological replicates per genotype per stage were collected. Samples were grinded as described in 2.2.9. Subsequently, 210 µl of protein extraction mix containing 50 µl 4x PEB (Agrisera, Vännas, Sweden), 2 µl protease inhibitor cocktail, 4 µl phosphatase inhibitor cocktail 2, 4 µl phosphatase inhibitor cocktail 3 (Sigma-Aldrich, St. Louis, USA) and 150 µl ddH_2O were added. Samples were centrifuged at 10,000 rpm for 3 min at 4 °C. The supernatant was transferred into a fresh 1.5 ml tube. The concentration of protein extracts was determined using Pierce 660 nm protein assay. An aliquot corresponding to 500 µg total protein extract from stamen was digested using a filter aided sample preparation protocol adapted from Wiśniewski et al. (2009). First, samples were reduced by adding 1/10 vol of 1 M DTT (100 mM final) and samples were incubated for 30 min at RT. Samples were then diluted with 8 M urea in 0.1 M Tris/HCl ph 8.5 (UA) to 800 µl and loaded onto filters (Vivacon 500, 30 kDa cutoff (Sartorius, Göttingen, Germany)) followed by centrifuging for 10 min at 14,000 g. Samples were then washed with UA and centrifuged for 10 min at 14000 g. Further, samples were alkylated using 100 µl 55 mm chloracetamide in UA and incubation for 20 min in the dark, followed by centrifugation for 10 min at 14,000 g. After washing 2x with UA and 2x with 100 mM Tris pH 8.5 1 mM $CaCl_2$, the filter was transferred to a new tube and samples were digested with 2.5 µg LysC (1 µg/µl Lys-C (WAKO, Richmond, USA) in 50 mM NH_4HCO_3 working solution diluted with UA to an enzyme-protein ratio 1:100) for 2 h at RT. Next, 2.5 µg trypsin (1 µg/µl in 1 mM HCl, working solution diluted with UA to an enzyme-protein ratio 1:100) was added, the samples were mixed and incubated overnight at RT. After centrifugation, 50 µl of 100 mM Tris pH 8.5 1 mM $CaCl_2$ were added and samples were centrifuged for 10 min at 14000 g. The flow through containing the peptides was acidified with trifluoroacetic acid (TFA) to 0.5% final concentration and samples were desalted using C18 SepPaks (1 cc cartridge, 100 mg (Waters, Milford, USA)). In brief, SepPaks were conditioned using methanol (1 ml), buffer B (80% acetonitrile (ACN), 0.1% TFA) (1 ml) and buffer A (0.1% TFA) (2 ml). Samples were loaded by gravity flow, washed with buffer A (1 x 1 ml, 1x 2 ml) and eluted with buffer B (2 x 400 µl). 80 µl of eluates were used for peptide measurement and concentrated for total proteome analysis and fractionation.

Phosphopeptide enrichment was conducted using metal-oxide chromatography (MOC) and the protocol adapted from Nakagami (2014). The remaining samples were evaporated to a sample volume of 50 µl and diluted with sample buffer (2 ml ACN, 820 µl lactic acid (LA), 2.5 µl TFA / 80% ACN, 0.1% TFA, 300 mg/ml LA, final concentrations) (282 µl). MOC tips were prepared by loading a slurry of 3 mg/sample TiO_2 beads (Titansphere TiO_2 beads 10 µm; GL Science Inc, Japan) in 100 µl MeOH onto a C8 micro column and centrifugation for 5 min at 1500 g. Tips were washed with centrifugation at 1,500 g for 5 min using 80 µl of solution B (80% ACN, 0.1% TFA) and 80 µl of solution C (300 mg/ml LA in solution B). To simplify the processing, samples tips were fitted onto a 96/500 µl deep well plate (Protein LoBind; Eppendorf, Germany). After washing, MOC tips were transferred to a fresh plate, samples were loaded onto the equilibrated tips and centrifuged for 10 min at 1,000 g. The flow through was reloaded onto the tips and centrifugation was repeated. Tips were washed with centrifugation at 1,500 g for 5 min using 80 µl of solution C and 3x 80 µl of solution B. For the elution of the enriched phosphopeptides, the tips were transferred to a fresh 96/500 µl deep well plate containing 100 µl/well of acidification buffer (20% phosphoric acid). Peptides were eluted first with 50 µl elution buffer 1 (5% NH_4OH) and centrifugation for 5 min at 800 g, followed by 50 µl of elution buffer 2 (10% piperidine) and centrifugation for 5 min at 800 g. Next, the samples were desalted using StageTips with C18 Empore disk membranes (3 M) (Rappsilber et al., 2003), dried in a vacuum evaporator, and dissolved in 10 µl 2% ACN, 0.1% TFA (A* buffer) for MS analysis.

For the library samples, aliquots from all samples corresponding to 2 µg peptides (60 µg in total) were mixed and submitted to SCX fractionation. To this end, StageTips were prepared using 6 layers of SPE disk (Empore Cation 2251 material) activated with acetonitrile and 1% TFA (100 µl each) and washed with buffer A (water, 0.2% TFA) (100 µl) by spinning 5 min (1.5k x g). Next, samples were acidified to 1% TFA, loaded by centrifugation (10 min, 800 x g) and washed with buffer A (5 min, 1.5k x g) (100 µl). Fractionation was carried out using an ammonium acetate gradient (20% ACN, 0.5% TFA) starting from 25 mM to 500 mM for 9 fractions and two final elution steps using 1% ammonium hydroxide, 80% ACN and finally 5% ammonium hydroxide, 80% ACN. All fractions were eluted by centrifugation (5 min, 500 x g) using 2 x 30 µl eluent. The fractions were dried and taken up in 10 µl A* buffer. Peptide concentration was determined by Nanodrop and samples were diluted to 0.1 µg/µl for measurement.

For the data-dependent analysis (DDA) analysis, the remaining eluted peptides from the 80 µl aliquots were dried and then taken up in 10 µl A* buffer. Peptide concentration was determined by Nanodrop and samples were diluted to 0.1 µg/µl for measurement.

3.2.5 Proteome data acquisition by LC-MS/MS

Total proteome and fractionated (library) samples were analyzed using an EASY-nLC 1000 (Thermo Fisher Scientific, Waltham, USA) coupled to an Orbitrap Exploris 480 mass spectrometer equipped with a FAIMS Pro interface (Thermo Fisher Scientific, Waltham, USA) for field asymmetric ion mobility separation. Peptides were separated on a 50 cm µPAC column (Thermo Fisher Scientific, Waltham, USA). Peptides were loaded on the column and eluted for 115 min using a segmented linear gradient of 5% to 95% solvent B (0 min : 5%B; 0-5 min -> 5%B; 5-65 min -> 20%B; 65-90 min ->35%B; 90-100 min -> 55%; 100-105 min ->95%, 105-115 min ->95%) (solvent A 0% ACN, 0.1% TFA; solvent B 80% ACN, 0.1% TFA) at a flow rate of 300 nl/min. Mass spectra were acquired in data-dependent acquisition mode with a TOP_S method using a cycle time of 2 seconds. For field asymmetric ion mobility separation, two compensation voltages (-45 and -60) were applied, the cycle time for each experiment was set to 1 second. MS spectra were acquired in the Orbitrap analyzer with a mass range of 320–1200 m/z at a resolution of 60,000 FWHM and a normalized AGC target of 300%. Precursors were filtered using the “MIPS” option, the intensity threshold was set to 5000, Precursors were selected with an isolation window of 1.6 m/z. HCD fragmentation was performed at a normalized collision energy of 30%. MS/MS spectra were acquired with a target value of 75% ions at a resolution of 15,000 FWHM, at an automated injection time and a fixed first mass of m/z 100. Peptides with a charge of +1, greater than 6, or with unassigned charge state were excluded from fragmentation for MS^2, dynamic exclusion for 40 s prevented repeated selection of precursors.

3.2.6 Phosphoproteome data acquisition by LC-MS/MS

Phospho-enriched samples were analyzed using an EASY-nLC 1200 (Thermo Fisher Scientific, Waltham, USA) coupled to a Q Exactive Plus mass spectrometer (Thermo Fisher Scientific, Waltham, USA). Peptides were separated on 16 cm frit-less silica emitters (New Objective, 75 µm inner diameter), packed in-house with reversed-phase ReproSil-Pur C18 AQ 1.9 µm resin (Dr. Maisch, Ammerbuch-Entringen, Germany). Peptides were loaded on the column and eluted for 115 min using a segmented linear gradient of 5% to 95% solvent B (0 min, 5% B; 0-5 min, 5% B; 5-65 min, 20% B; 65-90 min, 35% B; 90-100 min, 55%; 100-105 min, 95%, 105-115 min, 95%) (solvent A 0% ACN, 0.1% TFA; solvent B 80% ACN, 0.1%FA) at a flow rate of 300 nl/min. Mass spectra were acquired in data-dependent acquisition mode with a TOP15 method. MS spectra were acquired in the Orbitrap analyzer with a mass range of 300–1750 m/z at a resolution of 70,000 FWHM and a target value of 3×10^6 ions. Precursors were selected with an isolation window of 1.3 m/z. HCD fragmentation was performed at a normalized collision energy of 25. MS/MS spectra were acquired with a target value of 10^5 ions at a resolution of 17,500 FWHM, a maximum injection time of 120 ms and a fixed first mass of m/z 100. Peptides with a charge of +1, greater than 6, or with unassigned charge state were

excluded from fragmentation for MS^2, dynamic exclusion for 30 s prevented repeated selection of precursors.

3.2.7 Deep proteome data analysis

Raw data were processed using MaxQuant software (version 1.6.3.4, http://www.maxquant.org/) (Cox and Mann, 2008) with label-free quantification (LFQ) and iBAQ enabled (Tyanova et al., 2016). Library samples and DDA samples were grouped into separate parameter groups. In the group specific parameters, in the Misc. setting the Match type for library samples was set to “match from” and for DDA to “match from and to”.

MS/MS spectra were searched by the Andromeda search engine against a combined database containing the sequences from the barley Morex V2 genome (Monat et al., 2019), and sequences of 248 common contaminant proteins and decoy sequences. Trypsin specificity was required and a maximum of two missed cleavages allowed. Minimal peptide length was set to seven amino acids. Carbamidomethylation of cysteine residues was set as fixed and oxidation of methionine and protein N-terminal acetylation as variable modifications. The match between runs option was enabled. Peptide-spectrum-matches and proteins were retained if they were below a false discovery rate of 1% in both cases.

Statistical analysis of the MaxLFQ values was carried out using Perseus (version 1.6.14.0, http://www.maxquant.org/). Quantified proteins were filtered for reverse hits and hits “only identified by site” and MaxLFQ values were log2 transformed and samples were grouped by condition and separated according to type of comparison (i. e. genotype or timepoint comparison). Next, the data was separated for a mixed imputation processing: hits were filtered for 4 valid values in one of the conditions, next the data was separated into two sets: one set containing mostly missing at random (MAR) hits and the other set containing mostly missing not at random (MNAR) hits by filtering the data for 1 valid hit in each group and splitting the resulting matrices (Lazar et al., 2016). The resulting matrix with at least 1 valid hit in each group is the MAR dataset, the matrix with the hits filtered out is the MNAR dataset. The missing values of each dataset were then imputed using different options of the “imputeLCMD” R package (Lazar, 2015) integrated into Perseus: the missing values from the MAR dataset were imputed using a nearest neighbor approach (KNN, n=5), the missing values from the MNAR dataset were imputed using the MinProb option (q=0.01. tune.sigma=1). After merging of the imputed datasets two-sample Student’s *t*-tests were performed using a permutation-based FDR of 5%. The Perseus output was exported and further processed using Excel and R software.

3.2.8 Phosphoproteomics data analysis

Raw data were processed using MaxQuant software (version 1.6.3.4 http://www.maxquant.org/) (Cox & Mann, 2008) with label-free quantification (LFQ) and iBAQ enabled (Tyanova et al., 2016).

MS/MS spectra were searched by the Andromeda search engine against a combined database containing the sequences from the barley Morex V2 genome (Monat et al., 2019) and sequences of 248 common contaminant proteins and decoy sequences. Trypsin specificity was required and a maximum of two missed cleavages allowed. Minimal peptide length was set to seven amino acids. Carbamidomethylation of cysteine residues was set as fixed, phosphorylation of serine, threonine and tyrosine, oxidation of methionine and protein N-terminal acetylation as variable modifications. The match between runs option was enabled. Peptide-spectrum-matches and proteins were retained if they were below a false discovery rate of 1% in both cases.

Statistical analysis was carried out on phospho peptide level using the intensities obtained from the "modificationSpecificPeptides" output using Perseus (version 1.5.8.5, http://www.maxquant.org/). Quantified sites were filtered for reverse hits and contaminant hits and results were filtered to retain only phospho-modified peptides. Intensities were log2 transformed and samples were grouped by condition and separated according to type of comparison (i. e. genotype or timepoint comparison). After grouping the samples only those sites were retained for the subsequent analysis that had 4 valid values in one of the conditions, for the remaining hits intensities were normalized by subtraction of the median per column and missing values were imputed from a normal distribution with a downshift of 1.8 and separately for each column. Two-sample Student's *t*-tests were performed using permutation-based FDR of 0.05. The Perseus output was exported and further processed using Excel and R software.

3.2.9 Removal of redundant (phospho-)protein entries

In order to reduce redundancy of protein entries, we manually curated proteins related to auxin response and signaling, sugar transport and energy production and starch metabolism, using the previously acquired stamen transcriptomes as reference. Redundant proteins, which share a peptide sequence with at least one more protein in the proteome, were kept in the analysis if they were sufficiently supported by gene expression. A similar procedure was applied to reduce the number of redundant phosphoproteins entries, using the stamen proteome as reference.

3.3 Results

3.3.1 Transcriptome analysis of Bowman and *msg38* stamens during maturation

The transcriptional response to auxin in barley stamens was previously investigated at stages W9.25 and W9.35, at which starch granule deposition in pollen takes place, in the mutant *msg38* and cultivar Bowman, its corresponding fertile counterpart (Amanda et al., 2022). To define the kinetics of auxin-dependent molecular changes in across barley stamen maturation, we obtained additional transcriptomes at stages W8.5, W8.75 and W9 in these two genotypes. We detected 19,707 transcripts, covering ~60% of the annotated barley transcriptome. Principal component analysis and mapping of Euclidean sample distances revealed that the differences between stages account for the majority of total variance (Figure 11A, B). This may indicate that the genotypic differences are not as pronounced as in W9.25 and W9.35 transcriptomes, where both genotype and stage explain a similar portion of the total variance (Amanda et al., 2022). We identified 1,863 differentially expressed genes [DEGs, $|FC| \geq 1.5$; FDR-adjusted $P \leq 0.05$] of which 38, 596 and 1503 were found at stages W8.5, W8.75 and W9, respectively.

Hierarchical clustering distributed DEGs in 5 clusters (Figure 11C). The majority of DEGs (61%) were downregulated in *msg38* stamens and fell in clusters 2, 3 and 5, while the remaining clusters contained genes upregulated in *msg38* (Figure 11D). In Bowman, cluster 2 genes are expressed at very low levels in W8.5 stamens and then increase exponentially at W8.75 and W9. This increase in gene expression takes place only mildly in *msg38* stamens (Figure 11D). On the other hand, Bowman genes in clusters 3 and 5 are already expressed at medium levels in W8.5 and W8.75 stamens levels but then take sudden divergent paths at W9: increased expression for cluster 5 genes and decreased expression in cluster 3. In *msg38*, cluster 5 genes are already downregulated at stages W8.5, W8.75 and the increased expression observed in Bowman at W9 does not take place. Cluster 3 genes are slightly downregulated in *msg38* at W8.5 and W8.75; however, the most remarkable feature of this cluster is that the decreased gene expression observed in Bowman at W9 is even stronger in *msg38*. Overall, cluster 5 seems to contain the earliest gene set activated by auxin in maturing barley stamens. Moreover, GO analysis revealed that this cluster is enriched for genes related to auxin catabolism and auxin signaling, such as *Aux-IAAs*, *GH3s* and *SAURs*, which are known to early respond to auxin (Abel and Theologis, 1996). In cluster 2 and 3, we found multiple GO terms related to sugar metabolism. Since cluster 2 genes are activated from W8.75, it is plausible that they are part of a second wave of auxin-dependent gene expression, which goes on to increase exponentially, possibly all the way to the starch-filling stages W9.25 and W9.35. On the other hand, it is remarkable that sets of genes of the same category contained in cluster 3, are actually switched off at stage W9.

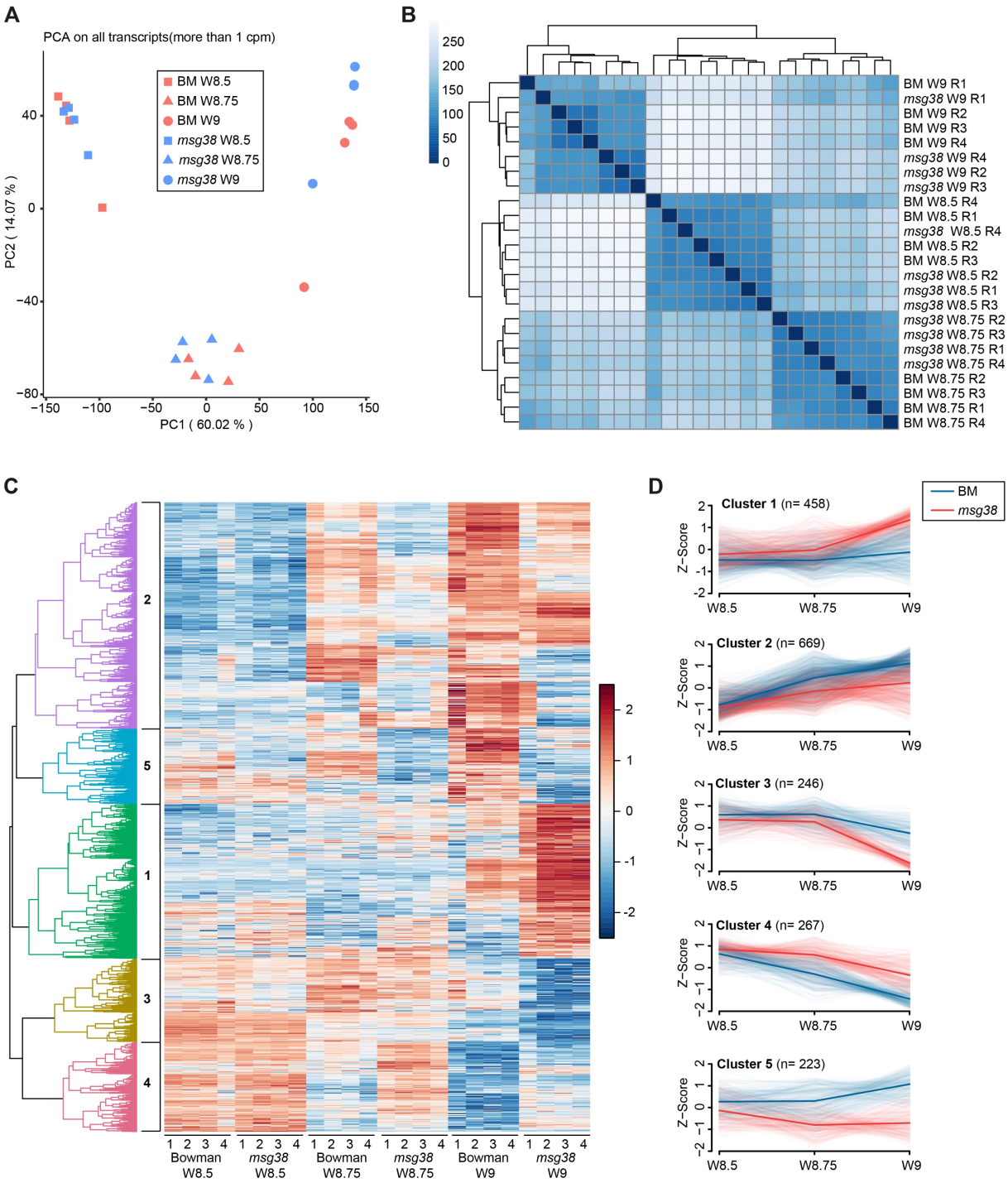

Figure 11. Transcriptomic analysis of Bowman and *msg38* stamens. A) Principal component analysis of normalized expression levels (counts per million, cpm) of all expressed genes. **B**) Heatmap of Euclidean distances between samples calculated from normalized cpm values of all expressed genes. **C**) Hierarchical clustering of DEGs. Scale represents mean-centered log_2 cpm values. Each column is a biological replicate (n=4 per treatment and stage). **D**) Expression profiles of all DEGs within each cluster. Z-scores are mean-centered and scaled transcript levels in cpm. Light-colored thin lines connect Z-scores at each stage of individual transcripts. Dark-colored thick lines connect the mean Z-Scores across all transcripts at each stage.

Next, we explored the expression kinetics of MSG38-dependent genes associated to auxin signaling, sugar transport and heterotrophic ATP production over the entire course of stamen maturation, including the W8.5, W8.75 and W9 transcriptomes presented here, and the W9.25 and W9.35 transcriptomes reported by Amanda et al. (2022). We found 34 auxin-responsive genes and 6 ARF genes that are differentially expressed in *msg38* and most of which are downregulated in at least one Waddington stage (Figure 12). These genes form subsets according to their expression kinetics in *msg38*: Some are downregulated at all stages, while others only at either early (W8.5 – W9) or late stages (W9.25 – W9.35). This confirms that auxin signaling is already ongoing as early as W8.5 and that it has target genes that require constant activation, while others have transient and stage-dependent expression.

Furthermore, there are 25 sugar transporter genes differentially expressed in *msg38*, predominantly at stages W9.25 and W9.5, and mostly are downregulated in the mutant. Moreover, no DEGs in this category occur at W8.5 (Figure 12). Energy generation genes follow a similar trend: Although there are 125 DEGs in this category, none is found at W8.5, only ~10% show significantly altered expression in at stages W8.75 and W9 (a mix of up- and downregulated transcripts), and the vast majority are differentially expressed (mostly downregulated), only at W9.25 and W9.35 (Figure 12). These findings support that the expression of energy genes that are dependent on auxin, mainly occurs during advanced stamen maturation, at the height of pollen starch accumulation. Besides, we noticed that most genes in these categories that were downregulated at stage W9 are involved in sucrose degradation and glycolysis, suggesting that they are the first line of energy generation genes that is activated by auxin. This agrees with the location of these processes at the top of the pathways for heterotrophic energy production and with the over accumulation of sugars and reduced pyruvate production in the *msg38* mutant (Amanda et al., 2022).

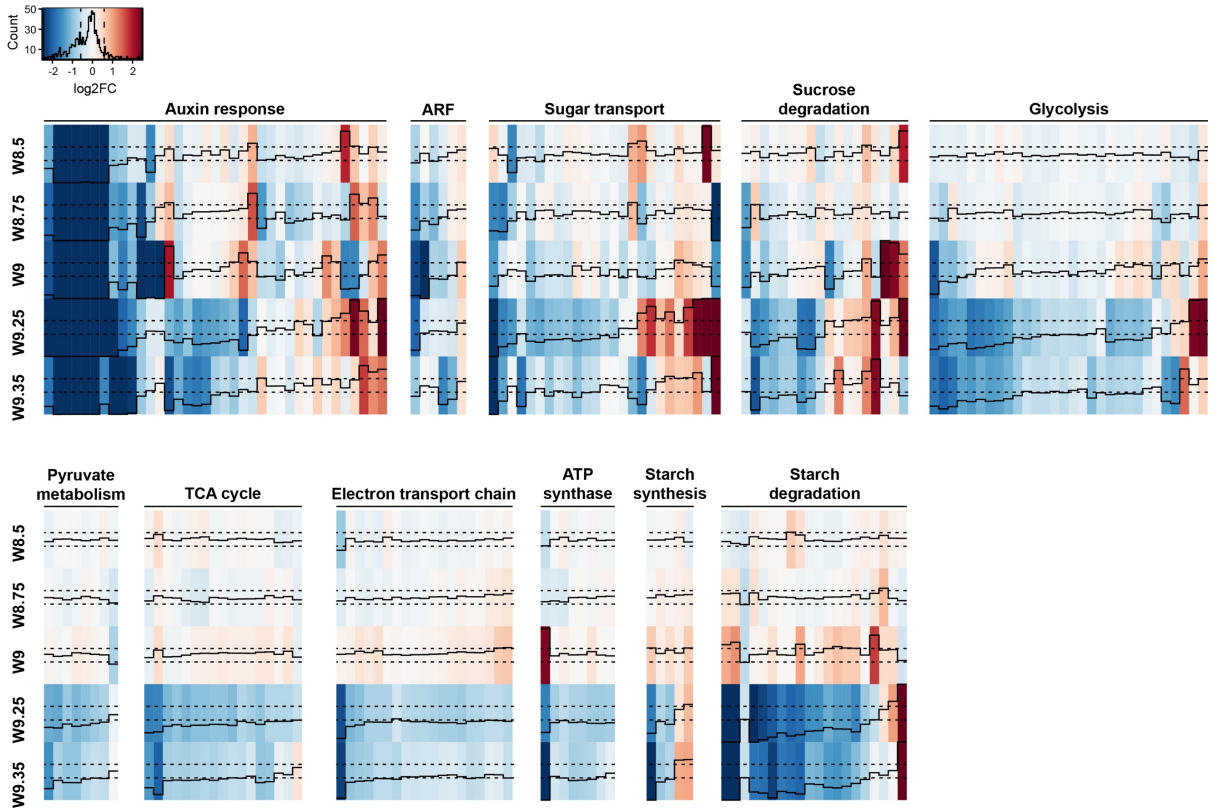

Figure 12. Differentially expressed genes related to auxin signaling, sugar transport and energy metabolism. Heatmaps showing log2 fold change values (FC, black solid line) of genes from different pathways that are differentially expressed in *msg38* stamens at least at one Waddington stage. Dashed black lines indicate $\log_2$ FC values of +/- 1.5, representing the threshold of significance for up- and downregulation, respectively. FC values for stages W9.25 and W9.35 were acquired from Amanda et al. (2022).

3.3.2 Comparative proteome analysis of Bowman and *msg38* stamens during advanced maturation

It is a common view that transcript levels and changes are not necessarily matched by protein quantifications (Vogel and Marcotte, 2012). Thus, we tested the hypothesis that the transcriptome changes activated by auxin result in measurable corresponding changes in the stamen proteome. Thus, we used LC-MS/MS-based proteomics on Bowman and *msg38* stamens, and detected 13,065 (8,689 non-redundant) proteins. Approximately 83% of these proteins were also expressed as genes in at least one of the stages between W8.5 – W9.35. Comparative analysis revealed 4,733 differentially abundant proteins [DAPs, |FC| ≥ 1.5; FDR-adjusted P ≤ 0.05], between Bowman and *msg38* stamens, of which 1,832, 2,179 and 3,093 are found at stages W9, W9.25 and W9.35, respectively. Only 1,326 (28%) auxin-dependent DAPs showed significantly changed gene expression in the stamen transcriptome, indicating that auxin-mediated posttranscriptional mechanisms influence the protein landscape in stamens. Conversely, only 27% out of 4,873 identified DEGs at stages W8.5 – W9.35 also were DAPs in the stamen proteome.

Next, we focused on proteins related to auxin responses and carbohydrate metabolism. We detected 14 auxin-signaling-related proteins in the entire proteome. This lower number is explained because most of them are low-abundance transcription factors (Aux-IAAs or ARFs), which are not detectable in standard proteomic analysis. Yet 9 of those 14 proteins were less abundant in *msg38* stamens (Figure 13), consistent with the transcriptome.

Furthermore, we found 34 sugar transport proteins, 12 of which are DAPs in *msg38*, approximately half upregulated and half downregulated (Figure 13). Moreover, half of these 12 proteins show similar gene expression changes in the transcriptome. Additionally, the stamen proteome contains 239 proteins related to heterotrophic ATP production and starch metabolism, 77 of which are DAPs in *msg38*, mostly at lower levels in the mutant (Figure 13), consistent with the findings of the transcriptome analysis (Figure 12; Amanda et al., 2022). Approximately 80% of energy metabolism proteins with decreased abundance show reduced transcripts of the corresponding genes. Thus, in contrast to the overall proteome, protein abundance of these protein class is mostly dependent on gene expression and auxin synthesis via HvYUC4-MSG38.

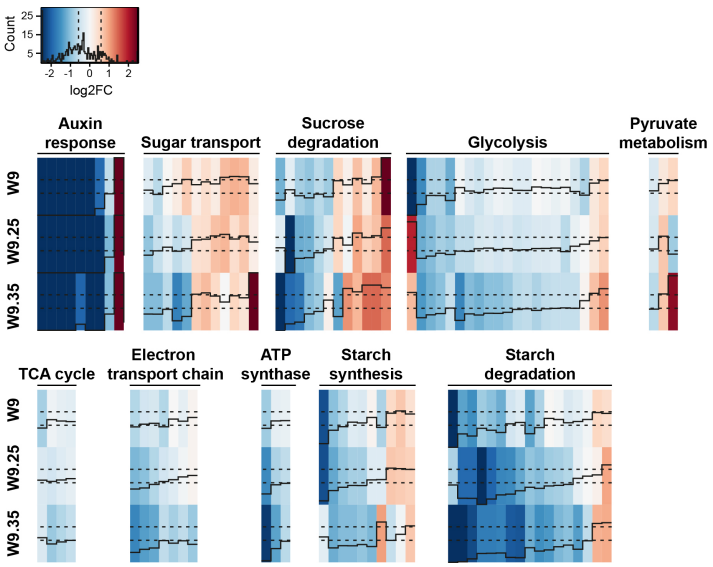

Figure 13. Differentially abundant proteins related to auxin, sugar transport and energy generation pathways. Heatmaps show log2 fold change values (FC, black solid line) of proteins from different pathways that are differentially abundant in *msg38* stamens at least at one Waddington stage. Dashed black lines indicate $\log_2$ FC values of +/- 1.5, representing the threshold of significance for up- and downregulation, respectively.

3.3.3 Analysis of phosphoproteins involved in carbohydrate metabolism during advanced stamen maturation

To further elucidate the regulatory effect of auxin on the function of proteins involved in sugar transport and energy metabolism, we performed a phosphoproteome screen of stamens during late maturation stages. We detected 4,249 (3,633 non-redundant) phosphopeptides corresponding to 2,377 proteins of which 86% were also detected in the proteome. We identified 1,663 differentially phosphorylated proteins [DPPs, |FC| ≥ 1.5; FDR-adjusted P ≤ 0.05]. Among them, 956, 869 and 1039 show significantly altered phosphorylation at stages W9, W9.25 and W9.35, respectively. Protein levels of 1,095 DPPs are not different between Bowman and *msg38*, indicating that most DPPs reflect actual changes in phosphorylation status and not simply protein abundance.

The data revealed 14 sugar transporters and 19 energy metabolism proteins with significantly altered phosphorylation of one or more phosphosites at least at one Waddington stage during late stamen maturation (Figure 14). Most of those DPPs (75%) are part of the sugar transporter, sucrose degradation and glycolysis categories, and contain phosphosites with decreased phosphorylation in *msg38* stamens (Figure 14). However, half DPPs in the sugar transporter category contained phosphosites with increased phosphorylation in the mutant Overall, the data suggests that auxin-dependent protein phosphorylation is an important mechanism to enhance sugar transport and top level pathways of energy production in stamens during pollen starch filling.

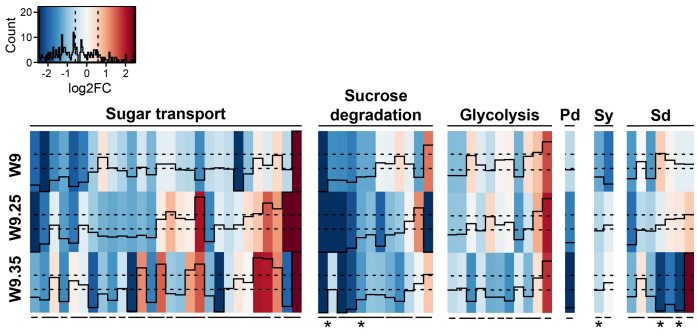

Figure 14. Auxin-dependent sugar transporter and energy generation phosphoproteins and their phosphosites. Heatmaps show log2 fold change values (FC, black solid line) of phosphosites of proteins from different pathways that are differentially phosphorylated in *msg38* stamens at least at one Waddington stage. Dashed black lines indicate log_2 FC values of +/- 1.5, representing the threshold of significance for up- and downregulation, respectively. Each column represents a single phosphosite of a protein. Individual proteins and their phosphosites are indicated by the black solid line below the heatmaps. Asterisks indicate proteins that show similar changes in their abundance in *msg38* stamens as the phosphorylation status. Pd, Pyruvate decarboxylase; Sy, Starch synthesis; Sd, Starch degradation.

3.4 Discussion

Auxin has a critical role in various processes required for male reproductive development (Sundberg and Østergaard, 2009). In barley, stamens accumulate auxin during post-meiotic development to enhance the expression of genes related to energy production at terminal maturation stages W9.25 and W9.35, thereby ensuring that enough ATP is available for pollen starch synthesis (Amanda et al., 2022). In this chapter, we analyzed the stamen transcriptome, proteome and phosphoproteome of the cultivar Bowman and the auxin-deficient mutant *msg38* at different stages of maturation, to gain additional insights into the auxin response and auxin-regulated energy metabolism in barley stamens.

Our RNA-Seq analysis of *msg38* and Bowman stamens revealed that auxin increasingly regulates gene expression in stamens between stage W8.5 and W9, covering approximately 9% of the stamen transcriptome. This proportion increases to approximately 16% of all expressed genes at subsequent stages W9.25 and W9.35 (Amanda et al., 2022), suggesting that auxin mainly acts during the terminal maturation phase in barley stamens. Using both transcriptome datasets, we investigated the expression kinetics of genes related to auxin response, sugar transport and energy metabolism over an expanded time course of stamen maturation (W8.5 – W9.35). We found that several auxin-response genes in *msg38* stamens were expressed at lower levels at earlier stamen maturation stages W8.5 – W9 (Figure 2), which is consistent with the decreased IAA concentrations in *msg38* stamens (Amanda et al., 2022). Furthermore, the data revealed different groups of auxin response genes with distinct expression patterns during stamen maturation (Figure 2). One set comprises consistently downregulated auxin response genes, including putative *Aux/IAAs* and members of the auxin-amido synthetase encoding *GH3* family that plays a crucial role in auxin homeostasis (Aoi et al., 2019). Furthermore, decreased expression of four *GH3* genes at stages W9 – W9.35 is supported by lower proteins levels at the same stages (Figure 3). We propose that these primary auxin-response genes might be valuable reporters of the auxin status in developing barley stamens. Moreover, some auxin-response genes were temporarily up- or downregulated at stages W8.75 and W9, respectively, while others showed altered expression only at stages W9.25 and W9.35 (Figure 2). This suggests that auxin may activate temporally separate components of its signaling network that control different processes of stamen maturation.

Proteins of the DNA-binding ARF family are key players in auxin-mediated gene expression (Liscum and Reed, 2002; Li et al., 2016). In the past, it has been shown that ARFs are crucial for male gametophyte development (Nagpal et al., 2005; Yang et al., 2013). Here, we identified several ARF encoding genes that are regulated by auxin throughout during stamen maturation. We propose that these *ARFs* are good candidates for auxin-mediated transcription factors

required for pollen maturation in barley. It will be interesting to create loss-of function mutants of some of these *ARFs* to test whether they exhibit the same male-sterile phenotype as *msg38*. Furthermore, identification of ARF protein DNA-binding targets via ChIP-qPCR would open the possibility to more precisely define the downstream cascade of auxin signaling in stamens and test if the expression boost of energy metabolism genes is directly or indirectly controlled by auxin.

We found that only few MSG38-dependent genes related to carbohydrate metabolism show expression changes during earlier maturation stages W8.75 – W9. This contrasts with the subsequent stages W9.25 and W9.35, when genes of sugar transport and every step of heterotrophic ATP-generation pathways are downregulated (Amanda et al., 2022). This finding supports the proposal by Amanda et al. (2022) that auxin shifts central carbohydrate metabolism in stamens to a state of high energy production during the peak stages at starch accumulation. It is thought that the effects of auxin depend on its local concentration (Teale et al., 2006; Casanova-Sáez et al., 2021), thus we propose that auxin may need to reach a threshold concentration in stamens to boost the expression of genes participating in energy-generation steps. This hypothesis might be supported by the observation that the concentration of bioactive IAA in stamens of fertile Bowman stamens already increases between stages W8 and W8.75/W9 by more than 10-fold (Amanda et al., 2022). Our data also shows that multiple *ARFs* are downregulated in *msg38* stamens at stages W8.75 and W9, which is accompanied by decreased expression of energy-generation genes at stage W9. Thus, it is possible that a critical auxin level in stamens might be reached around this phase of maturation. Notably, most auxin-dependent energy generation genes identified at stage W9 are involved in sucrose degradation and glycolysis, suggesting that they are the earliest processes of the stamen carbohydrate metabolism that are transcriptionally regulated by auxin.

Our proteome analysis shows that the abundance of more than a third of detected stamen proteins at stages W9 – W9.35 are regulated by auxin. However, the overall low overlap between DEGs and DAPs suggests that most auxin-mediated changes in protein levels are independently of gene expression. These findings are similar to studies Arabidopsis seedlings, where IAA treatment of seedlings resulted in a global remodeling of the protein landscape but only a small overlap between transcriptome and proteome analysis was found (Xing and Xue, 2012; Clark et al., 2019). Such discrepancies between transcript and protein abundance could possibly be explained by posttranscriptional events that influence mRNA processing and translation (Floris et al., 2009; Vélez-Bermúdez and Schmidt, 2014; Clark et al., 2019). On the other hand, we found a much better correspondence between transcriptome and proteome when considering only genes and proteins of sugar metabolism and energy generation, that

is, low abundance of these factors at the protein level in the *msg38* mutant can mostly be explained by decreased gene expression. This result emphasizes that auxin-mediated increase in the expression of energy-generation genes translates into elevated protein levels, thus promoting sugar utilization, mitochondrial respiration and ATP generation. On the other hand, some downregulated energy-generation proteins do not show altered gene expression, suggesting that auxin may also regulate proteins involved in stamen energy metabolism on a posttranscriptional level.

Reversible protein phosphorylation carried out by kinases and phosphatases is a common posttranslational modification to regulate protein activity (Li and Liu, 2021). In Arabidopsis, multiple key anther development proteins are phosphorylated, suggesting that phosphorylation is an important regulatory mechanism in male reproductive organ development (Ye et al., 2016). Our data shows that auxin modulates the phosphorylation status in the majority of detected phosphoproteins independently of their abundance, which suggests a central role for auxin in posttranslational protein modification during stamen maturation. Our finding that phosphorylation of several energy metabolism proteins requires auxin, further supports this conclusion (Figure 14). The activity of some of these auxin-regulated phosphoproteins, such as sugar transporters, invertases or pyruvate dehydrogenases, is known to be regulated by phosphorylation (Holness and Sugden, 2003; Gao et al., 2014; Yamada et al., 2016). Thus, we can hypothesize that auxin-mediated phosphorylation of energy metabolism proteins is an additional mechanism that favors pollen starch accumulation, hence male gametophyte development and function in barley.

Past studies have reported a connection between auxin and respiration rates in Arabidopsis and tomato (Ivanova et al., 2014; Batista-Silva et al., 2019). The work by Amanda et al. (2022) and the findings in this chapter show that auxin also enhances components of sugar metabolism and mitochondrial respiration in barley stamens during maturation. However, the link between auxin and central carbon metabolism remains poorly understood (Batista-Silva et al., 2019; Tivendale and Millar, 2022). Recently, it was demonstrated in rice that OsARF18 and OsARF2 regulate the expression of the sucrose transporter *OsSUT1* by binding to sucrose-responsive elements in its promoter, providing evidence of a direct interaction between auxin-signaling and carbohydrate transport (Zhao et al., 2022). On the other hand, it is possible that auxin exerts its regulatory effect on the primary metabolism in stamens in a more indirect manner. For instance, auxin was shown to activate the protein kinase TARGET OF RAPAMYCIN (TOR) (Li et al., 2017; Schepetilnikov et al., 2017), which orchestrates plant growth and development by controlling the carbon and energy metabolism (Xiong et al., 2013; Dong et al., 2015). Alternatively, SnRK1 could also play a role in mediating the auxin-dependent boost of energy metabolism in stamens. In fact, expression of the antisense *SnRK1*

gene in transgenic barley caused abnormal pollen with no starch (Zhang et al., 2001). However, it should be noted that the lack of pollen starch accumulation in the mutant pollen could be a secondary consequence of the observed arrest in pollen development at the binucleate stage (Zhang et al., 2001). Moreover, recent studies in peach roots suggest that *SnRK1* rather acts upstream of auxin signaling (Zhang et al., 2020). Clearly, further investigations are needed to elucidate the crosstalk between auxin and its downstream targets in developing stamens.

3.5 Conclusion

In summary, our results indicate that shifting the energy metabolism at stages of pollen starch accumulation is a major function of auxin in stamens during post-meiotic maturation. During this phase, auxin does not only act on a transcriptional but also on a posttranscriptional and posttranslational level, underlining its role as central hormone participating in male reproductive development. Our analysis reveals a set of auxin-related genes that might act as critical mediators to drive the metabolic shift in stamens. Moreover, we present candidate targets of auxin signaling and auxin-mediated phosphorylation that participate in sugar metabolism and ATP generation, and may be essential for the metabolic shift in stamens. In this study, we have focused on categories related to auxin and carbohydrate metabolism. However, our data is a valuable resource to explore other processes of stamen and male gametophyte development that are regulated by auxin.

4 General discussion and conclusion

Providing sufficient food for the growing global population is one of the major challenges that the world has to face in the coming decades. It is forecasted that climate change will facilitate future environmental conditions that reduce crop productivity, thereby intensifying global food insecurity and malnutrition. Drought, one of the most important abiotic stresses, can significantly decrease yields of economically important cereal crops by impairing the development of the stamens and male gametophytes. A common defect of drought stress-induced male sterility is the failure of starch synthesis in developing pollen. In barley, pollen starch accumulation is an essential prerequisite of male fertility that is controlled by the hormone auxin. In this work, we investigated the effects of drought and the role of auxin in barley stamen and pollen maturation. Understanding the molecular mechanisms that govern important stamen maturation steps, such as pollen starch synthesis, and investigating their role in regulating male development under drought, will help to develop new strategies to improve yields in increasingly dry environments, thus contribute to future food security.

To our knowledge, this is the first report of the molecular effects of drought on barley stamen maturation in a detailed stage-dependent manner. We show that barley spikelet fertility is maintained when the drought stress occurs during the terminal phase of reproductive organ development, whereas a drought spell started at the early stamen maturation phase significantly reduces spikelet fertility. Our results indicate that male sterility is the major contributor to loss of spikelet fertility under drought, however, female reproductive development seems negatively affected too. Therefore, improving barley fertility and yield under drought stress will require not only an understanding of the drought-induced defects on the male side but also of drought-sensitive processes participating in female organ development.

Our work shows that the absence of pollen starch accumulation is a major defect in drought-stressed sterile barley pollen, which can be linked to impaired carbohydrate metabolism and energy production. Accordingly, drought-affected stamens showed reduced expression of sugar-metabolism and energy-production genes, of which half are regulated by auxin in the *msg38* mutant. Moreover, we found that drought downregulates genes related to auxin that, based on the findings in chapter II, might be critical to enhance carbon metabolism and respiration for the synthesis of pollen starch. Thus, the observed disruption of central carbon metabolism in drought-affected stamens can be partly attributed to impaired auxin homeostasis and signaling. We propose that regulation of auxin signaling offers a potential mechanism to improve pollen starch synthesis and male fertility in barley under drought stress. In rice, it was already reported that application of exogenous auxin on panicles positively correlated with spikelet fertility under drought (Sharma et al., 2018).

On the other hand, it should be noted that the adverse effects of drought on stamen carbohydrate metabolism go beyond the control of MSG38. Most obviously, *msg38* stamens over accumulate sugars (Amanda et al., 2022) while drought-affected Scarlett stamens show decreased sugar levels. Thus, further studies are needed to fully understand the molecular effects of drought on stamen carbohydrate metabolism. Our results also indicate that drought may result in the accumulation ABA in stamens and effects in the synthesis of other hormones such as ethylene or JA. Therefore, it would be interesting to elucidate the role of those hormones in male reproductive development under drought in future studies.

The comparative analyses of omics datasets between Bowman and the *msg38* mutant, conducted by Amanda et al. (2022) and in chapter II of this work, suggest that upregulation of sugar metabolism and energy production for pollen starch synthesis is a major function of auxin in barley stamens. This is supported by the observations that i) *msg38* stamens show altered expression in relatively few genes at stages that precede the pollen starch-filling; ii) the auxin-mediated increase in energy-production genes also leads to higher abundance of the corresponding proteins; iii) auxin regulates the phosphorylation status, hence activity, of proteins that perform essential steps in sugar metabolism and energy production. Moreover, we identified MSG38-dependent auxin-response genes and *ARF*s that may convey the signal to enhance the central carbon metabolism. Collectively, the candidate genes identified in this work open the avenue for future in-depth studies. Knowledge of the auxin-signaling cascade and its direct targets will not only help to understand the canonical array of events that lead to successful maturation of the male gametophyte but also provide basis for engineering varieties with robust pollen development under drought.

A more classical approach to improve crops is introgression breeding, which requires the identification of tolerant genetic resources that can be found in exotic germplasms. Here, we screened a subset of the introgression line population S42IL for drought tolerance, using our established watering regime and short-term drought method. Among all tested S42IL accessions, S42IL-120 and S42IL-121 showed the most robust spikelet fertility upon drought in the initial screening. However, as the results of the initial screening could not consistently be reproduced in repeated experiments, it is necessary to conduct further testing of these lines. Additionally, extensive screening of the remaining genotypes of the S42IL collection could expose other drought-tolerant accessions of the population. Drought stress under a slightly changed watering regime reduced spikelet fertility in GB2 but not in GPF, suggesting them as valuable pair of contrasting genotypes that could be used to identify mechanisms of drought tolerance. Further experiments as conducted in this work could help to pinpoint the source of vulnerability in GB2 and the molecular basis for enhanced drought tolerance in GPF.

In summary, this dissertation gives novel insight into post-meiotic stamen and pollen maturation under drought and presents hints of molecular mechanisms that can be potentially used to engineer drought stress tolerance.

5 References

Abel S, Theologis A (1996) Early genes and auxin action. Plant Physiology 111: 9-17. doi: 10.1104/pp.111.1.9.

Alexa A, Rahnenführer J, Lengauer T (2006) Improved scoring of functional groups from gene expression data by decorrelating GO graph structure. Bioinformatics 22: 1600-1607. doi: 10.1093/bioinformatics/btl140.

Amanda D, Frey FP, Neumann U, Przybyl M, Šimura J, Zhang Y, Chen Z, Gallavotti A, Fernie AR, Ljung K, Acosta IF (2022) Auxin boosts energy generation pathways to fuel pollen maturation in barley. Current Biology 32: 1798-1811. doi: 10.1016/j.cub.2022.02.073.

Aoi Y, Tanaka K, Cook SD, Hayashi K-I, Kasahara H (2019) GH3 auxin-amido synthetases alter the ratio of indole-3-acetic acid and phenylacetic acid in Arabidopsis. Plant and Cell Physiology 61: 596-605. doi: 10.1093/pcp/pcz223.

Awika JM (2011) Major cereal grains production and use around the world. In: Awika JM, Piironene V, Bean S (Eds.), Advances in Cereal Science: Implications to Food Processing and Health Promotion, vol. 1089. American Chemical Society, Washington DC, 1-13. doi: 10.1021/bk-2011-1089.ch001.

Aya K, Ueguchi-Tanaka M, Kondo M, Hamada K, Yano K, Nishimura M, Matsuoka M (2009) Gibberellin modulates anther development in rice via the transcriptional regulation of GAMYB. The Plant Cell 21: 1453-1472. doi: 10.1105/tpc.108.062935.

Baik B-K, Ullrich SE (2008) Barley for food: Characteristics, improvement, and renewed interest. Journal of Cereal Science 48: 233-242. doi: 10.1016/j.jcs.2008.02.002.

Barnabas B, Jager K, Feher A (2008) The effect of drought and heat stress on reproductive processes in cereals. Plant, Cell & Environment 31: 11-38. doi: 10.1111/j.1365-3040.2007.01727.x.

Basu S, Ramegowda V, Kumar A, Pereira A (2016) Plant adaptation to drought stress. F1000Research 5: F1000 Faculty Rev-1554. doi: 10.12688/f1000research.7678.1.

Batista-Silva W, Medeiros DB, Rodrigues-Salvador A, Daloso DM, Omena-Garcia RP, Oliveira FS, Pino LE, Peres LEP, Nunes-Nesi A, Fernie AR, Zsögön A, Araújo WL (2019) Modulation of auxin signalling through *DIAGETROPICA* and *ENTIRE* differentially affects tomato plant growth via changes in photosynthetic and mitochondrial metabolism. Plant, Cell & Environment 42: 448-465. doi: 10.1111/pce.13413.

Bechtold U, Field B (2018) Molecular mechanisms controlling plant growth during abiotic stress. Journal of Experimental Botany 69: 2753-2758. doi: 10.1093/jxb/ery157.

Bingham J (1966) Varietal response in wheat to water supply in the field, and male sterility caused by a period of drought in a glasshouse experiment. Annals of Applied Biology 57: 365-377. doi: 10.1111/j.1744-7348.1966.tb03830.x.

Brás TA, Seixas J, Carvalhais N, Jägermeyr J (2021) Severity of drought and heatwave crop losses tripled over the last five decades in Europe. Environmental Research Letters 16: 065012. doi: 10.1088/1748-9326/abf004.

Brisson N, Gate P, Gouache D, Charmet G, Oury F-X, Huard F (2010) Why are wheat yields stagnating in Europe? A comprehensive data analysis for France. Field Crops Research 119: 201-212. doi: 10.1016/j.fcr.2010.07.012.

Casanova-Sáez R, Mateo-Bonmatí E, Ljung K (2021) Auxin metabolism in plants. Cold Spring Harbor Perspectives in Biology 13: a039867. doi: 10.1101/cshperspect.a039867.

Castro AJ, Clément C (2007) Sucrose and starch catabolism in the anther of Lilium during its development: a comparative study among the anther wall, locular fluid and microspore/pollen fractions. Planta 225: 1573-1582. doi: 10.1007/s00425-006-0443-5.

Cecchetti V, Altamura MM, Falasca G, Costantino P, Cardarelli M (2008) Auxin regulates Arabidopsis anther dehiscence, pollen maturation, and filament elongation. The Plant Cell 20: 1760-1774. doi: 10.1105/tpc.107.057570.

Cheng H, Song S, Xiao L, Soo HM, Cheng Z, Xie D, Peng J (2009) Gibberellin acts through jasmonate to control the expression of *MYB21*, *MYB24*, and *MYB57* to promote stamen filament growth in Arabidopsis. PLoS Genetics 5: e1000440. doi: 10.1371/journal.pgen.1000440.

Cheng Y, Dai X, Zhao Y (2006) Auxin biosynthesis by the YUCCA flavin monooxygenases controls the formation of floral organs and vascular tissues in Arabidopsis. Genes & Development 20: 1790-1799. doi: 10.1101/gad.1415106.

Christensen JE, Horner HT, Lersten NR (1972) Pollen wall and tapetal orbicular wall development in *Sorghum bicolor* (Gramineae). American Journal of Botany 59: 43-58. doi: 10.2307/2441229.

Ciais P, Reichstein M, Viovy N, Granier A, Ogée J, Allard V, Aubinet M, Buchmann N, Bernhofer C, Carrara A, Chevallier F, De Noblet N, Friend AD, Friedlingstein P, Grünwald T, Heinesch B, Keronen P, Knohl A, Krinner G, Loustau D, Manca G, Matteucci G, Miglietta F, Ourcival JM, Papale D, Pilegaard K, Rambal S, Seufert G, Soussana JF, Sanz MJ, Schulze ED, Vesala T, Valentini R (2005) Europe-wide reduction in primary productivity caused by the heat and drought in 2003. Nature 437: 529-533. doi: 10.1038/nature03972.

Claeyssen E, Rivoal J (2007) Isozymes of plant hexokinase: occurrence, properties and functions. Phytochemistry 68: 709-731. doi: 10.1016/j.phytochem.2006.12.001.

Clark NM, Shen Z, Briggs SP, Walley JW, Kelley DR (2019) Auxin induces widespread proteome remodeling in Arabidopsis seedlings. Proteomics 19: 1900199. doi: 10.1002/pmic.201900199.

Clément C, Burrus M, Audran J-C (1996) Floral organ growth and carbohydrate content during pollen development in Lilium. American Journal of Botany 83: 459-469. doi: 10.1002/j.1537-2197.1996.tb12727.x.

Clément C, Chavant L, Burrus M, Audran JC (1994) Anther starch variations in Lilium during pollen development. Sexual Plant Reproduction 7: 347-356. doi: 10.1007/bf00230513.

Cook BI, Ault TR, Smerdon JE (2015) Unprecedented 21st century drought risk in the American Southwest and Central Plains. Science Advances 1: e1400082. doi: doi:10.1126/sciadv.1400082.

Cox J, Mann M (2008) MaxQuant enables high peptide identification rates, individualized p.p.b.-range mass accuracies and proteome-wide protein quantification. Nature Biotechnology 26: 1367-1372. doi: 10.1038/nbt.1511.

Dai A (2011) Drought under global warming: a review. WIREs Climate Change 2: 45-65. doi: 10.1002/wcc.81.

Dai A (2013) Increasing drought under global warming in observations and models. Nature Climate Change 3: 52-58. doi: 10.1038/nclimate1633.

de Storme N, Geelen D (2014) The impact of environmental stress on male reproductive development in plants: biological processes and molecular mechanisms. Plant, Cell & Environment 37: 1-18. doi: 10.1111/pce.12142.

Dickinson DB (1968) Rapid starch synthesis associated with increased respiration in germinating lily pollen. Plant Physiology 43: 1-8. doi: 10.1104/pp.43.1.1.

Ding Z, Wang B, Moreno I, Dupláková N, Simon S, Carraro N, Reemmer J, Pěnčík A, Chen X, Tejos R, Skůpa P, Pollmann S, Mravec J, Petrášek J, Zažímalová E, Honys D, Rolčík J, Murphy A, Orellana A, Geisler M, Friml J (2012) ER-localized auxin transporter PIN8 regulates auxin homeostasis and male gametophyte development in Arabidopsis. Nature Communications 3: 941. doi: 10.1038/ncomms1941.

Dolferus R, Ji X, Richards RA (2011) Abiotic stress and control of grain number in cereals. Plant Science 181: 331-341. doi: 10.1016/j.plantsci.2011.05.015.

Dong B, Zheng X, Liu H, Able JA, Yang H, Zhao H, Zhang M, Qiao Y, Wang Y, Liu M (2017) Effects of drought stress on pollen sterility, grain yield, abscisic acid and protective enzymes in two winter wheat cultivars. Frontiers in Plant Science 8: 1008. doi: 10.3389/fpls.2017.01008.

Dong P, Xiong F, Que Y, Wang K, Yu L, Li Z, Ren M (2015) Expression profiling and functional analysis reveals that TOR is a key player in regulating photosynthesis and phytohormone signaling pathways in Arabidopsis. Frontiers in Plant Science 6: 677. doi: 10.3389/fpls.2015.00677.

Dorion S, Lalonde S, Saini HS (1996) Induction of male sterility in wheat by meiotic-stage water deficit Is preceded by a decline in invertase activity and changes in carbohydrate metabolism in anthers. Plant Physiology 111: 137-145. doi: 10.1104/pp.111.1.137.

Druka A, Franckowiak J, Lundqvist U, Bonar N, Alexander J, Houston K, Radovic S, Shahinnia F, Vendramin V, Morgante M, Stein N, Waugh R (2011) Genetic dissection of barley morphology and development. Plant Physiology 155: 617-627. doi: 10.1104/pp.110.166249.

Du Y, Zhao Q, Chen L, Yao X, Zhang W, Zhang B, Xie F (2020) Effect of drought stress on sugar metabolism in leaves and roots of soybean seedlings. Plant Physiology and Biochemistry 146: 1-12. doi: 10.1016/j.plaphy.2019.11.003.

Eady C, Lindsey K, Twell D (1995) The significance of microspore division and division symmetry for vegetative cell-specific transcription and generative cell differentiation. The Plant Cell 7: 65-74. doi: 10.1105/tpc.7.1.65.

Emenecker RJ, Strader LC (2020) Auxin-abscisic acid interactions in plant growth and development. Biomolecules 10: 281. doi: 10.3390/biom10020281.

FAO (2022a) The State of Food Security and Nutrition in the World 2022. FAO, Rome. doi: 10.4060/cc0639en.

FAO (2022b) Crop Prospects and Food Situation – Quarterly Global Report No. 1. FAO, Rome. doi: 10.4060/cb8893en.

FAOStat (2022) https://www.fao.org/faostat/en/#data/QCL/visualize.

Farooq M, Wahid A, Kobayashi N, Fujita D, Basra SMA (2009) Plant drought stress: effects, mechanisms and management. Agronomy for Sustainable Development 29: 185-212. doi: 10.1051/agro:2008021.

Fatland BL, Nikolau BJ, Wurtele ES (2005) Reverse genetic characterization of cytosolic acetyl-CoA generation by ATP-citrate lyase in Arabidopsis. The Plant Cell 17: 182-203. doi: 10.1105/tpc.104.026211.

Fernie AR, Carrari F, Sweetlove LJ (2004) Respiratory metabolism: glycolysis, the TCA cycle and mitochondrial electron transport. Current Opinion in Plant Biology 7: 254-261. doi: 10.1016/j.pbi.2004.03.007.

Floris M, Mahgoub H, Lanet E, Robaglia C, Menand B (2009) Post-transcriptional regulation of gene expression in plants during abiotic stress. International Journal of Molecular Sciences 10: 3168-3185. doi: 10.3390/ijms10073168.

Franchi GG, Bellani L, Nepi M, Pacini E (1996) Types of carbohydrate reserves in pollen: localization, systematic distribution and ecophysiological significance. Flora 191: 143-159. doi: 10.1016/S0367-2530(17)30706-5.

Franckowiak JD, Hockett EA (1988) Identification of three new loci which control male sterility of barley. Barley Genetics Newsletter 18: 11–13.

Franckowiak JD, Lundqvist U (2012) Descriptions of barley genetics stocks for 2012. Barley Genetics Newsletter 42: 36–173.

Gao J, van Kleeff PJM, Oecking C, Li KW, Erban A, Kopka J, Hincha DK, de Boer AH (2014) Light modulated activity of root alkaline/neutral invertase involves the interaction with 14-3-3 proteins. The Plant Journal 80: 785-796. doi: 10.1111/tpj.12677.

Gebaly SG, Ahmed FMM, Namich AAM (2013) Effect of spraying some organic, amino acids and potassium citrate on alleviation of drought stress in cotton plant. Journal of Plant Production 4: 1369-1381. doi: 10.21608/jpp.2013.74149.

Geigenberger P, Stitt M, Fernie AR (2004) Metabolic control analysis and regulation of the conversion of sucrose to starch in growing potato tubers. Plant, Cell & Environment 27: 655-673. doi: 10.1111/j.1365-3040.2004.01183.x.

Giraldo P, Benavente E, Manzano-Agugliaro F, Gimenez E (2019) Worldwide research trends on wheat and barley: a bibliometric comparative analysis. Agronomy 9: 352. doi: 10.3390/agronomy9070352.

Gol L, Haraldsson EB, von Korff M (2021) *Ppd-H1* integrates drought stress signals to control spike development and flowering time in barley. Journal of Experimental Botany 72: 122-136. doi: 10.1093/jxb/eraa261.

Gómez JF, Talle B, Wilson ZA (2015) Anther and pollen development: a conserved developmental pathway. Journal of Integrative Plant Biology 57: 876-891. doi: 10.1111/jipb.12425.

Grando S, Gomez-Macpherson H (2005) Food barley: importance, uses and local knowledge. ICARDA, Aleppo, Syria.

Guicherd P, Peltier JP, Gout E, Bligny R, Marigo G (1997) Osmotic adjustment in *Fraxinus excelsior* L.: malate and mannitol accumulation in leaves under drought conditions. Trees 11: 155-161. doi: 10.1007/PL00009664.

Guo C, Ge X, Ma H (2013) The rice *OsDIL* gene plays a role in drought tolerance at vegetative and reproductive stages. Plant Molecular Biology 82: 239-253. doi: 10.1007/s11103-013-0057-9.

Guo C, Yao L, You C, Wang S, Cui J, Ge X, Ma H (2016) *MID1* plays an important role in response to drought stress during reproductive development. The Plant Journal 88: 280-293. doi: 10.1111/tpj.13250.

Gürel F, Öztürk ZN, Uçarlı C, Rosellini D (2016) Barley genes as tools to confer abiotic stress tolerance in crops. Frontiers in Plant Science 7: 1137. doi: 10.3389/fpls.2016.01137.

Hafidh S, Honys D (2021) Reproduction Multitasking: The male gametophyte. Annual Review of Plant Biology 72: 581-614. doi: 10.1146/annurev-arplant-080620-021907.

Haile GG, Tang Q, Hosseini-Moghari S-M, Liu X, Gebremicael TG, Leng G, Kebede A, Xu X, Yun X (2020) Projected impacts of climate change on drought patterns over East Africa. Earth's Future 8: e2020EF001502. doi: 10.1029/2020EF001502.

Hari V, Rakovec O, Markonis Y, Hanel M, Kumar R (2020) Increased future occurrences of the exceptional 2018–2019 Central European drought under global warming. Scientific Reports 10: 12207. doi: 10.1038/s41598-020-68872-9.

Harris JM (2015) Abscisic acid: hidden architect of root system structure. Plants (Basel) 4: 548-572. doi: 10.3390/plants4030548.

Hasegawa T, Sakurai G, Fujimori S, Takahashi K, Hijioka Y, Masui T (2021) Extreme climate events increase risk of global food insecurity and adaptation needs. Nature Food 2: 587-595. doi: 10.1038/s43016-021-00335-4.

He M, He C-Q, Ding N-Z (2018) Abiotic stresses: general defenses of land plants and chances for engineering multistress tolerance. Frontiers in Plant Science 9: 1771. doi: 10.3389/fpls.2018.01771.

Hirano K, Aya K, Hobo T, Sakakibara H, Kojima M, Shim RA, Hasegawa Y, Ueguchi-Tanaka M, Matsuoka M (2008) Comprehensive transcriptome analysis of phytohormone biosynthesis and signaling genes in microspore/pollen and tapetum of rice. Plant and Cell Physiology 49: 1429-1450. doi: 10.1093/pcp/pcn123.

Hirose T, Zhang Z, Miyao A, Hirochika H, Ohsugi R, Terao T (2010) Disruption of a gene for rice sucrose transporter, *OsSUT1*, impairs pollen function but pollen maturation is unaffected. Journal of Experimental Botany 61: 3639-3646. doi: 10.1093/jxb/erq175.

Hoerling M, Eischeid J, Perlwitz J, Quan X, Zhang T, Pegion P (2012) On the increased frequency of Mediterranean drought. Journal of Climate 25: 2146-2161. doi: 10.1175/JCLI-D-11-00296.1.

Holleman C, Rembold F, Crespo O, Conti V (2020) The impact of climate variability and extremes on agriculture and food security – an analysis of the evidence and case studies. Background paper for The State of Food Security and Nutrition in the World 2018. FAO Agricultural Development Economics Technical Study No. 4. FAO, Rome, Italy.

Holness MJ, Sugden MC (2003) Regulation of pyruvate dehydrogenase complex activity by reversible phosphorylation. Biochemical Society Transactions 31: 1143-1151. doi: 10.1042/bst0311143.

Honsdorf N, March TJ, Berger B, Tester M, Pillen K (2014) High-throughput phenotyping to detect drought tolerance QTL in wild barley introgression lines. PLoS One 9: e97047. doi: 10.1371/journal.pone.0097047.

Honsdorf N, March TJ, Pillen K (2017) QTL controlling grain filling under terminal drought stress in a set of wild barley introgression lines. PLoS One 12: e0185983. doi: 10.1371/journal.pone.0185983.

Huang Y, Guo Y, Liu Y, Zhang F, Wang Z, Wang H, Wang F, Li D, Mao D, Luan S, Liang M, Chen L (2018) 9-*cis*-epoxycarotenoid dioxygenase 3 regulates plant growth and enhances multi-abiotic stress tolerance in rice. Frontiers in Plant Science 9: 162. doi: 10.3389/fpls.2018.00162.

Ivanova A, Law SR, Narsai R, Duncan O, Lee J-H, Zhang B, Van Aken O, Radomiljac JD, van der Merwe M, Yi K, Whelan J (2014) A functional antagonistic relationship between auxin and mitochondrial retrograde signaling regulates *Alternative Oxidase1a* expression in Arabidopsis. Plant Physiology 165: 1233-1254. doi: 10.1104/pp.114.237495.

Ji X, Dong B, Shiran B, Talbot MJ, Edlington JE, Hughes T, White RG, Gubler F, Dolferus R (2011) Control of abscisic acid catabolism and abscisic acid homeostasis is important for reproductive stage stress tolerance in cereals. Plant Physiology 156: 647-662. doi: 10.1104/pp.111.176164.

Ji X, Shiran B, Wan J, Lewis DC, Jenkins CL, Condon AG, Richards RA, Dolferus R (2010) Importance of pre-anthesis anther sink strength for maintenance of grain number during reproductive stage water stress in wheat. Plant, Cell & Environment 33: 926-942. doi: 10.1111/j.1365-3040.2010.02130.x.

Ji XM, Raveendran M, Oane R, Ismail A, Lafitte R, Bruskiewich R, Cheng SH, Bennett J (2005) Tissue-specific expression and drought responsiveness of cell-wall invertase genes of rice at flowering. Plant Molecular Biology 59: 945-964. doi: 10.1007/s11103-005-2415-8.

Jin Y, Yang H, Wei Z, Ma H, Ge X (2013) Rice male development under drought stress: phenotypic changes and stage-dependent transcriptomic reprogramming. Molecular Plant 6: 1630-1645. doi: 10.1093/mp/sst067.

Kasahara H (2016) Current aspects of auxin biosynthesis in plants. Bioscience, Biotechnology, and Biochemistry 80: 34-42. doi: 10.1080/09168451.2015.1086259.

Kim W, Iizumi T, Nishimori M (2019) Global patterns of crop production losses associated with droughts from 1983 to 2009. Journal of Applied Meteorology and Climatology 58: 1233-1244. doi: 10.1175/jamc-d-18-0174.1.

Koonjul P, Minhas J, Nunes C, Sheoran I, Saini H (2005) Selective transcriptional down-regulation of anther invertases precedes the failure of pollen development in water-stressed wheat. Journal of Experimental Botany 56: 179-190. doi: 10.1093/jxb/eri018.

Kopka J, Schauer N, Krueger S, Birkemeyer C, Usadel B, Bergmüller E, Dörmann P, Weckwerth W, Gibon Y, Stitt M, Willmitzer L, Fernie AR, Steinhauser D (2005) GMD@CSB.DB: the Golm metabolome database. Bioinformatics 21: 1635-1638. doi: 10.1093/bioinformatics/bti236.

Kushiro T, Okamoto M, Nakabayashi K, Yamagishi K, Kitamura S, Asami T, Hirai N, Koshiba T, Kamiya Y, Nambara E (2004) The Arabidopsis cytochrome P450 CYP707A encodes ABA 8'-hydroxylases: key enzymes in ABA catabolism. The EMBO Journal 23: 1647-1656. doi: 10.1038/sj.emboj.7600121.

Lakew B, Eglinton J, Henry RJ, Baum M, Grando S, Ceccarelli S (2011) The potential contribution of wild barley (*Hordeum vulgare* ssp. *spontaneum*) germplasm to drought tolerance of cultivated barley (*H. vulgare* ssp. *vulgare*). Field Crops Research 120: 161-168. doi: 10.1016/j.fcr.2010.09.011.

Lalonde S, Beebe DU, Saini HS (1997) Early signs of disruption of wheat anther development associated with the induction of male sterility by meiotic-stage water deficit. Sexual Plant Reproduction 10: 40-48. doi: 10.1007/s004970050066.

Lamin-Samu AT, Farghal M, Ali M, Lu G (2021) Morpho-physiological and transcriptome changes in tomato anthers of different developmental stages under drought stress. Cells 10: 1809. doi: 10.3390/cells10071809.

Lazar C (2015) imputeLCMD: a collection of methods for left-censored missing data imputation. R package, version 2.0. https://cran.r-project.org/web/packages/imputeLCMD/index.html.

Lazar C, Gatto L, Ferro M, Bruley C, Burger T (2016) Accounting for the multiple natures of missing values in label-free quantitative proteomics data sets to compare imputation strategies. Journal of Proteome Research 15: 1116-1125. doi: 10.1021/acs.jproteome.5b00981.

Lee CP, Elsässer M, Fuchs P, Fenske R, Schwarzländer M, Millar AH (2021) The versatility of plant organic acid metabolism in leaves is underpinned by mitochondrial malate–citrate exchange. The Plant Cell 33: 3700-3720. doi: 10.1093/plcell/koab223.

Lee S-K, Eom J-S, Hwang S-K, Shin D, An G, Okita TW, Jeon J-S (2016) Plastidic phosphoglucomutase and ADP-glucose pyrophosphorylase mutants impair starch synthesis in rice pollen grains and cause male sterility. Journal of Experimental Botany 67: 5557-5569. doi: 10.1093/jxb/erw324.

Lee S-K, Kim H, Cho J-I, Nguyen CD, Moon S, Park JE, Park HR, Huh JH, Jung K-H, Guiderdoni E, Jeon J-S (2020) Deficiency of rice hexokinase HXK5 impairs synthesis and utilization of starch in pollen grains and causes male sterility. Journal of Experimental Botany 71: 116-125. doi: 10.1093/jxb/erz436.

Lehner F, Coats S, Stocker TF, Pendergrass AG, Sanderson BM, Raible CC, Smerdon JE (2017) Projected drought risk in 1.5°C and 2°C warmer climates. Geophysical Research Letters 44: 7419-7428. doi: 10.1002/2017GL074117.

Lesk C, Rowhani P, Ramankutty N (2016) Influence of extreme weather disasters on global crop production. Nature 529: 84-87. doi: 10.1038/nature16467.

Levi A, Paterson AH, Cakmak I, Saranga Y (2011) Metabolite and mineral analyses of cotton near-isogenic lines introgressed with QTLs for productivity and drought-related traits. Physiologia Plantarum 141: 265-275. doi: 10.1111/j.1399-3054.2010.01438.x.

Li P, Liu J (2021) Protein phosphorylation in plant cell signaling. In: Wu XN (Eds.), Plant Phosphoproteomics: Methods and Protocols. Springer US, New York, 45-71. doi: doi.org/10.1007/978-1-0716-1625-3_3.

Li SB, Xie ZZ, Hu CG, Zhang J-Z (2016) A review of auxin response factors (ARFs) in plants. Frontiers in Plant Sciene 7: 47. doi: 10.3389/fpls.2016.00047.

Li X, Cai W, Liu Y, Li H, Fu L, Liu Z, Xu L, Liu H, Xu T, Xiong Y (2017) Differential TOR activation and cell proliferation in Arabidopsis root and shoot apexes. Proceedings of the National Academy of Sciences of the United States of America 114: 2765-2770. doi: 10.1073/pnas.1618782114.

Li X, Lawas LM, Malo R, Glaubitz U, Erban A, Mauleon R, Heuer S, Zuther E, Kopka J, Hincha DK, Jagadish KS (2015) Metabolic and transcriptomic signatures of rice floral organs reveal sugar starvation as a factor in reproductive failure under heat and drought stress. Plant, Cell & Environment 38: 2171-2192. doi: 10.1111/pce.12545.

Li Y, Guan K, Schnitkey GD, DeLucia E, Peng B (2019) Excessive rainfall leads to maize yield loss of a comparable magnitude to extreme drought in the United States. Global Change Biology 25: 2325-2337. doi: 10.1111/gcb.14628.

Liscum E, Reed JW (2002) Genetics of Aux/IAA and ARF action in plant growth and development. Plant Molecular Biology 49: 387-400. doi: 10.1023/A:1015255030047.

Liu H, Searle IR, Mather DE, Able AJ, Able JA (2015) Morphological, physiological and yield responses of durum wheat to pre-anthesis water-deficit stress are genotype-dependent. Crop and Pasture Science 66: 1024-1038. doi: 10.1071/CP15013.

Liu JX, Bennett J (2011) Reversible and irreversible drought-induced changes in the anther proteome of rice (*Oryza sativa* L.) genotypes IR64 and Moroberekan. Molecular Plant 4: 59-69. doi: 10.1093/mp/ssq039.

Liu JX, Liao DQ, Oane R, Estenor L, Yang XE, Li ZC, Bennett J (2006) Genetic variation in the sensitivity of anther dehiscence to drought stress in rice. Field Crops Research 97: 87-100. doi: 10.1016/j.fcr.2005.08.019.

Liu S, Li Z, Wu S, Wan X (2021) The essential roles of sugar metabolism for pollen development and male fertility in plants. The Crop Journal 9: 1223-1236. doi: 10.1016/j.cj.2021.08.003.

Ma X, Su Z, Ma H (2020) Molecular genetic analyses of abiotic stress responses during plant reproductive development. Journal of Experimental Botany 71: 2870-2885. doi: 10.1093/jxb/eraa089.

Mall RK, Gupta A, Sonkar G (2017) Effect of climate change on agricultural crops. In: Dubey SK, Pandey A, Sangwan RS (Eds.), Current Developments in Biotechnology and Bioengineering: Crop Modification, Nutrition, and Food Production. Elsevier, Amsterdam, 23-46.

Mandaokar A, Thines B, Shin B, Markus Lange B, Choi G, Koo YJ, Yoo YJ, Choi YD, Choi G, Browse J (2006) Transcriptional regulators of stamen development in Arabidopsis identified by transcriptional profiling. The Plant Journal 46: 984-1008. doi: 10.1111/j.1365-313X.2006.02756.x.

Mashiguchi K, Tanaka K, Sakai T, Sugawara S, Kawaide H, Natsume M, Hanada A, Yaeno T, Shirasu K, Yao H, McSteen P, Zhao Y, Hayashi K-i, Kamiya Y, Kasahara H (2011) The main auxin biosynthesis pathway in Arabidopsis. Proceedings of the National Academy of Sciences of the United States of America 108: 18512. doi: 10.1073/pnas.1108434108.

Mehri N, Fotovat R, Mirzaei M, Fard EM, Parsamatin P, Hasan MT, Wu Y, Ghaffari MR, Salekdeh GH (2020) Proteomic analysis of wheat contrasting genotypes reveals the interplay between primary metabolic and regulatory pathways in anthers under drought stress. Journal of Proteomics 226: 103895. doi: 10.1016/j.jprot.2020.103895.

Mendelsohn R, Dinar A, Williams L (2006) The distributional impact of climate change on rich and poor countries. Environment and Development Economics 11: 159-178. doi: 10.1017/S1355770X05002755.

Michard E, Simon AA, Tavares B, Wudick MM, Feijó JA (2017) Signaling with ions: the keystone for apical cell growth and morphogenesis in pollen tubes. Plant Physiology 173: 91-111. doi: 10.1104/pp.16.01561.

Mochida K, Saisho D, Hirayama T (2015) Crop improvement using life cycle datasets acquired under field conditions. Frontiers in Plant Science 6: 740. doi: 10.3389/fpls.2015.00740.

Monat C, Padmarasu S, Lux T, Wicker T, Gundlach H, Himmelbach A, Ens J, Li C, Muehlbauer GJ, Schulman AH, Waugh R, Braumann I, Pozniak C, Scholz U, Mayer KFX, Spannagl M, Stein N, Mascher M (2019) TRITEX: chromosome-scale sequence assembly of Triticeae genomes with open-source tools. Genome Biology 20: 284. doi: 10.1186/s13059-019-1899-5.

Morgan JM (1980) Possible role of abscisic acid in reducing seed set in water-stressed wheat plants. Nature 285: 655-657. doi: 10.1038/285655a0.

Muzammil S, Shrestha A, Dadshani S, Pillen K, Siddique S, Léon J, Naz AA (2018) An ancestral allele of *Pyrroline-5-carboxylate synthase1* promotes proline accumulation

and drought adaptation in cultivated barley. Plant Physiology 178: 771-782. doi: 10.1104/pp.18.00169.

Nagpal P, Ellis CM, Weber H, Ploense SE, Barkawi LS, Guilfoyle TJ, Hagen G, Alonso JM, Cohen JD, Farmer EE, Ecker JR, Reed JW (2005) Auxin response factors ARF6 and ARF8 promote jasmonic acid production and flower maturation. Development 132: 4107-4118. doi: 10.1242/dev.01955.

Nahar K, Ullah S (2018) Drought stress effects on plant water relations, growth, fruit quality and osmotic adjustment of tomato (*Solanum lycopersicum*) under subtropical condition. Asian Journal of Agricultural and Horticultural Research 1: 1-14. doi: 10.9734/AJAHR/2018/39824.

Nakagami H (2014) StageTip-based HAMMOC, an efficient and inexpensive phosphopeptide enrichment method for plant shotgun phosphoproteomics. Methods in Molecular Biology 1072: 595-607. doi: 10.1007/978-1-62703-631-3_40.

Nemhauser JL, Feldman LJ, Zambryski PC (2000) Auxin and ETTIN in Arabidopsis gynoecium morphogenesis. Development 127: 3877-3888. doi: 10.1242/dev.127.18.3877.

Nevo E, Chen G (2010) Drought and salt tolerances in wild relatives for wheat and barley improvement. Plant, Cell & Environment 33: 670-685. doi: 10.1111/j.1365-3040.2009.02107.x.

Nguyen GN, Hailstones DL, Wilkes M, Sutton BG (2010) DROUGHT STRESS: role of carbohydrate metabolism in drought-induced male sterility in rice anthers. Journal of Agronomy and Crop Science 196: 346-357. doi: 10.1111/j.1439-037X.2010.00423.x.

Nuccio ML, Wu J, Mowers R, Zhou H-P, Meghji M, Primavesi LF, Paul MJ, Chen X, Gao Y, Haque E, Basu SS, Lagrimini LM (2015) Expression of trehalose-6-phosphate phosphatase in maize ears improves yield in well-watered and drought conditions. Nature Biotechnology 33: 862-869. doi: 10.1038/nbt.3277.

O'Leary BM (2021) Playing with Pyr: alternate sources of mitochondrial pyruvate fuel plant respiration. The Plant Cell 33: 2519-2520. doi: 10.1093/plcell/koab147.

Obata T, Witt S, Lisec J, Palacios-Rojas N, Florez-Sarasa I, Yousfi S, Araus JL, Cairns JE, Fernie AR (2015) Metabolite profiles of maize leaves in drought, heat, and combined stress field trials reveal the relationship between metabolism and grain yield. Plant Physiology 169: 2665-2683. doi: 10.1104/pp.15.01164.

Oliver SN, Dennis ES, Dolferus R (2007) ABA regulates apoplastic sugar transport and is a potential signal for cold-induced pollen sterility in rice. Plant and Cell Physiology 48: 1319-1330. doi: 10.1093/pcp/pcm100.

Oliver SN, Van Dongen JT, Alfred SC, Mamun EA, Zhao X, Saini HS, Fernandes SF, Blanchard CL, Sutton BG, Geigenberger P, Dennis ES, Dolferus R (2005) Cold-induced repression of the rice anther-specific cell wall invertase gene *OSINV4* is correlated with sucrose accumulation and pollen sterility. Plant, Cell & Environment 28: 1534-1551. doi: 10.1111/j.1365-3040.2005.01390.x.

Onyemaobi I, Liu H, Siddique KHM, Yan G (2017) Both male and female malfunction contributes to yield reduction under water stress during meiosis in bread wheat. Frontiers in Plant Science 7: 2071. doi: 10.3389/fpls.2016.02071.

Owen HA, Makaroff CA (1995) Ultrastructure of microsporogenesis and microgametogenesis in *Arabidopsis thaliana* (L.) Heynh. ecotype Wassilewskija (Brassicaceae). Protoplasma 185: 7-21. doi: 10.1007/BF01272749.

Ozga JA, Kaur H, Savada RP, Reinecke DM (2016) Hormonal regulation of reproductive growth under normal and heat-stress conditions in legume and other model crop species. Journal of Experimental Botany 68: 1885-1894. doi: 10.1093/jxb/erw464.

Pacini E (2010) Relationships between tapetum, loculus, and pollen during development. International Journal of Plant Sciences 171: 1-11. doi: 10.1086/647923.

Plaut Z, Butow BJ, Blumenthal CS, Wrigley CW (2004) Transport of dry matter into developing wheat kernels and its contribution to grain yield under post-anthesis water deficit and elevated temperature. Field Crops Research 86: 185-198. doi: 10.1016/j.fcr.2003.08.005.

Poole N, Donovan J, Erenstein O (2021) Viewpoint: agri-nutrition research: revisiting the contribution of maize and wheat to human nutrition and health. Food Policy 100: 101976. doi: 10.1016/j.foodpol.2020.101976.

Pradhan AK, Rehman M, Saikia D, Jyoti SY, Poudel J, Tanti B (2020) Biochemical and molecular mechanism of abiotic stress tolerance in plants. In: Hasanuzzaman M (Eds.), Plant Ecophysiology and Adaptation under Climate Change: Mechanisms and Perspectives I. Springer, Singapore, 825-853. https://doi.org/10.1007/978-981-15-2156-0_29.

Rajala A, Hakala K, Mäkelä P, Peltonen-Sainio P (2011) Drought effect on grain number and grain weight at spike and spikelet level in six-row spring barley. Journal of Agronomy and Crop Science 197: 103-112. doi: 10.1111/j.1439-037X.2010.00449.x.

Rappsilber J, Ishihama Y, Mann M (2003) Stop and go extraction tips for matrix-assisted laser desorption/ionization, nanoelectrospray, and LC/MS sample pretreatment in proteomics. Analytical Chemistry 75: 663-670. doi: 10.1021/ac026117i.

Ray DK, Mueller ND, West PC, Foley JA (2013) Yield trends are insufficient to double global crop production by 2050. PLoS One 8: e66428. doi: 10.1371/journal.pone.0066428.

Ray DK, Ramankutty N, Mueller ND, West PC, Foley JA (2012) Recent patterns of crop yield growth and stagnation. Nature Communications 3: 1293. doi: 10.1038/ncomms2296.

Reeves PH, Ellis CM, Ploense SE, Wu MF, Yadav V, Tholl D, Chetelat A, Haupt I, Kennerley BJ, Hodgens C, Farmer EE, Nagpal P, Reed JW (2012) A regulatory network for coordinated flower maturation. PLoS Genetics 8: e1002506. doi: 10.1371/journal.pgen.1002506.

Ritchie ME, Phipson B, Wu D, Hu Y, Law CW, Shi W, Smyth GK (2015) limma powers differential expression analyses for RNA-sequencing and microarray studies. Nucleic Acids Research 43: e47-e47. doi: 10.1093/nar/gkv007.

Roitsch T, González M-C (2004) Function and regulation of plant invertases: sweet sensations. Trends in Plant Science 9: 606-613. doi: 10.1016/j.tplants.2004.10.009.

Rosado-Souza L, David LC, Drapal M, Fraser PD, Hofmann J, Klemens PAW, Ludewig F, Neuhaus HE, Obata T, Perez-Fons L, Schlereth A, Sonnewald U, Stitt M, Zeeman SC, Zierer W, Fernie AR (2019) Cassava metabolomics and starch quality. Current Protocols in Plant Biology 4: e20102. doi: 10.1002/cppb.20102.

Ruan YL, Jin Y, Yang YJ, Li GJ, Boyer JS (2010) Sugar input, metabolism, and signaling mediated by invertase: roles in development, yield potential, and response to drought and heat. Molecular Plant 3: 942-955. doi: 10.1093/mp/ssq044.

Ruijter JM, Ramakers C, Hoogaars WMH, Karlen Y, Bakker O, van den Hoff MJB, Moorman AFM (2009) Amplification efficiency: linking baseline and bias in the analysis

of quantitative PCR data. Nucleic Acids Research 37: e45-e45. doi: 10.1093/nar/gkp045.

Sağlam A, Terzi R, Nar H, Saruhan N, Ayaz FA, Kadıoğlu A (2010) Inorganic and organic solutes in apoplastic and symplastic spaces contribute to osmotic adjustment during leaf rolling in *Ctenanthe setosa*. Acta Biologica Cracoviensia Series Botanica 52: 37-44. doi: 10.2478/v10182-010-0005-9.

Sah SK, Reddy KR, Li J (2016) Abscisic acid and abiotic stress tolerance in crop plants. Frontiers in Plant Science 7: 571. doi: 10.3389/fpls.2016.00571.

Saini HS, Aspinall D (1981) Effect of water deficit on sporogenesis in wheat (*Triticum aestivum* L.). Annals of Botany 48: 623-633. doi: 10.1093/oxfordjournals.aob.a086170.

Saini HS, Sedgley M, Aspinall D (1984) Development anatomy in wheat of male sterility induced by heat stress, water deficit or abscisic acid. Functional Plant Biology 11: 243-253. doi: 10.1071/PP9840243.

Sakata T, Oshino T, Miura S, Tomabechi M, Tsunaga Y, Higashitani N, Miyazawa Y, Takahashi H, Watanabe M, Higashitani A (2010) Auxins reverse plant male sterility caused by high temperatures. Proceedings of the National Academy of Sciences of the United States of America 107: 8569-8574. doi: doi:10.1073/pnas.1000869107.

Salinas-Grenet H, Herrera-Vásquez A, Parra S, Cortez A, Gutiérrez L, Pollmann S, León G, Blanco-Herrera F (2018) Modulation of auxin levels in pollen grains affects stamen development and anther dehiscence in Arabidopsis. International Journal of Molecular Sciences 19: 2480. doi: 10.3390/ijms19092480.

Sallam A, Alqudah AM, Dawood MFA, Baenziger PS, Börner A (2019) Drought stress tolerance in wheat and barley: advances in physiology, breeding and genetics research. International Journal of Molecular Sciences 20: 3137. doi: 10.3390/ijms20133137.

Schepetilnikov M, Makarian J, Srour O, Geldreich A, Yang Z, Chicher J, Hammann P, Ryabova LA (2017) GTPase ROP2 binds and promotes activation of target of rapamycin, TOR, in response to auxin. The EMBO Journal 36: 886-903. doi: 10.15252/embj.201694816.

Schertl P, Braun H-P (2014) Respiratory electron transfer pathways in plant mitochondria. Frontiers in Plant Science 5: 163. doi: 10.3389/fpls.2014.00163.

Schmalenbach I, Korber N, Pillen K (2008) Selecting a set of wild barley introgression lines and verification of QTL effects for resistance to powdery mildew and leaf rust. Theoretical and Applied Genetics 117: 1093-1106. doi: 10.1007/s00122-008-0847-7.

Schmalenbach I, Léon J, Pillen K (2009) Identification and verification of QTLs for agronomic traits using wild barley introgression lines. Theoretical and Applied Genetics 118: 483-497. doi: 10.1007/s00122-008-0915-z.

Schonfeld MA, Johnson RC, Carver BF, Mornhinweg DW (1988) Water relations in winter wheat as drought resistance indicators. Crop Science 28: 526-531. doi: 10.2135/cropsci1988.0011183X002800030021x.

Scott RJ, Spielman M, Dickinson HG (2004) Stamen structure and function. The Plant Cell 16 (Suppl): 46-60. doi: 10.1105/tpc.017012.

Senapati N, Stratonovitch P, Paul MJ, Semenov MA (2019) Drought tolerance during reproductive development is important for increasing wheat yield potential under climate change in Europe. Journal of Experimental Botany 70: 2549-2560. doi: 10.1093/jxb/ery226.

Sharma L, Dalal M, Verma RK, Kumar SVV, Yadav SK, Pushkar S, Kushwaha SR, Bhowmik A, Chinnusamy V (2018) Auxin protects spikelet fertility and grain yield under drought and heat stresses in rice. Environmental and Experimental Botany 150: 9-24. doi: 10.1016/j.envexpbot.2018.02.013.

Shavrukov Y, Kurishbayev A, Jatayev S, Shvidchenko V, Zotova L, Koekemoer F, de Groot S, Soole K, Langridge P (2017) Early flowering as a drought escape mechanism in plants: how can it aid wheat production? Frontiers in Plant Science 8: 1950. doi: 10.3389/fpls.2017.01950.

Sheoran IS, Saini HS (1996) Drought-induced male sterility in rice: changes in carbohydrate levels and enzyme activities associated with the inhibition of starch accumulation in pollen. Sexual Plant Reproduction 9: 161-169. doi: 10.1007/BF02221396.

Shi H, Chen L, Ye T, Liu X, Ding K, Chan Z (2014) Modulation of auxin content in Arabidopsis confers improved drought stress resistance. Plant Physiology and Biochemistry 82: 209-217. doi: 10.1016/j.plaphy.2014.06.008.

Singh PK, Srivastava D, Tiwari P, Tiwari M, Verma G, Chakrabarty D (2019) Drought tolerance in plants: molecular mechanism and regulation of signaling molecules. In: Khan MIR, Reddy PS, Ferrante A, Khan NA (Eds.), Plant Signaling Molecules. Woodhead Publishing, Swaston, 105-123.

Song S, Qi T, Huang H, Ren Q, Wu D, Chang C, Peng W, Liu Y, Peng J, Xie D (2011) The jasmonate-ZIM domain proteins interact with the *R2R3-MYB* transcription factors *MYB21* and *MYB24* to affect jasmonate-regulated stamen development in Arabidopsis. The Plant Cell 23: 1000-1013. doi: 10.1105/tpc.111.083089.

Sukiran NL, Ma JC, Ma H, Su Z (2019) ANAC019 is required for recovery of reproductive development under drought stress in Arabidopsis. Plant Molecular Biology 99: 161-174. doi: 10.1007/s11103-018-0810-1.

Sun L, Sui X, Lucas WJ, Li Y, Feng S, Ma S, Fan J, Gao L, Zhang Z (2019) Down-regulation of the sucrose transporter *CsSUT1* causes male sterility by altering carbohydrate supply. Plant Physiology 180: 986-997. doi: 10.1104/pp.19.00317.

Sundberg E, Østergaard L (2009) Distinct and dynamic auxin activities during reproductive development. Cold Spring Harbor Perspectives in Biology 1: a001628. doi: 10.1101/cshperspect.a001628.

Tahjib-Ul-Arif M, Zahan MI, Karim MM, Imran S, Hunter CT, Islam MS, Mia MA, Hannan MA, Rhaman MS, Hossain MA, Brestic M, Skalicky M, Murata Y (2021) Citric acid-mediated abiotic stress tolerance in plants. International Journal of Molecular Sciences 22. doi: 10.3390/ijms22137235.

Taiz L, Zeiger E (2010) Plant Physiology. Fifth Edition. Sinauer Associates, Sunderland, Massachusetts.

Teale WD, Paponov IA, Palme K (2006) Auxin in action: signalling, transport and the control of plant growth and development. Nature Reviews Molecular Cell Biology 7: 847-859. doi: 10.1038/nrm2020.

Tester M, Langridge P (2010) Breeding technologies to increase crop production in a changing world. Science 327: 818-822. doi: 10.1126/science.1183700.

Tilman D, Balzer C, Hill J, Befort BL (2011) Global food demand and the sustainable intensification of agriculture. Proceedings of the National Academy of Sciences of the United States of America 108: 20260-20264. doi: 10.1073/pnas.1116437108.

Timpa JD, Burke JJ, Quisenberry JE, Wendt CW (1986) Effects of water stress on the organic acid and carbohydrate compositions of cotton plants. Plant Physiology 82: 724-728. doi: 10.1104/pp.82.3.724.

Tivendale ND, Millar AH (2022) How is auxin linked with cellular energy pathways to promote growth? New Phytologist 233: 2397-2404. doi: 10.1111/nph.17946.

Turner NC, Wright GC, Siddique KHM (2001) Adaptation of grain legumes (pulses) to water-limited environments. Advances in Agronomy 71: 193-231. doi: 10.1016/s0065-2113(01)71015-2.

Tuteja N (2007) Abscisic acid and abiotic stress signaling. Plant Signaling & Behavior 2: 135-138. doi: 10.4161/psb.2.3.4156.

Tyanova S, Temu T, Cox J (2016) The MaxQuant computational platform for mass spectrometry-based shotgun proteomics. Nature Protocols 11: 2301-2319. doi: 10.1038/nprot.2016.136.

United Nations, Department of Economic and Social Affairs, Population Division (2019) World Population Prospects 2019: Highlights (ST/ESA/SER.A/423).

Vélez-Bermúdez IC, Schmidt W (2014) The conundrum of discordant protein and mRNA expression. Are plants special? Frontiers in Plant Science 5: 619. doi: 10.3389/fpls.2014.00619.

Vogel C, Marcotte EM (2012) Insights into the regulation of protein abundance from proteomic and transcriptomic analyses. Nature Reviews Genetics 13: 227-232. doi: 10.1038/nrg3185.

von Korff M, Wang H, Leon J, Pillen K (2004) Development of candidate introgression lines using an exotic barley accession (*Hordeum vulgare* ssp. *spontaneum*) as donor. Theoretical and Applied Genetics 109: 1736-1745. doi: 10.1007/s00122-004-1818-2.

Wang D, Li J, Sun L, Hu Y, Yu J, Wang C, Zhang F, Hou H, Liang W, Zhang D (2021) Two rice MYB transcription factors maintain male fertility in response to photoperiod by modulating sugar partitioning. New Phytologist 231: 1612-1629. doi: 10.1111/nph.17512.

Weiste C, Pedrotti L, Selvanayagam J, Muralidhara P, Fröschel C, Novák O, Ljung K, Hanson J, Dröge-Laser W (2017) The Arabidopsis bZIP11 transcription factor links low-energy signalling to auxin-mediated control of primary root growth. PLoS Genet 13: e1006607. doi: 10.1371/journal.pgen.1006607.

Wilson ZA, Song J, Taylor B, Yang C (2011) The final split: the regulation of anther dehiscence. Journal of Experimental Botany 62: 1633-1649. doi: 10.1093/jxb/err014.

Wilson ZA, Zhang D-B (2009) From Arabidopsis to rice: pathways in pollen development. Journal of Experimental Botany 60: 1479-1492. doi: 10.1093/jxb/erp095.

Wiśniewski JR, Zougman A, Mann M (2009) Combination of FASP and StageTip-based fractionation allows in-depth analysis of the hippocampal membrane proteome. Journal of Proteome Research 8: 5674-5678. doi: 10.1021/pr900748n.

Xing M, Xue H (2012) A proteomics study of auxin effects in *Arabidopsis thaliana*. Acta Biochimica et Biophysica Sinica 44: 783-796. doi: 10.1093/abbs/gms057.

Xiong Y, McCormack M, Li L, Hall Q, Xiang C, Sheen J (2013) Glucose–TOR signalling reprograms the transcriptome and activates meristems. Nature 496: 181-186. doi: 10.1038/nature12030.

Yamada K, Saijo Y, Nakagami H, Takano Y (2016) Regulation of sugar transporter activity for antibacterial defense in Arabidopsis. Science 354: 1427-1430. doi: 10.1126/science.aah5692.

Yang J, Tian L, Sun MX, Huang XY, Zhu J, Guan YF, Jia QS, Yang ZN (2013) AUXIN RESPONSE FACTOR17 is essential for pollen wall pattern formation in Arabidopsis. Plant Physiology 162: 720-731. doi: 10.1104/pp.113.214940.

Yao X, Tian L, Yang J, Zhao YN, Zhu YX, Dai X, Zhao Y, Yang ZN (2018) Auxin production in diploid microsporocytes is necessary and sufficient for early stages of pollen development. PLoS Genetics 14: e1007397. doi: 10.1371/journal.pgen.1007397.

Ye J, Zhang Z, You C, Zhang X, Lu J, Ma H (2016) Abundant protein phosphorylation potentially regulates Arabidopsis anther development. Journal of Experimental Botany 67: 4993-5008. doi: 10.1093/jxb/erw293.

Yu J, Jiang M, Guo C (2019) Crop pollen development under drought: from the phenotype to the mechanism. International Journal of Molecular Sciences 20: 1550. doi: 10.3390/ijms20071550.

Zamir D (2001) Improving plant breeding with exotic genetic libraries. Nature Reviews Genetics 2: 983-989. doi: 10.1038/35103590.

Zhang H, Liang W, Yang X, Luo X, Jiang N, Ma H, Zhang D (2010) Carbon starved anther encodes a MYB domain protein that regulates sugar partitioning required for rice pollen development. Plant Cell 22: 672-689. doi: 10.1105/tpc.109.073668.

Zhang J, Zhang S, Cheng M, Jiang H, Zhang X, Peng C, Lu X, Zhang M, Jin J (2018) Effect of drought on agronomic traits of rice and wheat: a meta-analysis. International Journal of Environmental Research and Public Health 15: 839. doi: 10.3390/ijerph15050839.

Zhang S, Peng F, Xiao Y, Wang W, Wu X (2020) Peach PpSnRK1 participates in sucrose-mediated root growth through auxin signaling. Frontiers in Plant Science 11: 409. doi: 10.3389/fpls.2020.00409.

Zhang X, Cai X (2011) Climate change impacts on global agricultural land availability. Environmental Research Letters 6: 014014. doi: 10.1088/1748-9326/6/1/014014.

Zhang Y, Fernie AR (2018) On the role of the tricarboxylic acid cycle in plant productivity. Journal of Integrative Plant Biology 60: 1199-1216. doi: 10.1111/jipb.12690.

Zhang Y, Shewry PR, Jones H, Barcelo P, Lazzeri PA, Halford NG (2001) Expression of antisense SnRK1 protein kinase sequence causes abnormal pollen development and male sterility in transgenic barley. The Plant Journal 28: 431-441. doi: 10.1046/j.1365-313x.2001.01167.x.

Zhao Z, Wang C, Yu X, Tian Y, Wang W, Zhang Y, Bai W, Yang N, Zhang T, Zheng H, Wang Q, Lu J, Lei D, He X, Chen K, Gao J, Liu X, Liu S, Jiang L, Wang H, Wan J (2022) Auxin regulates source-sink carbohydrate partitioning and reproductive organ development in rice. Proceedings of the National Academy of Sciences of the United States of America 119: e2121671119. doi: 10.1073/pnas.2121671119.

Zheng Y, Deng X, Qu A, Zhang M, Tao Y, Yang L, Liu Y, Xu J, Zhang S (2018) Regulation of pollen lipid body biogenesis by MAP kinases and downstream WRKY transcription factors in Arabidopsis. PLoS Genetics 14: e1007880. doi: 10.1371/journal.pgen.1007880.

Zhong J, van Esse GW, Bi X, Lan T, Walla A, Sang Q, Franzen R, von Korff M (2021) *INTERMEDIUM-M* encodes an *HvAP2L-H5* ortholog and is required for inflorescence indeterminacy and spikelet determinacy in barley. Proceedings of the National

Academy of Sciences of the United States of America 118: e2011779118. doi: 10.1073/pnas.2011779118.

6 Acknowledgements

First, I would like to express my sincere gratitude to Dr. Ivan Acosta for giving me the opportunity to work as a PhD student in his group at the Max Planck Institute for Plant Breeding in Cologne. Thanks to his continuous supervision, guidance and support, I was able to complete my doctoral studies. It was a great pleasure for me to learn from him and discuss all the ideas and questions that came up during the project.

I would like to thank Prof. Dr. Lukas Schreiber for his advice and support to finalize and submit my thesis and being the first examiner of my doctoral committee. I would also like to thank Prof. Dr. Frank Hochholdinger, Prof. Dr. Peter Dörmann and Prof. Dr. Gabriel Schaaf for being part of my doctoral committee.

I would also like to thank my collaborators: Prof. Dr. Alisdair Fernie and Dr. Youjun Zhang from the Max Planck Institute of Molecular Plant Biology for providing valuable metabolite profiling data. Dr. Hirofumi Nakagami and Dr. Sara Stolze from the Max Planck Institute for Plant Breeding for conducting the proteome analysis.

I am thankful to the former members of the Acosta group, who were part of my life and work at the MPIPZ. I thank Marine and Dhika for their support during my early days as PhD student. I would like to thank Edelgard and Susanne, our wonderful technicians, for the aid in the lab and the refreshing talks about everything. Special thanks go to my colleague Mohamed for the countless hours that we've spent together in the office, lab and greenhouse. I consider myself lucky that he was part of my PhD journey and I've found in him a good friend.

I would also like to thank the members of the greenhouse staff Caren and Astrid for taking care of my barley plants.

My heartfelt gratitude and appreciation go to my parents and my sister Eva for making this journey possible. Your love and belief in me have been and always will be the foundation of my success, growth and happiness.

I would also like to thank all my friends, especially Christian and Torben, for having my back and the fun times that we had together. Life feels much easier with you!

Finally, I would like to thank my fiancée Esther for the unwavering support and motivation. Simultaneously pursuing a PhD was a challenging task and we went through many ups and downs, but eventually, we have not only completed our studies but also started a small family and have our daughter Johanna. I will always be grateful that I could walk this path with you on my side.